Electromagnetic scattering by a bounded obstacle in a parallel plate waveguide

Kristensson, Gerhard

2012

CODEN:LUTEDX/(TEAT-7220)/1-54/(2012)

Revision No. 1: January 2013

Electromagnetic scattering by a bounded obstacle in a parallel plate waveguide

Gerhard Kristensson

Electromagnetic Theory
Department of Electrical and Information Technology
Lund University
Sweden

Gerhard Kristensson
Gerhard.Kristensson@eit.lth.se

Department of Electrical and Information Technology
Electromagnetic Theory
Lund University
P.O. Box 118
SE-221 00 Lund
Sweden

Editor: Gerhard Kristensson

Abstract

This paper concerns scattering of an electromagnetic wave by a bounded object located inside a parallel plate waveguide. The exciting field in the waveguide is either an arbitrary source located at a finite distance from the obstacle or a plane wave generated in the far zone. In the latter case, the generating field corresponds to the lowest propagating mode (TEM) in the waveguide. The analytic treatment of the problem relies on an extension of the null field approach, or T-matrix method, originally developed by Peter Waterman, and later generalized to deal with object close to an interface. The present paper generalizes this approach further to deal with obstacles inside a parallel waveguide. This problem shows features that reflect both the two-dimensional geometry, as well as the three-dimensional scattering characteristics. The analysis is illustrated by several numerical examples.

1 Introduction

Recent theoretical progress in the development of useful scattering identities — sum rules [2, 14, 15, 28] – have initiated several attempts to verify these identities experimentally [15, 22–26]. These sum rules relate the dynamical behavior of the scattering and absorption behavior of the scatterer to the static properties of the scatterer (polarizability dyadics). A detailed investigation of the static properties of an obstacle between two parallel plates has been reported recently [20].

The scattering identities have successfully been verified in free space [23–26]. In many respects, the parallel plate waveguide shows a more controlled environment for these measurements. Initial investigations show that this geometry is accessible [15, 22].

The analysis of wave propagation in a parallel plate waveguide shows many similarities with wave propagation in stratified media. An excellent introduction to the topic of wave propagation in stratified media is found in [10]. The presence of the parallel plates is usually solved by the introduction of an appropriate Green's dyadic. In particular, wave propagation in an empty parallel plate waveguide from a given source configuration can be solved with this technique.

The complexity of the solution increases dramatically if an obstacle is introduced in the waveguide. In the vicinity of the scatterer, the scattered field behaves as a solution of a three-dimensional scattering problem. However, far away from the scatterer, the field does not decline as $1/r$, as it does for a three-dimensional problem, but vanishes as $1/\sqrt{\rho}$, where the distance to the vertical axis is denoted ρ. Nevertheless, far away from the scatterer, the problem is still a three-dimensional scattering problem, since there are variations in the fields in the vertical direction. Only at frequencies below the first cutoff frequency, defined by $k_0 d = \pi$, where k_0 is the wave number in vacuum, and d is the distance between the plates, the problem is two-dimensional, in that there are no variations in the vertical direction of the fields below this frequency.

Again, the introduction of an appropriate Green's dyadic can be useful in the solution of the scattering problem. However, in this paper, we do not pursue this

line of solution technique further. Instead, we use the free space Green's dyadic, and solve the problem with parallel plates and scatterer simultaneously. The entire solution employs the integral representation of the solution. This integral representation approach to solve the scattering problem was originally introduced by Peter Waterman [30], and it has proven to be a very powerful and useful technique to solve a large variety of scattering problems, not only electromagnetic, but also acoustic and elastodynamic problems.

This paper solves the complex wave propagation problem in a planar waveguide with finite obstacles, and the present geometry is an extension of the results with buried obstacle close to a planar interface — layered or not [4, 5, 8, 17–19, 21]. Similar technique to solve the electromagnetic scattering problem by obstacles inside a cylindrical waveguide has also been reported [7]. Problems with two planar surfaces have been addressed before, but not for the electromagnetic problem [16]. The present scattering problem is to some extent equivalent to a scattering problem with infinite number of images of the scatterer distributed periodically in space. The bookkeeping problems associated with such an approach are, however, an inconceivable task, and the solution of the problem asks for a more systematic approach. This paper such an attempt.

The results presented in this paper are inclined towards microwave applications. There are, however, no such limitations in the results. The technique applies equally well to applications at higher frequencies, *e.g.*, THz and IR, such as the computation of the scattering effects of impurities in thin films *etc.*

2 Formulation of the problem

A finite scatterer with bounding surface S_s defines the region V_s. Two infinite, perfectly conducting planes, S_+ and S_-, confine the two disjoint regions V_e and V_s, see Figure 1. These planes are parameterized by $z = z_+$ and $z = z_-$, respectively, and without loss of generality, it is assumed that $z_+ > 0$ and $z_- < 0$. The location of the origin O is arbitrary, but it is important for the analysis that it is located somewhere in V_s. The regions above S_+ and below S_- are denoted by V_+ and V_-, respectively. The sources of the problem are assumed to be locates in $V_\mathrm{i} \subset V_\mathrm{e}$, between the surfaces S_+ and S_-.

To proceed, he time-harmonic electric and magnetic fields satisfy the free-space Maxwell equations in V_e (we use the time convention $\exp\{-\mathrm{i}\omega t\}$),

$$\begin{cases} \nabla \times \boldsymbol{E}(\boldsymbol{r}) = \mathrm{i}k_0\eta_0\boldsymbol{H}(\boldsymbol{r}) \\ \nabla \times \eta_0\boldsymbol{H}(\boldsymbol{r}) = -\mathrm{i}k_0\boldsymbol{E}(\boldsymbol{r}) \end{cases} \qquad \boldsymbol{r} \in V_\mathrm{e} \tag{2.1}$$

where $k_0 = \omega/c_0$ and η_0 are the angular wave number and wave impedance in free space, respectively. The boundary conditions on the bounding surfaces are

$$\begin{cases} \hat{\boldsymbol{z}} \times \boldsymbol{E}(\boldsymbol{r}) = \boldsymbol{0}, & \boldsymbol{r} \in S_+ \cup S_- \\ \hat{\boldsymbol{\nu}} \times \boldsymbol{E}(\boldsymbol{r}) = \boldsymbol{0}, & \boldsymbol{r} \in S_\mathrm{s} \end{cases} \tag{2.2}$$

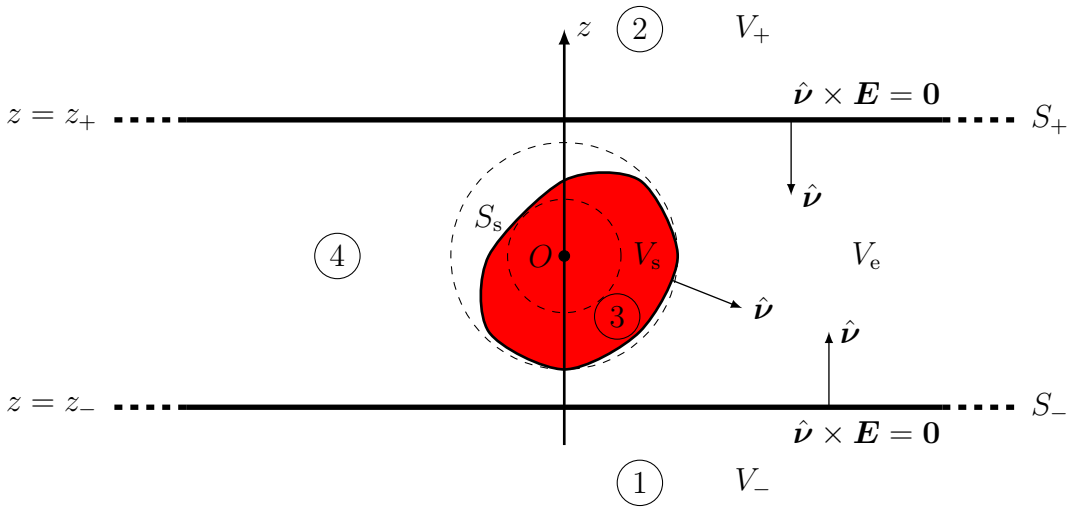

Figure 1: The geometry of the direct scattering problem with two perfectly conducting planes S_+ and S_- and a scatterer with bounding surface S_s.

The scatterer V_s is here assumed to be a perfectly conducting body. This assumption can easily be relaxed, see below. With an appropriate radiation condition in V_e at large lateral distances, (2.1) has a unique solution.

2.1 Integral representation of the solution

Let $\boldsymbol{E}_\mathrm{i}$ denote the incident electric field with sources located in V_e, and define the scattered electric field $\boldsymbol{E}_\mathrm{s} = \boldsymbol{E} - \boldsymbol{E}_\mathrm{i}$. The incident field $\boldsymbol{E}_\mathrm{i}$ is the field with no obstacle or plates present. With the directions of the unit normals defined as in Figure 1, the solution of (2.1) and (2.2) satisfies the surface integral representation [29]

$$-\frac{1}{\mathrm{i}k_0}\nabla\times\left(\nabla\times\iint\limits_{S_+\cup S_-\cup S_\mathrm{s}} g(k_0,|\boldsymbol{r}-\boldsymbol{r}'|)(\hat{\boldsymbol{\nu}}(\boldsymbol{r}')\times\eta_0\boldsymbol{H}(\boldsymbol{r}'))\,\mathrm{d}S'\right)$$

$$+\nabla\times\iint\limits_{S_+\cup S_-\cup S_\mathrm{s}} g(k_0,|\boldsymbol{r}-\boldsymbol{r}'|)\,(\hat{\boldsymbol{\nu}}(\boldsymbol{r}')\times\boldsymbol{E}(\boldsymbol{r}'))\,\mathrm{d}S' = \begin{cases}\boldsymbol{E}_\mathrm{s}(\boldsymbol{r}), & \boldsymbol{r}\in V_\mathrm{e}\\ -\boldsymbol{E}_\mathrm{i}(\boldsymbol{r}), & \boldsymbol{r}\in V_+\cup V_-\cup V_\mathrm{s}\end{cases}$$

where the free-space Green's function for the scalar Helmholtz equation is

$$g(k_0,|\boldsymbol{r}-\boldsymbol{r}'|) = \frac{\mathrm{e}^{\mathrm{i}k_0|\boldsymbol{r}-\boldsymbol{r}'|}}{4\pi|\boldsymbol{r}-\boldsymbol{r}'|}$$

The integral representation also contains a surface integral evaluated at large lateral distances, but proper radiation conditions at large lateral distances make this

integral vanish. Due to (2.2), the surface integral representation simplifies to

$$-\frac{1}{\mathrm{i}k_0}\nabla\times\left(\nabla\times\iint\limits_{S_+\cup S_-\cup S_\mathrm{s}}\mathbf{G}_\mathrm{e}(k_0,|\boldsymbol{r}-\boldsymbol{r}'|)\cdot\boldsymbol{K}(\boldsymbol{r}')\,\mathrm{d}S'\right)=\begin{cases}\boldsymbol{E}_\mathrm{s}(\boldsymbol{r}), & \boldsymbol{r}\in V_\mathrm{e}\\ -\boldsymbol{E}_\mathrm{i}(\boldsymbol{r}), & \boldsymbol{r}\in V_+\cup V_-\cup V_\mathrm{s}\end{cases}\tag{2.3}$$

where $\boldsymbol{K}=\hat{\boldsymbol{\nu}}\times\eta_0\boldsymbol{H}$, and the electric Green's dyadic

$$\mathbf{G}_\mathrm{e}(k_0,|\boldsymbol{r}-\boldsymbol{r}'|)=\left(\mathbf{I}_3+\frac{1}{k_0^2}\nabla\nabla\right)g(k_0,|\boldsymbol{r}-\boldsymbol{r}'|)$$

This surface integral representation is the starting point in the null-field approach, which is the approach that we adopt to solve this scattering problem.

3 Basis functions and expansions

3.1 Spherical vector waves

We introduce the out-going or radiating spherical vector waves, $\boldsymbol{u}_n(k\boldsymbol{r})$, defined as [6] ($\boldsymbol{u}_{\tau\sigma ml}(k\boldsymbol{r})=\boldsymbol{u}_{\tau n}(k\boldsymbol{r})=\boldsymbol{u}_n(k\boldsymbol{r})$)

$$\begin{cases}\boldsymbol{u}_{1n}(k\boldsymbol{r})=h_l^{(1)}(kr)\boldsymbol{A}_{1n}(\hat{\boldsymbol{r}})\\ \boldsymbol{u}_{2n}(k\boldsymbol{r})=\dfrac{(krh_l^{(1)}(kr))'}{kr}\boldsymbol{A}_{2n}(\hat{\boldsymbol{r}})+\sqrt{l(l+1)}\dfrac{h_l^{(1)}(kr)}{kr}\boldsymbol{A}_{3n}(\hat{\boldsymbol{r}})\end{cases}\tag{3.1}$$

and regular spherical vector waves $\boldsymbol{v}_{\tau\sigma ml}(k\boldsymbol{r})$ as

$$\begin{cases}\boldsymbol{v}_{1n}(k\boldsymbol{r})=j_l(kr)\boldsymbol{A}_{1n}(\hat{\boldsymbol{r}})\\ \boldsymbol{v}_{2n}(k\boldsymbol{r})=\dfrac{(krj_l(kr))'}{kr}\boldsymbol{A}_{2n}(\hat{\boldsymbol{r}})+\sqrt{l(l+1)}\dfrac{j_l(kr)}{kr}\boldsymbol{A}_{3n}(\hat{\boldsymbol{r}})\end{cases}\tag{3.2}$$

where $j_l(kr)$ and $h_l^{(1)}(kr)$ denote the spherical Bessel functions and the spherical Hankel functions of the first kind, respectively, and where the vector spherical harmonics,

$$\boldsymbol{A}_{\tau\sigma ml}(\hat{\boldsymbol{r}})=\boldsymbol{A}_{\tau n}(\hat{\boldsymbol{r}})=\boldsymbol{A}_n(\hat{\boldsymbol{r}})\qquad\begin{cases}\tau=1,2,3\\ \sigma=\mathrm{e},\mathrm{o}\\ m=0,1,\ldots,l-1,l\\ l=0,1,2,3,\ldots\end{cases}$$

where $\hat{\boldsymbol{r}}=\boldsymbol{r}/|\boldsymbol{r}|$. The index n is a multi-index that consists of three or four different indices, *i.e.*, $n=\sigma ml$ or $n=\tau\sigma ml$, depending on the context, where $\tau=1,2,3$, $\sigma=\mathrm{e},\mathrm{o}$, $m=0,1,2,\ldots,l$, and $l=0,1,2,\ldots$. Their definitions are,

$$\begin{cases}\boldsymbol{A}_{1n}(\hat{\boldsymbol{r}})=\dfrac{1}{\sqrt{l(l+1)}}\nabla\times(\boldsymbol{r}Y_n(\hat{\boldsymbol{r}}))=\dfrac{1}{\sqrt{l(l+1)}}\nabla Y_n(\hat{\boldsymbol{r}})\times\boldsymbol{r}\\ \boldsymbol{A}_{2n}(\hat{\boldsymbol{r}})=\dfrac{1}{\sqrt{l(l+1)}}r\nabla Y_n(\hat{\boldsymbol{r}})\\ \boldsymbol{A}_{3n}(\hat{\boldsymbol{r}})=\hat{\boldsymbol{r}}Y_n(\hat{\boldsymbol{r}})\end{cases}$$

The spherical harmonics, $Y_n(\hat{\boldsymbol{r}}) = Y_{\sigma ml}(\theta, \phi)$, are defined by [6]

$$Y_{\sigma ml}(\theta, \phi) = C_{lm} P_l^m(\cos\theta) \begin{Bmatrix} \cos m\phi \\ \sin m\phi \end{Bmatrix}$$

where

$$C_{lm} = \sqrt{\frac{\varepsilon_m}{2\pi}} \sqrt{\frac{2l+1}{2} \frac{(l-m)!}{(l+m)!}}$$

and the Neumann factor is defined as $\varepsilon_m = 2 - \delta_{m0}$. The spherical harmonics are orthonormal on the unit sphere Ω, *i.e.*,

$$\iint_\Omega Y_n(\hat{\boldsymbol{r}}) Y_{n'}(\hat{\boldsymbol{r}}) \, \mathrm{d}\Omega = \delta_{nn'} = \delta_{\sigma\sigma'} \delta_{mm'} \delta_{ll'}$$

3.2 Planar vector waves

In a geometry where the medium is laterally homogeneous in the variables x and y, it is natural to decompose the electromagnetic field outside the source region in a spectrum of planar vector waves. The plane wave decomposition amounts to a Fourier transformation of the electric and magnetic fields and flux densities with respect to the lateral variables x and y. The Fourier transform of a time-harmonic field, *e.g.*, the electric field $\boldsymbol{E}(\boldsymbol{r}, \omega)$, is denoted by

$$\boldsymbol{E}(z, \boldsymbol{k}_\mathrm{t}, \omega) = \iint_{\mathbb{R}^2} \boldsymbol{E}(\boldsymbol{r}, \omega) \mathrm{e}^{-\mathrm{i}\boldsymbol{k}_\mathrm{t} \cdot \boldsymbol{\rho}} \, \mathrm{d}x \, \mathrm{d}y$$

where the transverse (tangential) wave vector and the spatial position vector in the plane are

$$\boldsymbol{k}_\mathrm{t} = \hat{\boldsymbol{x}} k_x + \hat{\boldsymbol{y}} k_y = k_\mathrm{t} \hat{\boldsymbol{e}}_\parallel, \quad \boldsymbol{\rho} = x\hat{\boldsymbol{x}} + y\hat{\boldsymbol{y}}$$

The length of the transverse wave vector is always a real non-negative number, *viz.*,

$$k_\mathrm{t} = \sqrt{k_x^2 + k_y^2} \geq 0$$

The unit vector of the transverse wave vector in the x-y-plane is $\hat{\boldsymbol{e}}_\parallel = \boldsymbol{k}_\mathrm{t}/k_\mathrm{t}$.

The inverse Fourier transform is defined by

$$\boldsymbol{E}(\boldsymbol{r}, \omega) = \frac{1}{4\pi^2} \iint_{\mathbb{R}^2} \boldsymbol{E}(z, \boldsymbol{k}_\mathrm{t}, \omega) \mathrm{e}^{\mathrm{i}\boldsymbol{k}_\mathrm{t} \cdot \boldsymbol{\rho}} \, \mathrm{d}k_x \, \mathrm{d}k_y \tag{3.3}$$

Notice that the same letter is used to denote the Fourier transform of the field and the field itself. The arguments and the dimensions of the fields differ. The argument of the field shows what field is intended.

This solution is most conveniently expressed in terms of the two sets of dimensionless, vector-valued plane waves, $\boldsymbol{\varphi}_j^{\pm}(\boldsymbol{k}_{\mathrm{t}};\boldsymbol{r})$, and, $\boldsymbol{\varphi}_j^{\pm\dagger}(\boldsymbol{k}_{\mathrm{t}};\boldsymbol{r})$, $j=1,2$, which are defined as:

$$\begin{cases} \boldsymbol{\varphi}_1^{\pm}(\boldsymbol{k}_{\mathrm{t}};\boldsymbol{r}) = \dfrac{\hat{\boldsymbol{z}}\times\boldsymbol{k}_{\mathrm{t}}}{4\pi \mathrm{i} k_{\mathrm{t}}} \mathrm{e}^{\mathrm{i}\boldsymbol{k}_{\mathrm{t}}\cdot\boldsymbol{\rho}\pm\mathrm{i}k_z z} \\ \boldsymbol{\varphi}_2^{\pm}(\boldsymbol{k}_{\mathrm{t}};\boldsymbol{r}) = \dfrac{\mp\boldsymbol{k}_{\mathrm{t}}k_z + k_{\mathrm{t}}^2\hat{\boldsymbol{z}}}{4\pi k_0 k_{\mathrm{t}}} \mathrm{e}^{\mathrm{i}\boldsymbol{k}_{\mathrm{t}}\cdot\boldsymbol{\rho}\pm\mathrm{i}k_z z} \end{cases} \qquad \begin{cases} \boldsymbol{\varphi}_1^{\pm\dagger}(\boldsymbol{k}_{\mathrm{t}};\boldsymbol{r}) = -\dfrac{\hat{\boldsymbol{z}}\times\boldsymbol{k}_{\mathrm{t}}}{4\pi \mathrm{i} k_{\mathrm{t}}} \mathrm{e}^{-\mathrm{i}\boldsymbol{k}_{\mathrm{t}}\cdot\boldsymbol{\rho}\pm\mathrm{i}k_z z} \\ \boldsymbol{\varphi}_2^{\pm\dagger}(\boldsymbol{k}_{\mathrm{t}};\boldsymbol{r}) = \dfrac{\pm\boldsymbol{k}_{\mathrm{t}}k_z + k_{\mathrm{t}}^2\hat{\boldsymbol{z}}}{4\pi k_0 k_{\mathrm{t}}} \mathrm{e}^{-\mathrm{i}\boldsymbol{k}_{\mathrm{t}}\cdot\boldsymbol{\rho}\pm\mathrm{i}k_z z} \end{cases} \tag{3.4}$$

where, as above, $k_{\mathrm{t}} = |\boldsymbol{k}_{\mathrm{t}}|$, and k_z is defined by

$$k_z = \left(k_0^2 - k_{\mathrm{t}}^2\right)^{1/2} = \begin{cases} \sqrt{k_0^2 - k_{\mathrm{t}}^2} \text{ for } k_{\mathrm{t}} < k_0 \\ \mathrm{i}\sqrt{k_{\mathrm{t}}^2 - k_0^2} \text{ for } k_{\mathrm{t}} > k_0 \end{cases}$$

Both solutions, $\boldsymbol{\varphi}_j^{\pm}(\boldsymbol{k}_{\mathrm{t}};\boldsymbol{r})$, and, $\boldsymbol{\varphi}_j^{\pm\dagger}(\boldsymbol{k}_{\mathrm{t}};\boldsymbol{r})$, $j=1,2$, satisfy the electric field equation, *i.e.*,

$$\nabla\times\left(\nabla\times\boldsymbol{\varphi}_j^{\pm}(\boldsymbol{k}_{\mathrm{t}};\boldsymbol{r})\right) - k_0^2\boldsymbol{\varphi}_j^{\pm}(\boldsymbol{k}_{\mathrm{t}};\boldsymbol{r}) = \boldsymbol{0}$$

The plus super index denotes an exponentially decreasing inhomogeneous (evanescent) wave as $z\to\infty$, and similarly for the minus super index as $z\to-\infty$. The index $j=1$ labels the TE-waves, and $j=2$ labels the TM-waves. Notice that the symbol dagger (†) corresponds to the transformation $\boldsymbol{k}_{\mathrm{t}}\to-\boldsymbol{k}_{\mathrm{t}}$, *i.e.*,

$$\boldsymbol{\varphi}_j^{\pm\dagger}(\boldsymbol{k}_{\mathrm{t}};\boldsymbol{r}) = \boldsymbol{\varphi}_j^{\pm}(-\boldsymbol{k}_{\mathrm{t}};\boldsymbol{r})$$

and that $\boldsymbol{k}^{\pm}\cdot\boldsymbol{\varphi}_j^{\pm}(\boldsymbol{k}_{\mathrm{t}};\boldsymbol{r}) = \boldsymbol{k}^{\mp}\cdot\boldsymbol{\varphi}_j^{\pm\dagger}(\boldsymbol{k}_{\mathrm{t}};\boldsymbol{r}) = 0$, where $\boldsymbol{k}^{\pm} = \boldsymbol{k}_{\mathrm{t}} \pm k_z\hat{\boldsymbol{z}}$.

Notice also that an alternative definition of the planar vector waves is

$$\begin{cases} \boldsymbol{\varphi}_1^{\pm}(\boldsymbol{k}_{\mathrm{t}};\boldsymbol{r}) = \dfrac{1}{4\pi k_{\mathrm{t}}}\nabla\times\left(\hat{\boldsymbol{z}}\mathrm{e}^{\mathrm{i}\boldsymbol{k}_{\mathrm{t}}\cdot\boldsymbol{\rho}\pm\mathrm{i}k_z z}\right) \\ \boldsymbol{\varphi}_2^{\pm}(\boldsymbol{k}_{\mathrm{t}};\boldsymbol{r}) = \dfrac{1}{4\pi k_0 k_{\mathrm{t}}}\nabla\times\left(\nabla\times\left(\hat{\boldsymbol{z}}\mathrm{e}^{\mathrm{i}\boldsymbol{k}_{\mathrm{t}}\cdot\boldsymbol{\rho}\pm\mathrm{i}k_z z}\right)\right) \end{cases} \tag{3.5}$$

which implies

$$\begin{cases} \nabla\times\boldsymbol{\varphi}_1^{\pm}(\boldsymbol{k}_{\mathrm{t}};\boldsymbol{r}) = k_0\boldsymbol{\varphi}_2^{\pm}(\boldsymbol{k}_{\mathrm{t}};\boldsymbol{r}) \\ \nabla\times\boldsymbol{\varphi}_2^{\pm}(\boldsymbol{k}_{\mathrm{t}};\boldsymbol{r}) = k_0\boldsymbol{\varphi}_1^{\pm}(\boldsymbol{k}_{\mathrm{t}};\boldsymbol{r}) \end{cases} \qquad \begin{cases} \nabla\times\boldsymbol{\varphi}_1^{\pm\dagger}(\boldsymbol{k}_{\mathrm{t}};\boldsymbol{r}) = k_0\boldsymbol{\varphi}_2^{\pm\dagger}(\boldsymbol{k}_{\mathrm{t}};\boldsymbol{r}) \\ \nabla\times\boldsymbol{\varphi}_2^{\pm\dagger}(\boldsymbol{k}_{\mathrm{t}};\boldsymbol{r}) = k_0\boldsymbol{\varphi}_1^{\pm\dagger}(\boldsymbol{k}_{\mathrm{t}};\boldsymbol{r}) \end{cases}$$

Notice also that

$$\hat{\boldsymbol{z}}\mathrm{e}^{\mathrm{i}\boldsymbol{k}_{\mathrm{t}}\cdot\boldsymbol{\rho}\pm\mathrm{i}k_z z} = \frac{4\pi k_0}{k_{\mathrm{t}}}\hat{\boldsymbol{z}}\left(\hat{\boldsymbol{z}}\cdot\boldsymbol{\varphi}_2^{\pm}(\boldsymbol{k}_{\mathrm{t}};\boldsymbol{r})\right)$$

These planar vector waves satisfy the following orthogonality relations on S,

which is the plane $z = z_0$, see Appendix A:

$$\begin{cases} \iint\limits_S \boldsymbol{\varphi}_j^{\mp}(\boldsymbol{k}_\mathrm{t};\boldsymbol{r}) \cdot \boldsymbol{\varphi}_{j'}^{\pm\dagger}(\boldsymbol{k}'_\mathrm{t};\boldsymbol{r})\ \mathrm{d}x\,\mathrm{d}y = \dfrac{1}{4}\delta_{jj'}\delta(\boldsymbol{k}_\mathrm{t} - \boldsymbol{k}'_\mathrm{t}) \\ \iint\limits_S \left(\hat{\boldsymbol{z}} \times \boldsymbol{\varphi}_j^{\mp}(\boldsymbol{k}_\mathrm{t};\boldsymbol{r})\right) \cdot \boldsymbol{\varphi}_{j'}^{\pm\dagger}(\boldsymbol{k}'_\mathrm{t};\boldsymbol{r})\ \mathrm{d}x\,\mathrm{d}y = \mp\dfrac{k_z}{4\mathrm{i}k_0}\delta_{\bar{j}j'}\delta(\boldsymbol{k}_\mathrm{t} - \boldsymbol{k}'_\mathrm{t}) \\ \iint\limits_S \left(\hat{\boldsymbol{z}} \times \boldsymbol{\varphi}_j^{\pm}(\boldsymbol{k}_\mathrm{t};\boldsymbol{r})\right) \cdot \boldsymbol{\varphi}_{j'}^{\pm\dagger}(\boldsymbol{k}'_\mathrm{t};\boldsymbol{r})\ \mathrm{d}x\,\mathrm{d}y = \pm(-1)^j\dfrac{k_z}{4\mathrm{i}k_0}\mathrm{e}^{\pm 2\mathrm{i}k_z z_0}\delta_{\bar{j}j'}\delta(\boldsymbol{k}_\mathrm{t} - \boldsymbol{k}'_\mathrm{t}) \end{cases} \tag{3.6}$$

where the dual index $\bar{j}$ is defined $\bar{1} = 2$ and $\bar{2} = 1$.

3.3 Green's dyadic decompositions

The Green's dyadic, $\mathbf{G}_\mathrm{e}(k_0, |\boldsymbol{r} - \boldsymbol{r}'|)$, is decomposed in spherical vector waves [6]

$$\mathbf{G}_\mathrm{e}(k_0, |\boldsymbol{r} - \boldsymbol{r}'|) = \mathrm{i}k_0 \sum_n \boldsymbol{v}_n(k_0\boldsymbol{r}_<)\boldsymbol{u}_n(k_0\boldsymbol{r}_>) = \mathrm{i}k_0 \sum_n \boldsymbol{u}_n(k_0\boldsymbol{r}_>)\boldsymbol{v}_n(k_0\boldsymbol{r}_<) \tag{3.7}$$

where $\boldsymbol{r}_<$ ($\boldsymbol{r}_>$) is the position vector with the smallest (largest) distance to the origin, *i.e.*, if $r < r'$ then $\boldsymbol{r}_< = \boldsymbol{r}$ and $\boldsymbol{r}_> = \boldsymbol{r}'$. The summation is over the divergence-free vector spherical vector waves, $\tau = 1, 2$. Moreover, we need the decomposition of the Green's dyadic in planar vector waves [6]

$$\mathbf{G}_\mathrm{e}(k_0, |\boldsymbol{r} - \boldsymbol{r}'|) = 2\mathrm{i}k_0 \sum_{j=1,2} \iint\limits_{\mathbb{R}^2} \boldsymbol{\varphi}_j^{\pm}(\boldsymbol{k}_\mathrm{t};\boldsymbol{r})\boldsymbol{\varphi}_j^{\mp\dagger}(\boldsymbol{k}_\mathrm{t};\boldsymbol{r}')\frac{k_0}{k_z}\frac{\mathrm{d}k_x\,\mathrm{d}k_y}{k_0^2} \tag{3.8}$$

where the upper (lower) indices are used if $z > z'$ ($z < z'$).

3.4 Transformation between solutions

To connect the spherical vector waves and the planar vector waves, we need transformation properties between the two sets of solutions. The results that are relevant in the analysis below are [6, p. 183]

$$\boldsymbol{u}_n(k_0\boldsymbol{r}) = 2\sum_{j=1,2} \iint\limits_{\mathbb{R}^2} B_{nj}^{\pm}(\boldsymbol{k}_\mathrm{t})\boldsymbol{\varphi}_j^{\pm}(\boldsymbol{k}_\mathrm{t};\boldsymbol{r})\frac{k_0}{k_z}\frac{\mathrm{d}k_x\,\mathrm{d}k_y}{k_0^2}, \quad z \gtrless 0 \tag{3.9}$$

where

$$B_{nj}^{\pm}(\boldsymbol{k}_\mathrm{t}) = \mathrm{i}^{-l+\tau}\boldsymbol{A}_n\left((\boldsymbol{k}_\mathrm{t} \pm k_z\hat{\boldsymbol{z}})/k_0\right) \cdot \left(\delta_{j1}\frac{\hat{\boldsymbol{z}} \times \boldsymbol{k}_\mathrm{t}}{k_\mathrm{t}} + \mathrm{i}\delta_{j2}\frac{\pm\boldsymbol{k}_\mathrm{t}k_z - k_\mathrm{t}^2\hat{\boldsymbol{z}}}{k_0 k_\mathrm{t}}\right) \tag{3.10}$$

The explicit components are

$$B_{nj}^{+}(\boldsymbol{k}_\mathrm{t}) = \mathrm{i}^{-l}C_{lm}\Bigg\{-\mathrm{i}\delta_{\tau j}\Delta_l^m(k_z/k_0)\begin{Bmatrix}\cos m\beta \\ \sin m\beta\end{Bmatrix} - \delta_{\tau\bar{j}}\pi_l^m(k_z/k_0)\begin{Bmatrix}-\sin m\beta \\ \cos m\beta\end{Bmatrix}\Bigg\} \tag{3.11}$$

where the dual index to j is defined $\overline{1} = 2$ and $\overline{2} = 1$, and where $\boldsymbol{k}_\mathrm{t} = k_\mathrm{t}(\hat{\boldsymbol{x}}\cos\beta + \hat{\boldsymbol{y}}\sin\beta)$, and

$$C_{lm} = \sqrt{\frac{\varepsilon_m}{2\pi}}\sqrt{\frac{2l+1}{2}\frac{(l-m)!}{(l+m)!}}$$

and

$$\Delta_l^m(t) = -\frac{(1-t^2)^{1/2}}{\sqrt{l(l+1)}}P_l^{m\prime}(t), \quad \pi_l^m(t) = \frac{m}{\sqrt{l(l+1)}\,(1-t^2)^{1/2}}P_l^m(t) \tag{3.12}$$

The coefficients $B_{nj}^-(\boldsymbol{k}_\mathrm{t})$ are obtained from $B_{nj}^+(\boldsymbol{k}_\mathrm{t})$ by the use of the parity relation $P_l^m(-t) = (-1)^{l+m}P_l^m(t)$)

$$B_{nj}^-(\boldsymbol{k}_\mathrm{t}) = \mathrm{i}^{-l}(-1)^{l+m}C_{lm}\left\{\mathrm{i}\delta_{\tau j}\Delta_l^m(k_z/k_0)\begin{Bmatrix}\cos m\beta\\ \sin m\beta\end{Bmatrix} - \delta_{\tau\bar{j}}\pi_l^m(k_z/k_0)\begin{Bmatrix}-\sin m\beta\\ \cos m\beta\end{Bmatrix}\right\}$$

or, in a more compact notation

$$B_{nj}^-(\boldsymbol{k}_\mathrm{t}) = (-1)^{l+m+j+\tau+1}B_{nj}^+(\boldsymbol{k}_\mathrm{t}), \quad j = 1,2$$

The coefficients $B_{nj}^\pm(\boldsymbol{k}_\mathrm{t})$ for different τ and j indices are not independent, *i.e.*,

$$B_{1\sigma ml1}^\pm(\boldsymbol{k}_\mathrm{t}) = B_{2\sigma ml2}^\pm(\boldsymbol{k}_\mathrm{t}), \quad B_{2\sigma ml1}^\pm(\boldsymbol{k}_\mathrm{t}) = B_{1\sigma ml2}^\pm(\boldsymbol{k}_\mathrm{t})$$

or in terms of the dual indices of τ and j.

$$B_{\overline{\tau}\sigma mlj}^\pm(\boldsymbol{k}_\mathrm{t}) = B_{\tau\sigma ml\overline{j}}^\pm(\boldsymbol{k}_\mathrm{t}) \tag{3.13}$$

where the dual index $\overline{j}$ and $\overline{\tau}$ are defined $\overline{1} = 2$ and $\overline{2} = 1$.

There is also a useful transformation between planar vector waves and regular spherical vector waves. This transformation is [6, p. 183]

$$\boldsymbol{\varphi}_j^\pm(\boldsymbol{k}_\mathrm{t};\boldsymbol{r}) = \sum_n B_{nj}^{\pm\dagger}(\boldsymbol{k}_\mathrm{t})\boldsymbol{v}_n(k_0\boldsymbol{r}) \tag{3.14}$$

where

$$B_{nj}^{\pm\dagger}(\boldsymbol{k}_\mathrm{t}) = \mathrm{i}^{l-\tau}\boldsymbol{A}_n\left((\boldsymbol{k}_\mathrm{t} \pm k_z\hat{\boldsymbol{z}})/k_0\right)\cdot\left(\delta_{j1}\frac{\hat{\boldsymbol{z}}\times\boldsymbol{k}_\mathrm{t}}{k_\mathrm{t}} - \mathrm{i}\delta_{j2}\frac{\pm\boldsymbol{k}_\mathrm{t}k_z - k_\mathrm{t}^2\hat{\boldsymbol{z}}}{k_0k_\mathrm{t}}\right)$$

This expansion is uniformly convergent in compact domains of $\mathbb{R}^3$. Notice that

$$B_{nj}^{\pm\dagger}(-\boldsymbol{k}_\mathrm{t}) = B_{nj}^\mp(\boldsymbol{k}_\mathrm{t}) \tag{3.15}$$

where we employed the parity of the vector spherical harmonics, $\boldsymbol{A}_{\tau\sigma ml}(-\hat{\boldsymbol{r}}) = (-1)^{l+\tau-1}\boldsymbol{A}_{\tau\sigma ml}(\hat{\boldsymbol{r}})$.

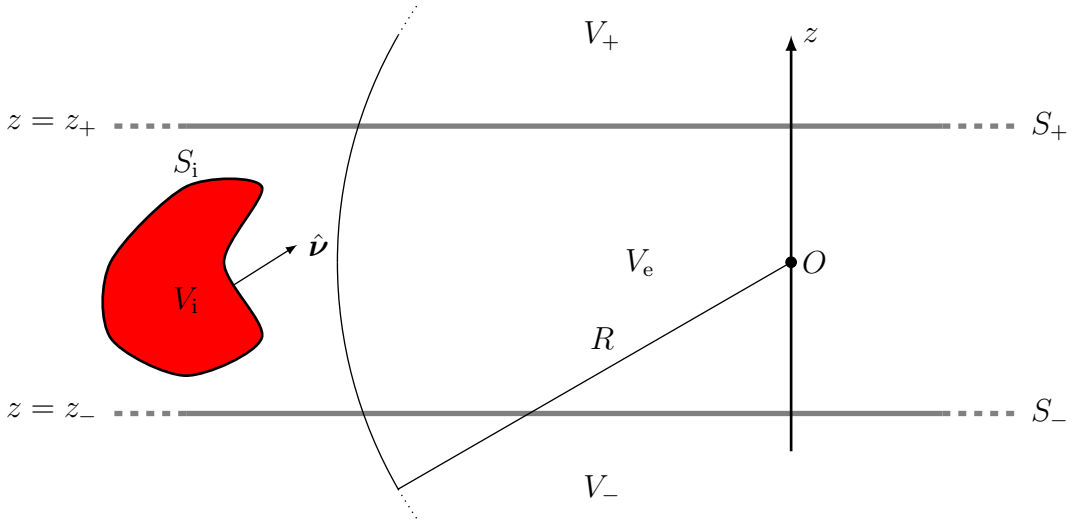

Figure 2: The geometry of the sources of the incident field between the two perfectly conducting planes S_+ and S_-. Notice, no scatterers or plates are physically present in this geometry.

4 Incident electric field

The sources of the incident field are assumed to be located between the plates $S_\pm$ and outside the scatterer V_s. We assume they are confined to the region $V_\mathrm{i} \subset V_\mathrm{e}$. Denote by V_R the largest spherical region centered at the origin not including V_i, see Figure 2.

Due to the completeness of the planar vector waves and the spherical vector waves, the incident electric field is assumed to have the following expansions in the three regions, $V_\pm$ and V_s:

$$\boldsymbol{E}_\mathrm{i}(\boldsymbol{r}) = \sum_{j=1,2} \iint_{\mathbb{R}^2} a_j^\pm(\boldsymbol{k}_\mathrm{t}) \boldsymbol{\varphi}_j^\pm(\boldsymbol{k}_\mathrm{t}; \boldsymbol{r}) \frac{\mathrm{d}k_x \, \mathrm{d}k_y}{k_0^2}, \quad \boldsymbol{r} \in V_\pm \tag{4.1}$$

where the upper (lower) sign holds for V_+ (V_-), and

$$\boldsymbol{E}_\mathrm{i}(\boldsymbol{r}) = \sum_n a_n \boldsymbol{v}_n(k_0 \boldsymbol{r}), \quad \boldsymbol{r} \in V_R \tag{4.2}$$

where V_R is a sphere of radius R that does not include the circumscribing sphere of the source region. These expansions represent the same incident field with different domains of convergence. In order to be consistent, the expansion coefficients are related to each other. We claim[1]

$$a_n = \sum_{j=1,2} \iint_{\mathbb{R}^2} a_j^\pm(\boldsymbol{k}_\mathrm{t}) B_{nj}^{\pm\dagger}(\boldsymbol{k}_\mathrm{t}) \frac{\mathrm{d}k_x \, \mathrm{d}k_y}{k_0^2} \tag{4.3}$$

[1]At this stage it is only an assumption. No formal proof exists. The relation holds for the examples in Section 11.

5 Utilizing the surface integral representation

The position vector, $\boldsymbol{r}$, can take four principle positions, $\boldsymbol{r} \in V_\pm$, $\boldsymbol{r} \in V_\mathrm{s}$, and $\boldsymbol{r} \in V_\mathrm{e}$. We now explore these possibilities. The decompositions of the Green's dyadic in spherical and planar vector waves, see (3.7) and (3.8) are now used.

5.1 Above and below the upper and lower surfaces $S_\pm$

When the position vector is either in V_+ or in V_-, the lower line of (2.3) using (3.7), (3.8), (3.9), and (4.1) yield

$$\begin{aligned}
&\sum_{j=1,2} \iint\limits_{\mathbb{R}^2} a_j^\pm(\boldsymbol{k}_\mathrm{t}) \boldsymbol{\varphi}_j^\pm(\boldsymbol{k}_\mathrm{t}; \boldsymbol{r}) \frac{\mathrm{d}k_x \, \mathrm{d}k_y}{k_0^2} \\
&\qquad = 2k_0^2 \sum_{j=1,2} \iint\limits_{\mathbb{R}^2} \boldsymbol{\varphi}_j^\pm(\boldsymbol{k}_\mathrm{t}; \boldsymbol{r}) \iint\limits_{S_+ \cup S_-} \boldsymbol{\varphi}_j^{\mp\dagger}(\boldsymbol{k}_\mathrm{t}; \boldsymbol{r}') \cdot \boldsymbol{K}(\boldsymbol{r}') \, \mathrm{d}S' \frac{k_0}{k_z} \frac{\mathrm{d}k_x \, \mathrm{d}k_y}{k_0^2} \\
&+ 2k_0^2 \sum_{j=1,2} \iint\limits_{\mathbb{R}^2} \boldsymbol{\varphi}_j^\pm(\boldsymbol{k}_\mathrm{t}; \boldsymbol{r}) \sum_n B_{nj}^\pm(\boldsymbol{k}_\mathrm{t}) \iint\limits_{S_\mathrm{s}} \boldsymbol{v}_n(k_0 \boldsymbol{r}') \cdot \boldsymbol{K}(\boldsymbol{r}') \, \mathrm{d}S' \frac{k_0}{k_z} \frac{\mathrm{d}k_x \, \mathrm{d}k_y}{k_0^2}, \quad \boldsymbol{r} \in V_\pm
\end{aligned}$$

Note that we have changed the order of the surface integral and the sum over n. Since the planar vector waves are linearly independent, we have

$$\begin{cases}
a_j^+(\boldsymbol{k}_\mathrm{t}) = 2k_0^2 \dfrac{k_0}{k_z} \displaystyle\iint\limits_{S_+ \cup S_-} \boldsymbol{\varphi}_j^{-\dagger}(\boldsymbol{k}_\mathrm{t}; \boldsymbol{r}') \cdot \boldsymbol{K}(\boldsymbol{r}') \, \mathrm{d}S' \\
\qquad\qquad + 2k_0^2 \dfrac{k_0}{k_z} \displaystyle\sum_n B_{nj}^+(\boldsymbol{k}_\mathrm{t}) \iint\limits_{S_\mathrm{s}} \boldsymbol{v}_n(k_0 \boldsymbol{r}') \cdot \boldsymbol{K}(\boldsymbol{r}') \, \mathrm{d}S' \\
a_j^-(\boldsymbol{k}_\mathrm{t}) = 2k_0^2 \dfrac{k_0}{k_z} \displaystyle\iint\limits_{S_+ \cup S_-} \boldsymbol{\varphi}_j^{+\dagger}(\boldsymbol{k}_\mathrm{t}; \boldsymbol{r}') \cdot \boldsymbol{K}(\boldsymbol{r}') \, \mathrm{d}S' \\
\qquad\qquad + 2k_0^2 \dfrac{k_0}{k_z} \displaystyle\sum_n B_{nj}^-(\boldsymbol{k}_\mathrm{t}) \iint\limits_{S_\mathrm{s}} \boldsymbol{v}_n(k_0 \boldsymbol{r}') \cdot \boldsymbol{K}(\boldsymbol{r}') \, \mathrm{d}S'
\end{cases} \tag{5.1}$$

This is the general expression of the expansion coefficients $a_j^\pm(\boldsymbol{k}_\mathrm{t})$ in terms of the surface field $\boldsymbol{K}(\boldsymbol{r})$. From these two expressions we conclude that $\tilde{a}^\pm = -a_j^\mp$, where $\tilde{a}^\pm$ denotes $a_j^\pm$ with $k_z \leftrightarrow -k_z$. To see this, use the definition of the planar vector waves in Section 3.2 and the definition of $B_{nj}^\pm(\boldsymbol{k}_\mathrm{t})$ in (3.10) to conclude that $\boldsymbol{\varphi}_j^{\mp\dagger}(\boldsymbol{k}_\mathrm{t}; \boldsymbol{r}) \leftrightarrow \boldsymbol{\varphi}_j^{\pm\dagger}(\boldsymbol{k}_\mathrm{t}; \boldsymbol{r})$ and $B_{nj}^\pm(\boldsymbol{k}_\mathrm{t}) \leftrightarrow B_{nj}^\mp(\boldsymbol{k}_\mathrm{t})$ when $k_z \leftrightarrow -k_z$. Thus, we get

$$\begin{aligned}
\tilde{a}_j^\pm(\boldsymbol{k}_\mathrm{t}) = -2k_0^2 \frac{k_0}{k_z} &\iint\limits_{S_+ \cup S_-} \boldsymbol{\varphi}_j^{\pm\dagger}(\boldsymbol{k}_\mathrm{t}; \boldsymbol{r}') \cdot \boldsymbol{K}(\boldsymbol{r}') \, \mathrm{d}S' \\
&- 2k_0^2 \frac{k_0}{k_z} \sum_n B_{nj}^\mp(\boldsymbol{k}_\mathrm{t}) \iint\limits_{S_\mathrm{s}} \boldsymbol{v}_n(k_0 \boldsymbol{r}') \cdot \boldsymbol{K}(\boldsymbol{r}') \, \mathrm{d}S' = -a_j^\mp(\boldsymbol{k}_\mathrm{t})
\end{aligned}$$

5.2 Inside the largest inscribed sphere of V_s

When the position vector is inside the largest sphere enclosed in V_s, the lower line of (2.3) using (3.7), (3.9), and (4.1) yield

$$\begin{aligned}\sum_n a_n \boldsymbol{v}_n(k_0\boldsymbol{r}) = k_0^2 \sum_n \boldsymbol{v}_n(k_0\boldsymbol{r}) \iint_{S_\mathrm{s}} \boldsymbol{u}_n(k_0\boldsymbol{r}') \cdot \boldsymbol{K}(\boldsymbol{r}')\, \mathrm{d}S' \\ + 2k_0^2 \sum_n \boldsymbol{v}_n(k_0\boldsymbol{r}) \sum_{j=1,2} \iint_{\mathbb{R}^2} B_{nj}^{+}(\boldsymbol{k}_\mathrm{t}) \iint_{S_+} \boldsymbol{\varphi}_j^{+}(\boldsymbol{k}_\mathrm{t};\boldsymbol{r}') \cdot \boldsymbol{K}(\boldsymbol{r}')\, \mathrm{d}S' \frac{k_0}{k_z} \frac{\mathrm{d}k_x\, \mathrm{d}k_y}{k_0^2} \\ + 2k_0^2 \sum_n \boldsymbol{v}_n(k_0\boldsymbol{r}) \sum_{j=1,2} \iint_{\mathbb{R}^2} B_{nj}^{-}(\boldsymbol{k}_\mathrm{t}) \iint_{S_-} \boldsymbol{\varphi}_j^{-}(\boldsymbol{k}_\mathrm{t};\boldsymbol{r}') \cdot \boldsymbol{K}(\boldsymbol{r}')\, \mathrm{d}S' \frac{k_0}{k_z} \frac{\mathrm{d}k_x\, \mathrm{d}k_y}{k_0^2}\end{aligned}$$

Note that we have changed the order of the surface integral and the sum over n. Since the regular spherical vector waves, $\boldsymbol{v}_n(k_0\boldsymbol{r})$, are linearly independent, we have

$$\begin{aligned}a_n = k_0^2 \iint_{S_\mathrm{s}} \boldsymbol{u}_n(k_0\boldsymbol{r}') \cdot \boldsymbol{K}(\boldsymbol{r}')\, \mathrm{d}S' \\ + 2k_0^2 \sum_{j=1,2} \iint_{\mathbb{R}^2} B_{nj}^{+}(\boldsymbol{k}_\mathrm{t}) \iint_{S_+} \boldsymbol{\varphi}_j^{+}(\boldsymbol{k}_\mathrm{t};\boldsymbol{r}') \cdot \boldsymbol{K}(\boldsymbol{r}')\, \mathrm{d}S' \frac{k_0}{k_z} \frac{\mathrm{d}k_x\, \mathrm{d}k_y}{k_0^2} \\ + 2k_0^2 \sum_{j=1,2} \iint_{\mathbb{R}^2} B_{nj}^{-}(\boldsymbol{k}_\mathrm{t}) \iint_{S_-} \boldsymbol{\varphi}_j^{-}(\boldsymbol{k}_\mathrm{t};\boldsymbol{r}') \cdot \boldsymbol{K}(\boldsymbol{r}')\, \mathrm{d}S' \frac{k_0}{k_z} \frac{\mathrm{d}k_x\, \mathrm{d}k_y}{k_0^2} \qquad (5.2)\end{aligned}$$

Alternatively, expand the Green's dyadic into planar vector waves, (3.8), and use (3.14). We get

$$\begin{aligned}a_n = k_0^2 \iint_{S_\mathrm{s}} \boldsymbol{u}_n(k_0\boldsymbol{r}') \cdot \boldsymbol{K}(\boldsymbol{r}')\, \mathrm{d}S' \\ + 2k_0^2 \sum_{j=1,2} \iint_{\mathbb{R}^2} B_{nj}^{-\dagger}(\boldsymbol{k}_\mathrm{t}) \iint_{S_+} \boldsymbol{\varphi}_j^{+\dagger}(\boldsymbol{k}_\mathrm{t};\boldsymbol{r}') \cdot \boldsymbol{K}(\boldsymbol{r}')\, \mathrm{d}S' \frac{k_0}{k_z} \frac{\mathrm{d}k_x\, \mathrm{d}k_y}{k_0^2} \\ + 2k_0^2 \sum_{j=1,2} \iint_{\mathbb{R}^2} B_{nj}^{+\dagger}(\boldsymbol{k}_\mathrm{t}) \iint_{S_-} \boldsymbol{\varphi}_j^{-\dagger}(\boldsymbol{k}_\mathrm{t};\boldsymbol{r}') \cdot \boldsymbol{K}(\boldsymbol{r}')\, \mathrm{d}S' \frac{k_0}{k_z} \frac{\mathrm{d}k_x\, \mathrm{d}k_y}{k_0^2}\end{aligned}$$

The symmetry properties $\boldsymbol{\varphi}_j^{\pm\dagger}(\boldsymbol{k}_\mathrm{t};\boldsymbol{r}) = \boldsymbol{\varphi}_j^{\pm}(-\boldsymbol{k}_\mathrm{t};\boldsymbol{r})$ and $B_{nj}^{\pm\dagger}(-\boldsymbol{k}_\mathrm{t}) = B_{nj}^{\mp}(\boldsymbol{k}_\mathrm{t})$ show that these expressions are identical.

5.3 In V_e outside the smallest sphere that circumscribes V_s

When the position vector is outside the circumscribing sphere of S_s in V_e, the upper line of (2.3) using (3.7), (3.8), (3.9), and (4.1) yield

$$\begin{aligned}\boldsymbol{E}_\mathrm{s}(\boldsymbol{r}) &= \sum_n f_n \boldsymbol{u}_n(k_0\boldsymbol{r}) \\ &+ \sum_{j=1,2} \iint_{\mathbb{R}^2} f_j^+(\boldsymbol{k}_\mathrm{t})\boldsymbol{\varphi}_j^+(\boldsymbol{k}_\mathrm{t};\boldsymbol{r})\,\frac{\mathrm{d}k_x\,\mathrm{d}k_y}{k_0^2} + \sum_{j=1,2} \iint_{\mathbb{R}^2} f_j^-(\boldsymbol{k}_\mathrm{t})\boldsymbol{\varphi}_j^-(\boldsymbol{k}_\mathrm{t};\boldsymbol{r})\,\frac{\mathrm{d}k_x\,\mathrm{d}k_y}{k_0^2}\end{aligned} \tag{5.3}$$

where

$$\begin{cases} f_n = -k_0^2 \displaystyle\iint_{S_\mathrm{s}} \boldsymbol{v}_n(k_0\boldsymbol{r}')\cdot\boldsymbol{K}(\boldsymbol{r}')\,\mathrm{d}S' \\ f_j^\pm(\boldsymbol{k}_\mathrm{t}) = -2k_0^2\dfrac{k_0}{k_z}\displaystyle\iint_{S_\mp} \boldsymbol{\varphi}_j^{\mp\dagger}(\boldsymbol{k}_\mathrm{t};\boldsymbol{r}')\cdot\boldsymbol{K}(\boldsymbol{r}')\,\mathrm{d}S' \end{cases} \tag{5.4}$$

6 Expansion and elimination of the surface fields

Expand the currents on the surfaces in planar vector waves and a complete set of tangential vector functions, $\hat{\boldsymbol{\nu}}\times\boldsymbol{\psi}_n$, on S_s. More precisely, we assume

$$\boldsymbol{K}(\boldsymbol{r}) = \begin{cases} \displaystyle\sum_{j=1,2}\iint_{\mathbb{R}^2} \alpha_j^+(\boldsymbol{k}_\mathrm{t})\hat{\boldsymbol{z}}\times\boldsymbol{\varphi}_{\overline{j}}^-(\boldsymbol{k}_\mathrm{t};\boldsymbol{r})\,\frac{\mathrm{d}k_x\,\mathrm{d}k_y}{k_0^2}, & \boldsymbol{r}\in S_+ \\ \displaystyle\sum_{j=1,2}\iint_{\mathbb{R}^2} \alpha_j^-(\boldsymbol{k}_\mathrm{t})\hat{\boldsymbol{z}}\times\boldsymbol{\varphi}_{\overline{j}}^+(\boldsymbol{k}_\mathrm{t};\boldsymbol{r})\,\frac{\mathrm{d}k_x\,\mathrm{d}k_y}{k_0^2}, & \boldsymbol{r}\in S_- \\ \displaystyle\sum_n \alpha_n\hat{\boldsymbol{\nu}}(\boldsymbol{r})\times\boldsymbol{\psi}_n(\boldsymbol{r}), & \boldsymbol{r}\in S_\mathrm{s} \end{cases}$$

where the dual index $\overline{j}$ is defined $\overline{1}=2$ and $\overline{2}=1$.

Introduce the dimension-less Q-matrices of the scatterer. They are defined as

$$Q'_{nn'} = k_0^2\iint_{S_\mathrm{s}} \boldsymbol{u}_n\cdot(\hat{\boldsymbol{\nu}}\times\boldsymbol{\psi}_{n'})\,\mathrm{d}S, \qquad Q_{nn'} = k_0^2\iint_{S_\mathrm{s}} \boldsymbol{v}_n\cdot(\hat{\boldsymbol{\nu}}\times\boldsymbol{\psi}_{n'})\,\mathrm{d}S$$

The orthogonality relations imply, see (3.6) (S is defined as $z=z_0$)

$$\begin{cases} \displaystyle\iint_S \boldsymbol{\varphi}_{j'}^{\pm\dagger}(\boldsymbol{k}_\mathrm{t};\boldsymbol{r})\cdot\Big(\hat{\boldsymbol{z}}\times\boldsymbol{\varphi}_{\overline{j}}^{\mp}(\boldsymbol{k}'_\mathrm{t};\boldsymbol{r})\Big)\,\mathrm{d}x\,\mathrm{d}y = \mp\frac{k_z}{4\mathrm{i}k_0}\delta_{jj'}\delta(\boldsymbol{k}_\mathrm{t}-\boldsymbol{k}'_\mathrm{t}) \\ \displaystyle\iint_S \boldsymbol{\varphi}_{j'}^{\mp\dagger}(\boldsymbol{k}_\mathrm{t};\boldsymbol{r})\cdot\Big(\hat{\boldsymbol{z}}\times\boldsymbol{\varphi}_{\overline{j}}^{\mp}(\boldsymbol{k}'_\mathrm{t};\boldsymbol{r})\Big)\,\mathrm{d}x\,\mathrm{d}y = \pm(-1)^j\frac{k_z}{4\mathrm{i}k_0}\mathrm{e}^{\mp 2\mathrm{i}k_z z_0}\delta_{jj'}\delta(\boldsymbol{k}_\mathrm{t}-\boldsymbol{k}'_\mathrm{t}) \end{cases}$$

Equation (5.1) implies

$$a_j^+(\boldsymbol{k}_\mathrm{t}) = \frac{1}{2\mathrm{i}}\left((-1)^j\alpha_j^+(\boldsymbol{k}_\mathrm{t})\mathrm{e}^{-2\mathrm{i}k_z z_+} + \alpha_j^-(\boldsymbol{k}_\mathrm{t})\right) + 2\frac{k_0}{k_z}\sum_{nn'} B_{nj}^+(\boldsymbol{k}_\mathrm{t})Q_{nn'}\alpha_{n'}$$

and

$$a_j^-(\boldsymbol{k}_\mathrm{t}) = \frac{1}{2\mathrm{i}}\left(-\alpha_j^+(\boldsymbol{k}_\mathrm{t}) - (-1)^j\alpha_j^-(\boldsymbol{k}_\mathrm{t})\mathrm{e}^{2\mathrm{i}k_z z_-}\right) + 2\frac{k_0}{k_z}\sum_{nn'} B_{nj}^-(\boldsymbol{k}_\mathrm{t})Q_{nn'}\alpha_{n'}$$

Denoting the distance between the plates by $d = z_+ - z_-$, the last two expressions lead to

$$\alpha_j^+(\boldsymbol{k}_\mathrm{t}) = -2\mathrm{i}\frac{a_j^-(\boldsymbol{k}_\mathrm{t}) + a_j^+(\boldsymbol{k}_\mathrm{t})(-1)^j\mathrm{e}^{2\mathrm{i}k_z z_-}}{1-\mathrm{e}^{-2\mathrm{i}k_z d}} + 4\mathrm{i}\frac{k_0}{k_z}\sum_{nn'}\frac{B_{nj}^-(\boldsymbol{k}_\mathrm{t}) + B_{nj}^+(\boldsymbol{k}_\mathrm{t})(-1)^j\mathrm{e}^{2\mathrm{i}k_z z_-}}{1-\mathrm{e}^{-2\mathrm{i}k_z d}}Q_{nn'}\alpha_{n'}$$

and

$$\alpha_j^-(\boldsymbol{k}_\mathrm{t}) = 2\mathrm{i}\frac{a_j^+(\boldsymbol{k}_\mathrm{t}) + a_j^-(\boldsymbol{k}_\mathrm{t})(-1)^j\mathrm{e}^{-2\mathrm{i}k_z z_+}}{1-\mathrm{e}^{-2\mathrm{i}k_z d}} - 4\mathrm{i}\frac{k_0}{k_z}\sum_{nn'}\frac{B_{nj}^+(\boldsymbol{k}_\mathrm{t}) + B_{nj}^-(\boldsymbol{k}_\mathrm{t})(-1)^j\mathrm{e}^{-2\mathrm{i}k_z z_+}}{1-\mathrm{e}^{-2\mathrm{i}k_z d}}Q_{nn'}\alpha_{n'}$$

Furthermore, from Appendix A, we get

$$\iint\limits_S \boldsymbol{\varphi}_{j'}^{\pm}(\boldsymbol{k}_\mathrm{t};\boldsymbol{r})\cdot\left(\hat{\boldsymbol{z}}\times\boldsymbol{\varphi}_j^{\mp}(\boldsymbol{k}'_\mathrm{t};\boldsymbol{r})\right)\mathrm{d}x\,\mathrm{d}y = \mp\frac{k_z}{4\mathrm{i}k_0}\delta_{jj'}\delta(\boldsymbol{k}_\mathrm{t}+\boldsymbol{k}'_\mathrm{t}) \tag{6.1}$$

and (5.2) imply

$$a_n = \sum_{n'} Q'_{nn'}\alpha_{n'} - \gamma_n$$

where

$$\gamma_n = \frac{1}{2\mathrm{i}}\sum_{j=1,2}\iint\limits_{\mathbb{R}^2}\left(\alpha_j^+(\boldsymbol{k}_\mathrm{t})B_{nj}^{-\dagger}(\boldsymbol{k}_\mathrm{t}) - \alpha_j^-(\boldsymbol{k}_\mathrm{t})B_{nj}^{+\dagger}(\boldsymbol{k}_\mathrm{t})\right)\frac{\mathrm{d}k_x\,\mathrm{d}k_y}{k_0^2} \tag{6.2}$$

The expansion coefficients α_n are formally extracted as

$$\alpha_n = \sum_{n'} Q'^{-1}_{nn'}\left(a_{n'} + \gamma_{n'}\right)$$

which leads to the expressions

$$\alpha_j^+(\boldsymbol{k}_\mathrm{t}) = -2\mathrm{i}\frac{a_j^-(\boldsymbol{k}_\mathrm{t}) + a_j^+(\boldsymbol{k}_\mathrm{t})(-1)^j\mathrm{e}^{2\mathrm{i}k_z z_-}}{1-\mathrm{e}^{-2\mathrm{i}k_z d}} - 4\mathrm{i}\frac{k_0}{k_z}\sum_{nn'}\frac{B_{nj}^-(\boldsymbol{k}_\mathrm{t}) + B_{nj}^+(\boldsymbol{k}_\mathrm{t})(-1)^j\mathrm{e}^{2\mathrm{i}k_z z_-}}{1-\mathrm{e}^{-2\mathrm{i}k_z d}}T_{nn'}\left(a_{n'} + \gamma_{n'}\right) \tag{6.3}$$

and

$$\alpha_j^-(\boldsymbol{k}_\mathrm{t}) = 2\mathrm{i}\frac{a_j^+(\boldsymbol{k}_\mathrm{t}) + a_j^-(\boldsymbol{k}_\mathrm{t})(-1)^j \mathrm{e}^{-2\mathrm{i}k_z z_+}}{1-\mathrm{e}^{-2\mathrm{i}k_z d}} + 4\mathrm{i}\frac{k_0}{k_z}\sum_{nn'}\frac{B_{nj}^+(\boldsymbol{k}_\mathrm{t}) + B_{nj}^-(\boldsymbol{k}_\mathrm{t})(-1)^j \mathrm{e}^{-2\mathrm{i}k_z z_+}}{1-\mathrm{e}^{-2\mathrm{i}k_z d}} T_{nn'}\left(a_{n'}+\gamma_{n'}\right) \quad (6.4)$$

where the T-matrix of the scatterer is

$$T_{nn'} = -\sum_{n''} Q_{nn''} Q'^{-1}_{n''n'}$$

Insert the formulas of $\alpha_j^\pm(\boldsymbol{k}_\mathrm{t})$ from above in the expression for γ_n in (6.2), and we get an infinite set of equations that can be solved for γ_n for every specified incident field, *i.e.*,

$$c_n = d_n + \sum_{n'n''} A_{nn'} T_{n'n''} c_{n''} \quad (6.5)$$

where the array $c_n = a_n + \gamma_n$, and the d_n vector is

$$d_n = -\sum_{j=1,2}\iint_{\mathbb{R}^2} a_j^+(\boldsymbol{k}_\mathrm{t})\frac{B_{nj}^{+\dagger}(\boldsymbol{k}_\mathrm{t}) + (-1)^j \mathrm{e}^{2\mathrm{i}k_z z_-} B_{nj}^{-\dagger}(\boldsymbol{k}_\mathrm{t})}{1-\mathrm{e}^{-2\mathrm{i}k_z d}}\,\frac{\mathrm{d}k_x\,\mathrm{d}k_y}{k_0^2} - \sum_{j=1,2}\iint_{\mathbb{R}^2} a_j^-(\boldsymbol{k}_\mathrm{t})\frac{B_{nj}^{-\dagger}(\boldsymbol{k}_\mathrm{t}) + (-1)^j \mathrm{e}^{-2\mathrm{i}k_z z_+} B_{nj}^{+\dagger}(\boldsymbol{k}_\mathrm{t})}{1-\mathrm{e}^{-2\mathrm{i}k_z d}}\,\frac{\mathrm{d}k_x\,\mathrm{d}k_y}{k_0^2} + a_n \quad (6.6)$$

and the $A_{nn'}$ matrix is

$$A_{nn'} = -2\sum_{j=1,2}\iint_{\mathbb{R}^2} B_{nj}^{-\dagger}(\boldsymbol{k}_\mathrm{t})\frac{B_{n'j}^-(\boldsymbol{k}_\mathrm{t}) + (-1)^j \mathrm{e}^{2\mathrm{i}k_z z_-} B_{n'j}^+(\boldsymbol{k}_\mathrm{t})}{1-\mathrm{e}^{-2\mathrm{i}k_z d}}\,\frac{k_0}{k_z}\,\frac{\mathrm{d}k_x\,\mathrm{d}k_y}{k_0^2} - 2\sum_{j=1,2}\iint_{\mathbb{R}^2} B_{nj}^{+\dagger}(\boldsymbol{k}_\mathrm{t})\frac{B_{n'j}^+(\boldsymbol{k}_\mathrm{t}) + (-1)^j \mathrm{e}^{-2\mathrm{i}k_z z_+} B_{n'j}^-(\boldsymbol{k}_\mathrm{t})}{1-\mathrm{e}^{-2\mathrm{i}k_z d}}\,\frac{k_0}{k_z}\,\frac{\mathrm{d}k_x\,\mathrm{d}k_y}{k_0^2} \quad (6.7)$$

The A matrix is independent of the excitation and the scatterer, and the entries can be computed once and for all and stored for later use, see Appendix B. We also conclude, using (3.15) and symmetry to a change of variables $\boldsymbol{k}_\mathrm{t} \to -\boldsymbol{k}_\mathrm{t}$, that the matrix $A_{nn'}$ is symmetric, *i.e.*, $A_{nn'} = A_{n'n}$.

Above, we assumed the scatterer was a perfectly conducting body. The main reason for this was to simplify the theoretical work. At this point, if any other, more general, scatterer is present, the only change that has to be made, is to replace the transition matrix of the scatterer with the appropriate one. Therefore, the results above hold for any scatterer — single or multiple, homogeneous or not — only the transition matrix is known.

Finally, we get the expansion coefficients of the scattered field as, see (5.4)

$$\begin{cases} f_n = \sum_{n'} T_{nn'} c_{n'} \\ f_j^{\pm}(\boldsymbol{k}_{\mathrm{t}}) = \mp \dfrac{1}{2\mathrm{i}} \alpha_j^{\mp}(\boldsymbol{k}_{\mathrm{t}}) \end{cases} \tag{6.8}$$

7 The primary and secondary fields

Equations (5.3), (6.8), (6.3), and (6.4) then give the scattered field

$$\boldsymbol{E}_{\mathrm{s}}(\boldsymbol{r}) = \boldsymbol{E}_{\mathrm{s}}^{\mathrm{dir}}(\boldsymbol{r}) + \boldsymbol{E}_{\mathrm{s}}^{\mathrm{anom}}(\boldsymbol{r})$$

where

$$\begin{aligned} \boldsymbol{E}_{\mathrm{s}}^{\mathrm{dir}}(\boldsymbol{r}) = &- \sum_{j=1,2} \iint_{\mathbb{R}^2} \frac{a_j^+(\boldsymbol{k}_{\mathrm{t}}) + a_j^-(\boldsymbol{k}_{\mathrm{t}})(-1)^j \mathrm{e}^{-2\mathrm{i}k_z z_+}}{1 - \mathrm{e}^{-2\mathrm{i}k_z d}} \boldsymbol{\varphi}_j^+(\boldsymbol{k}_{\mathrm{t}}; \boldsymbol{r}) \frac{\mathrm{d}k_x \, \mathrm{d}k_y}{k_0^2} \\ &- \sum_{j=1,2} \iint_{\mathbb{R}^2} \frac{a_j^-(\boldsymbol{k}_{\mathrm{t}}) + a_j^+(\boldsymbol{k}_{\mathrm{t}})(-1)^j \mathrm{e}^{2\mathrm{i}k_z z_-}}{1 - \mathrm{e}^{-2\mathrm{i}k_z d}} \boldsymbol{\varphi}_j^-(\boldsymbol{k}_{\mathrm{t}}; \boldsymbol{r}) \frac{\mathrm{d}k_x \, \mathrm{d}k_y}{k_0^2} \end{aligned}$$

and

$$\begin{aligned} \boldsymbol{E}_{\mathrm{s}}^{\mathrm{anom}}(\boldsymbol{r}) = \sum_{nn'} T_{nn'} c_{n'} \Bigg\{ &\boldsymbol{u}_n(k_0 \boldsymbol{r}) \\ &- 2 \sum_{j=1,2} \iint_{\mathbb{R}^2} \frac{B_{nj}^+(\boldsymbol{k}_{\mathrm{t}}) + B_{nj}^-(\boldsymbol{k}_{\mathrm{t}})(-1)^j \mathrm{e}^{-2\mathrm{i}k_z z_+}}{1 - \mathrm{e}^{-2\mathrm{i}k_z d}} \boldsymbol{\varphi}_j^+(\boldsymbol{k}_{\mathrm{t}}; \boldsymbol{r}) \frac{k_0}{k_z} \frac{\mathrm{d}k_x \, \mathrm{d}k_y}{k_0^2} \\ &- 2 \sum_{j=1,2} \iint_{\mathbb{R}^2} \frac{B_{nj}^-(\boldsymbol{k}_{\mathrm{t}}) + B_{nj}^+(\boldsymbol{k}_{\mathrm{t}})(-1)^j \mathrm{e}^{2\mathrm{i}k_z z_-}}{1 - \mathrm{e}^{-2\mathrm{i}k_z d}} \boldsymbol{\varphi}_j^-(\boldsymbol{k}_{\mathrm{t}}; \boldsymbol{r}) \frac{k_0}{k_z} \frac{\mathrm{d}k_x \, \mathrm{d}k_y}{k_0^2} \Bigg\} \end{aligned}$$

The total electric field $\boldsymbol{E}(\boldsymbol{r})$ between the plates can be decomposed in several ways. The incident field is $\boldsymbol{E}_{\mathrm{i}}(\boldsymbol{r})$, and the scattered field consists of two parts, $\boldsymbol{E}_{\mathrm{s}}^{\mathrm{dir}}(\boldsymbol{r})$ and $\boldsymbol{E}_{\mathrm{s}}^{\mathrm{anom}}(\boldsymbol{r})$. As an alternative to this decomposition of the electric field in an incident and a scattered field, we introduce a decomposition in terms of a primary and secondary field, *i.e.*,

$$\boldsymbol{E}(\boldsymbol{r}) = \boldsymbol{E}_{\mathrm{i}}(\boldsymbol{r}) + \boldsymbol{E}_{\mathrm{s}}(\boldsymbol{r}) = \boldsymbol{E}^{\mathrm{prim}}(\boldsymbol{r}) + \boldsymbol{E}^{\mathrm{sec}}(\boldsymbol{r})$$

where

$$\begin{cases} \boldsymbol{E}^{\mathrm{prim}}(\boldsymbol{r}) = \boldsymbol{E}_{\mathrm{i}}(\boldsymbol{r}) + \boldsymbol{E}_{\mathrm{s}}^{\mathrm{dir}}(\boldsymbol{r}) \\ \boldsymbol{E}^{\mathrm{sec}}(\boldsymbol{r}) = \boldsymbol{E}_{\mathrm{s}}^{\mathrm{anom}}(\boldsymbol{r}) \end{cases}$$

The field $\boldsymbol{E}_{\mathrm{i}}(\boldsymbol{r})$ is the total electric field in the absence of both the surfaces S_+ and S_-, and the scatterer S_{s}. The scattered electric field $\boldsymbol{E}_{\mathrm{s}}(\boldsymbol{r})$ is the additional field

due to these surfaces. In the second decomposition, $\boldsymbol{E}^{\mathrm{prim}}(\boldsymbol{r})$ is the total electric field in the absence of the scatterer (surfaces S_+ and S_- present), and $\boldsymbol{E}^{\mathrm{sec}}(\boldsymbol{r})$ is the correction due to the presence of the scatterer. The explicit expression of these fields are

$$\begin{aligned}\boldsymbol{E}^{\mathrm{prim}}(\boldsymbol{r}) = \boldsymbol{E}_{\mathrm{i}}(\boldsymbol{r}) &- \sum_{j=1,2} \iint\limits_{\mathbb{R}^2} \frac{a_j^+(\boldsymbol{k}_{\mathrm{t}}) + a_j^-(\boldsymbol{k}_{\mathrm{t}})(-1)^j \mathrm{e}^{-2\mathrm{i}k_z z_+}}{1-\mathrm{e}^{-2\mathrm{i}k_z d}} \boldsymbol{\varphi}_j^+(\boldsymbol{k}_{\mathrm{t}};\boldsymbol{r})\, \frac{\mathrm{d}k_x\,\mathrm{d}k_y}{k_0^2} \\ &- \sum_{j=1,2} \iint\limits_{\mathbb{R}^2} \frac{a_j^-(\boldsymbol{k}_{\mathrm{t}}) + a_j^+(\boldsymbol{k}_{\mathrm{t}})(-1)^j \mathrm{e}^{2\mathrm{i}k_z z_-}}{1-\mathrm{e}^{-2\mathrm{i}k_z d}} \boldsymbol{\varphi}_j^-(\boldsymbol{k}_{\mathrm{t}};\boldsymbol{r})\, \frac{\mathrm{d}k_x\,\mathrm{d}k_y}{k_0^2}\end{aligned} \tag{7.1}$$

and

$$\begin{aligned}\boldsymbol{E}^{\mathrm{sec}}(\boldsymbol{r}) = \sum_{nn'} T_{nn'} c_{n'} \Bigg\{ &\boldsymbol{u}_n(k_0\boldsymbol{r}) \\ &- 2\sum_{j=1,2} \iint\limits_{\mathbb{R}^2} \frac{B_{nj}^+(\boldsymbol{k}_{\mathrm{t}}) + B_{nj}^-(\boldsymbol{k}_{\mathrm{t}})(-1)^j \mathrm{e}^{-2\mathrm{i}k_z z_+}}{1-\mathrm{e}^{-2\mathrm{i}k_z d}} \boldsymbol{\varphi}_j^+(\boldsymbol{k}_{\mathrm{t}};\boldsymbol{r})\, \frac{k_0}{k_z} \frac{\mathrm{d}k_x\,\mathrm{d}k_y}{k_0^2} \\ &- 2\sum_{j=1,2} \iint\limits_{\mathbb{R}^2} \frac{B_{nj}^-(\boldsymbol{k}_{\mathrm{t}}) + B_{nj}^+(\boldsymbol{k}_{\mathrm{t}})(-1)^j \mathrm{e}^{2\mathrm{i}k_z z_-}}{1-\mathrm{e}^{-2\mathrm{i}k_z d}} \boldsymbol{\varphi}_j^-(\boldsymbol{k}_{\mathrm{t}};\boldsymbol{r})\, \frac{k_0}{k_z} \frac{\mathrm{d}k_x\,\mathrm{d}k_y}{k_0^2} \Bigg\} \\ &= \sum_{nn'} T_{nn'} c_{n'} \boldsymbol{F}_n(\boldsymbol{r})\end{aligned} \tag{7.2}$$

where the $\boldsymbol{F}_n(\boldsymbol{r})$ vector has the generic form

$$\begin{aligned}\boldsymbol{F}_n(\boldsymbol{r}) = &2\sum_{j=1,2} \iint\limits_{\mathbb{R}^2} B_{nj}^{\pm}(\boldsymbol{k}_{\mathrm{t}}) \boldsymbol{\varphi}_j^{\pm}(\boldsymbol{k}_{\mathrm{t}};\boldsymbol{r}) \frac{k_0}{k_z} \frac{\mathrm{d}k_x\,\mathrm{d}k_y}{k_0^2} \\ &- 2\sum_{j=1,2} \iint\limits_{\mathbb{R}^2} \frac{B_{nj}^+(\boldsymbol{k}_{\mathrm{t}}) + B_{nj}^-(\boldsymbol{k}_{\mathrm{t}})(-1)^j \mathrm{e}^{-2\mathrm{i}k_z z_+}}{1-\mathrm{e}^{-2\mathrm{i}k_z d}} \boldsymbol{\varphi}_j^+(\boldsymbol{k}_{\mathrm{t}};\boldsymbol{r})\, \frac{k_0}{k_z} \frac{\mathrm{d}k_x\,\mathrm{d}k_y}{k_0^2} \\ &- 2\sum_{j=1,2} \iint\limits_{\mathbb{R}^2} \frac{B_{nj}^-(\boldsymbol{k}_{\mathrm{t}}) + B_{nj}^+(\boldsymbol{k}_{\mathrm{t}})(-1)^j \mathrm{e}^{2\mathrm{i}k_z z_-}}{1-\mathrm{e}^{-2\mathrm{i}k_z d}} \boldsymbol{\varphi}_j^-(\boldsymbol{k}_{\mathrm{t}};\boldsymbol{r})\, \frac{k_0}{k_z} \frac{\mathrm{d}k_x\,\mathrm{d}k_y}{k_0^2}\end{aligned} \tag{7.3}$$

where the sign $\pm$ in the first $B_{nj}^{\pm}(\boldsymbol{k}_{\mathrm{t}})$ factor depends on whether $z \gtrless 0$, see (3.9).

As a check of the boundary condition, let $z = z_{\pm}$. We then have ($\boldsymbol{r}_{\pm} = \boldsymbol{\rho} + z_{\pm}\hat{\boldsymbol{z}}$)

$$\begin{aligned}\boldsymbol{E}^{\mathrm{prim}}(\boldsymbol{r}_{\pm})\big|_{\tan} = &\sum_{j=1,2} \iint\limits_{\mathbb{R}^2} a_j^{\pm}(\boldsymbol{k}_{\mathrm{t}})\, \boldsymbol{\varphi}_j^{\pm}(\boldsymbol{k}_{\mathrm{t}};\boldsymbol{r}_{\pm})\big|_{\tan}\, \frac{\mathrm{d}k_x\,\mathrm{d}k_y}{k_0^2} \\ &- \sum_{j=1,2} \iint\limits_{\mathbb{R}^2} \frac{a_j^+(\boldsymbol{k}_{\mathrm{t}}) + a_j^-(\boldsymbol{k}_{\mathrm{t}})(-1)^j \mathrm{e}^{-2\mathrm{i}k_z z_+}}{1-\mathrm{e}^{-2\mathrm{i}k_z d}}\, \boldsymbol{\varphi}_j^+(\boldsymbol{k}_{\mathrm{t}};\boldsymbol{r}_{\pm})\big|_{\tan}\, \frac{\mathrm{d}k_x\,\mathrm{d}k_y}{k_0^2} \\ &- \sum_{j=1,2} \iint\limits_{\mathbb{R}^2} \frac{a_j^-(\boldsymbol{k}_{\mathrm{t}}) + a_j^+(\boldsymbol{k}_{\mathrm{t}})(-1)^j \mathrm{e}^{2\mathrm{i}k_z z_-}}{1-\mathrm{e}^{-2\mathrm{i}k_z d}}\, \boldsymbol{\varphi}_j^-(\boldsymbol{k}_{\mathrm{t}};\boldsymbol{r}_{\pm})\big|_{\tan}\, \frac{\mathrm{d}k_x\,\mathrm{d}k_y}{k_0^2} = \boldsymbol{0}\end{aligned}$$

since

$$\boldsymbol{\varphi}_j^-(\boldsymbol{k}_\mathrm{t};\boldsymbol{r}_\pm)\big|_\mathrm{tan} = -(-1)^j\ \boldsymbol{\varphi}_j^+(\boldsymbol{k}_\mathrm{t};\boldsymbol{r}_\pm)\big|_\mathrm{tan}\,\mathrm{e}^{-2\mathrm{i}k_z z_\pm}$$

In a similar fashion, for the secondary field we get, see (3.9)

$$\begin{aligned}\boldsymbol{F}_n(\boldsymbol{r}_\pm)\big|_\mathrm{tan} &= 2\sum_{j=1,2}\iint\limits_{\mathbb{R}^2} B_{nj}^\pm(\boldsymbol{k}_\mathrm{t})\ \boldsymbol{\varphi}_j^\pm(\boldsymbol{k}_\mathrm{t};\boldsymbol{r}_\pm)\big|_\mathrm{tan}\,\frac{k_0}{k_z}\frac{\mathrm{d}k_x\,\mathrm{d}k_y}{k_0^2}\\ &- 2\sum_{j=1,2}\iint\limits_{\mathbb{R}^2}\frac{B_{nj}^+(\boldsymbol{k}_\mathrm{t})+B_{nj}^-(\boldsymbol{k}_\mathrm{t})(-1)^j\mathrm{e}^{-2\mathrm{i}k_z z_+}}{1-\mathrm{e}^{-2\mathrm{i}k_z d}}\ \boldsymbol{\varphi}_j^+(\boldsymbol{k}_\mathrm{t};\boldsymbol{r}_\pm)\big|_\mathrm{tan}\,\frac{k_0}{k_z}\frac{\mathrm{d}k_x\,\mathrm{d}k_y}{k_0^2}\\ &- 2\sum_{j=1,2}\iint\limits_{\mathbb{R}^2}\frac{B_{nj}^-(\boldsymbol{k}_\mathrm{t})+B_{nj}^+(\boldsymbol{k}_\mathrm{t})(-1)^j\mathrm{e}^{2\mathrm{i}k_z z_-}}{1-\mathrm{e}^{-2\mathrm{i}k_z d}}\ \boldsymbol{\varphi}_j^-(\boldsymbol{k}_\mathrm{t};\boldsymbol{r}_\pm)\big|_\mathrm{tan}\,\frac{k_0}{k_z}\frac{\mathrm{d}k_x\,\mathrm{d}k_y}{k_0^2} = \boldsymbol{0}\end{aligned}$$

This formally solves the scattering problem for a given incident field. The computational flow is:

1. For a given incident field, determine the expansion coefficients a_n and $a_j^\pm$, see (4.1) and (4.2)
2. Compute the d_n vector in (6.6) and the $A_{nn'}$ matrix in (6.7)
3. Determine the T-matrix of the scatterer, and solve the matrix equation (6.5) for c_n
4. Compute the $\boldsymbol{F}_n(\boldsymbol{r})$ vector for the points $\boldsymbol{r}$ of interest, see (7.3), and compute the secondary field $\boldsymbol{E}^\mathrm{sec}(\boldsymbol{r})$ in (7.2)

8 Evaluation of the fields

The fields in (7.1) and (7.2) are given as integral expressions of the transverse wave number $\boldsymbol{k}_\mathrm{t}$. Our aim here is to evaluate these integrals in terms of pole contributions (residue calculus).

The integrands have simple poles at

$$k_{\mathrm{t}p} = \pm\left(k_0^2 - \frac{p^2\pi^2}{d^2}\right)^{1/2}, \quad p = 0, 1, 2, \ldots \tag{8.1}$$

In particular, $k_{\mathrm{t}0} = \pm k_0$. At these poles, k_z is

$$k_z = \frac{p\pi}{d} \quad \Leftrightarrow \quad \mathrm{e}^{-2\mathrm{i}k_z d} = 1$$

These poles are identified as the parallel plate waveguide modes [11, 27], see Figure 3, which shows the locations of the poles.

8.1 Absence of branch point at $k_\mathrm{t} = \pm k_0$

Most integrands also seem to have a branch point at $k_\mathrm{t} = \pm k_0$ corresponding to $k_z = 0$. These branch points are, however, artificial, since for fixed value of $\boldsymbol{k}_\mathrm{t}$, the

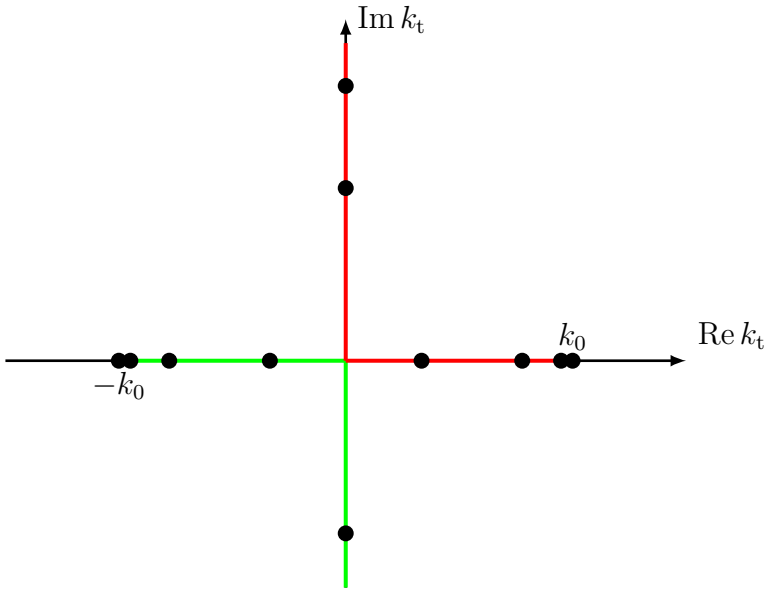

Figure 3: The locations of the poles $k_{\mathrm{t}p}$. The first poles are $k_{\mathrm{t}0} = \pm k_0$. The red and green contours depict the curves where $\operatorname{Im} k_z = 0$. The poles on the real axis are the propagating waveguide modes, and the ones on the imaginary axis are the modes under cutoff. In this particular case, the number of propagating modes are four.

integrands are even in $k_z \leftrightarrow -k_z$. In fact, if $\tilde{a}^\pm$ denotes $a_j^\pm$ with $k_z \leftrightarrow -k_z$, we have from above that $\tilde{a}^\pm = -a_j^\mp$, and from the definition of the planar vector waves in Section 3.2 we conclude that $\boldsymbol{\varphi}_j^\pm(\boldsymbol{k}_\mathrm{t}; \boldsymbol{r}) \leftrightarrow \boldsymbol{\varphi}_j^\mp(\boldsymbol{k}_\mathrm{t}; \boldsymbol{r})$ when $k_z \leftrightarrow -k_z$.

The integrand of $\boldsymbol{E}^{\mathrm{prim}}$ in (7.1) is even in $k_z \leftrightarrow -k_z$, since

$$
\begin{aligned}
&\left\{ a_j^\pm \boldsymbol{\varphi}_j^\pm - \frac{a_j^+ + a_j^-(-1)^j \mathrm{e}^{-2\mathrm{i}k_z z_+}}{1 - \mathrm{e}^{-2\mathrm{i}k_z d}} \boldsymbol{\varphi}_j^+ - \frac{a_j^- + a_j^+(-1)^j \mathrm{e}^{2\mathrm{i}k_z z_-}}{1 - \mathrm{e}^{-2\mathrm{i}k_z d}} \boldsymbol{\varphi}_j^- \right\} \\
&\quad - \left\{ -a_j^\mp \boldsymbol{\varphi}_j^\mp + \frac{a_j^- + a_j^+(-1)^j \mathrm{e}^{2\mathrm{i}k_z z_+}}{1 - \mathrm{e}^{2\mathrm{i}k_z d}} \boldsymbol{\varphi}_j^- + \frac{a_j^+ + a_j^-(-1)^j \mathrm{e}^{-2\mathrm{i}k_z z_-}}{1 - \mathrm{e}^{2\mathrm{i}k_z d}} \boldsymbol{\varphi}_j^+ \right\} \\
&\quad = a_j^+ \boldsymbol{\varphi}_j^+ - \frac{a_j^+ + a_j^-(-1)^j \mathrm{e}^{-2\mathrm{i}k_z z_+} - a_j^-(-1)^j \mathrm{e}^{-2\mathrm{i}k_z z_+} - a_j^+ \mathrm{e}^{-2\mathrm{i}k_z d}}{1 - \mathrm{e}^{-2\mathrm{i}k_z d}} \boldsymbol{\varphi}_j^+ \\
&\qquad + a_j^- \boldsymbol{\varphi}_j^- - \frac{a_j^+(-1)^j \mathrm{e}^{2\mathrm{i}k_z z_-} + a_j^- - a_j^- \mathrm{e}^{-2\mathrm{i}k_z d} - a_j^+(-1)^j \mathrm{e}^{2\mathrm{i}k_z z_-}}{1 - \mathrm{e}^{-2\mathrm{i}k_z d}} \boldsymbol{\varphi}_j^- = \boldsymbol{0}
\end{aligned}
$$

where the second bracket on the left-hand side is the transformed quantity of the first bracket.

Similarly, we also have for $\boldsymbol{E}^{\mathrm{sec}}$ or the $\boldsymbol{F}_n(\boldsymbol{r})$ in (7.3), using $B_{nj}^\pm(\boldsymbol{k}_\mathrm{t}) \leftrightarrow B_{nj}^\mp(\boldsymbol{k}_\mathrm{t})$

when $k_z \leftrightarrow -k_z$

$$\left\{ B_{nj}^{\pm}\boldsymbol{\varphi}_j^{\pm} - \frac{B_{nj}^{+} + B_{nj}^{-}(-1)^j \mathrm{e}^{-2\mathrm{i}k_z z_+}}{1-\mathrm{e}^{-2\mathrm{i}k_z d}}\boldsymbol{\varphi}_j^{+} - \frac{B_{nj}^{-} + B_{nj}^{+}(-1)^j \mathrm{e}^{2\mathrm{i}k_z z_-}}{1-\mathrm{e}^{-2\mathrm{i}k_z d}}\boldsymbol{\varphi}_j^{-} \right\}$$
$$+ \left\{ B_{nj}^{\mp}\boldsymbol{\varphi}_j^{\mp} - \frac{B_{nj}^{-} + B_{nj}^{+}(-1)^j \mathrm{e}^{2\mathrm{i}k_z z_+}}{1-\mathrm{e}^{2\mathrm{i}k_z d}}\boldsymbol{\varphi}_j^{-} - \frac{B_{nj}^{+} + B_{nj}^{-}(-1)^j \mathrm{e}^{-2\mathrm{i}k_z z_-}}{1-\mathrm{e}^{2\mathrm{i}k_z d}}\boldsymbol{\varphi}_j^{+} \right\}$$
$$= B_{nj}^{+}\boldsymbol{\varphi}_j^{+} - \frac{B_{nj}^{+} + B_{nj}^{-}(-1)^j \mathrm{e}^{-2\mathrm{i}k_z z_+} - B_{nj}^{+}\mathrm{e}^{-2\mathrm{i}k_z d} - B_{nj}^{-}(-1)^j \mathrm{e}^{-2\mathrm{i}k_z z_+}}{1-\mathrm{e}^{-2\mathrm{i}k_z d}}\boldsymbol{\varphi}_j^{+}$$
$$+ B_{nj}^{-}\boldsymbol{\varphi}_j^{-} - \frac{B_{nj}^{-} + B_{nj}^{+}(-1)^j \mathrm{e}^{2\mathrm{i}k_z z_-} - B_{nj}^{-}\mathrm{e}^{-2\mathrm{i}k_z d} - B_{nj}^{+}(-1)^j \mathrm{e}^{2\mathrm{i}k_z z_-}}{1-\mathrm{e}^{-2\mathrm{i}k_z d}}\boldsymbol{\varphi}_j^{-} = \mathbf{0}$$

We therefore conclude that the only singularities in these integrals are simple poles.

8.2 Interaction terms

The interaction between the scatterer and the parallel plates is quantified by the d_n vector in (6.6) and the $A_{nn'}$ matrix in (6.7), which both have an integrand that have the same simple poles as the integrand of the scattered field. Moreover, to investigate whether $k_\mathrm{t} = k_0$ is a branch point of the integrand of the d_n vector or not, we evaluate

$$\left\{ -a_j^{+}\frac{(-1)^j \mathrm{e}^{2\mathrm{i}k_z z_-} B_{nj}^{-\dagger} + B_{nj}^{+\dagger}}{1-\mathrm{e}^{-2\mathrm{i}k_z d}} - a_j^{-}\frac{(-1)^j \mathrm{e}^{-2\mathrm{i}k_z z_+} B_{nj}^{+\dagger} + B_{nj}^{-\dagger}}{1-\mathrm{e}^{-2\mathrm{i}k_z d}} + a_j^{\pm} B_{nj}^{\pm\dagger} \right\}$$
$$- \left\{ a_j^{-}\frac{(-1)^j \mathrm{e}^{-2\mathrm{i}k_z z_-} B_{nj}^{+\dagger} + B_{nj}^{-\dagger}}{1-\mathrm{e}^{2\mathrm{i}k_z d}} + a_j^{+}\frac{(-1)^j \mathrm{e}^{2\mathrm{i}k_z z_+} B_{nj}^{-\dagger} + B_{nj}^{+\dagger}}{1-\mathrm{e}^{2\mathrm{i}k_z d}} - a_j^{\mp} B_{nj}^{\mp\dagger} \right\} = 0$$

The choice of the plus or minus sign in this expression depends on whether $\hat{\boldsymbol{z}}\cdot\boldsymbol{r}_0 \gtrless 0$. This shows that the integrand of the d_n vector is even as $k_z \to -k_z$. The explicit evaluation of the d_n vector depends on the explicit form of the incident field. We postpone these calculations to Section 11.

Similarly, for the $A_{nn'}$ matrix

$$\left\{ -B_{nj}^{-\dagger}\frac{(-1)^j \mathrm{e}^{2\mathrm{i}k_z z_-} B_{n'j}^{+} + B_{n'j}^{-}}{1-\mathrm{e}^{-2\mathrm{i}k_z d}} - B_{nj}^{+\dagger}\frac{B_{n'j}^{+} + (-1)^j \mathrm{e}^{-2\mathrm{i}k_z z_+} B_{n'j}^{-}}{1-\mathrm{e}^{-2\mathrm{i}k_z d}} \right\}$$
$$+ \left\{ -B_{nj}^{+\dagger}\frac{(-1)^j \mathrm{e}^{-2\mathrm{i}k_z z_-} B_{n'j}^{-} + B_{n'j}^{+}}{1-\mathrm{e}^{2\mathrm{i}k_z d}} - B_{nj}^{-\dagger}\frac{B_{n'j}^{-} + (-1)^j \mathrm{e}^{2\mathrm{i}k_z z_+} B_{n'j}^{+}}{1-\mathrm{e}^{2\mathrm{i}k_z d}} \right\}$$
$$= -B_{nj}^{-\dagger} B_{n'j}^{-} - B_{nj}^{+\dagger} B_{n'j}^{+}$$

This shows that the $A_{nn'}$ matrix does not show any even symmetry as $k_z \to -k_z$. The explicit evaluation of these integrals in $A_{nn'}$, which are independent of the excitation, is found in Appendix B.

8.3 The primary field

The primary field depends on the explicit form of the incident field, *i.e.*, it depends on $a_j^{\pm}(\boldsymbol{k}_{\rm t})$ and a_n. We postpone the treatment of this field to the examples in Section 11.

8.4 The secondary field

The secondary field assumes the value $\boldsymbol{E}^{\rm sec}(\boldsymbol{r}) = \sum_{nn'} T_{nn'} c_{n'} \boldsymbol{F}_n(\boldsymbol{r})$. We evaluate the $\boldsymbol{F}_n(\boldsymbol{r})$ in terms of residue contributions in the upper half $k_{\rm t}$-plane. This is analyzed in detail in Appendix C. In terms of the circular cylindrical coordinate system, the components are, see (C.7), (C.8), and (C.9) in Appendix C

$$\boldsymbol{F}_n(\boldsymbol{r}) = \hat{\boldsymbol{\rho}} F_{n\rho}(\boldsymbol{r}) + \hat{\boldsymbol{\phi}} F_{n\phi}(\boldsymbol{r}) + \hat{\boldsymbol{z}} F_{nz}(\boldsymbol{r})$$

where

$$\begin{aligned}
\hat{\boldsymbol{\rho}} \cdot \boldsymbol{F}_n(\boldsymbol{r}) &= -\frac{1}{k_0} \hat{\boldsymbol{\phi}} \cdot \nabla G_n(\boldsymbol{r}) - \frac{1}{k_0^2} \hat{\boldsymbol{\rho}} \cdot \nabla \frac{\partial}{\partial z} H_{\overline{n}} \\
&= \frac{{\rm i}\pi}{2k_0 d} \sum_{p=1}^{\infty} \varepsilon_p \Bigg\{ \frac{\partial g_n^+(k_{{\rm t}p}, \phi)}{\partial \phi} {\rm e}^{{\rm i}\pi p z_-/d} \sin(\pi p (z - z_-)/d) \frac{H_m^{(1)}(k_{{\rm t}p}\rho)}{k_{{\rm t}p}\rho} \\
&\quad - \frac{\partial g_n^-(k_{{\rm t}p}, \phi)}{\partial \phi} {\rm e}^{-{\rm i}\pi p z_+/d} \sin(\pi p (z - z_+)/d) \frac{H_m^{(1)}(k_{{\rm t}p}\rho)}{k_{{\rm t}p}\rho} \\
&\quad + {\rm i} \frac{p\pi}{k_0 d} g_{\overline{n}}^+(k_{{\rm t}p}, \phi) {\rm e}^{{\rm i}\pi p z_-/d} \sin(\pi p (z - z_-)/d) H_m^{(1)\prime}(k_{{\rm t}p}\rho) \\
&\quad + {\rm i} \frac{p\pi}{k_0 d} g_{\overline{n}}^-(k_{{\rm t}p}, \phi) {\rm e}^{-{\rm i}\pi p z_+/d} \sin(\pi p (z - z_+)/d) H_m^{(1)\prime}(k_{{\rm t}p}\rho) \Bigg\}
\end{aligned}$$

and

$$\begin{aligned}
\hat{\boldsymbol{\phi}} \cdot \boldsymbol{F}_n(\boldsymbol{r}) &= \frac{1}{k_0} \hat{\boldsymbol{\rho}} \cdot \nabla G_n(\boldsymbol{r}) - \frac{1}{k_0^2} \hat{\boldsymbol{\phi}} \cdot \nabla \frac{\partial}{\partial z} H_{\overline{n}} \\
&= \frac{{\rm i}\pi}{2k_0 d} \sum_{p=1}^{\infty} \varepsilon_p \Bigg\{ -g_n^+(k_{{\rm t}p}, \phi) {\rm e}^{{\rm i}\pi p z_-/d} \sin(\pi p (z - z_-)/d) H_m^{(1)\prime}(k_{{\rm t}p}\rho) \\
&\quad + g_n^-(k_{{\rm t}p}, \phi) {\rm e}^{-{\rm i}\pi p z_+/d} \sin(\pi p (z - z_+)/d) H_m^{(1)\prime}(k_{{\rm t}p}\rho) \\
&\quad + {\rm i} \frac{p\pi}{k_0 d} \frac{\partial g_{\overline{n}}^+(k_{{\rm t}p}, \phi)}{\partial \phi} {\rm e}^{{\rm i}\pi p z_-/d} \sin(\pi p (z - z_-)/d) \frac{H_m^{(1)}(k_{{\rm t}p}\rho)}{k_{{\rm t}p}\rho} \\
&\quad + {\rm i} \frac{p\pi}{k_0 d} \frac{\partial g_{\overline{n}}^-(k_{{\rm t}p}, \phi)}{\partial \phi} {\rm e}^{-{\rm i}\pi p z_+/d} \sin(\pi p (z - z_+)/d) \frac{H_m^{(1)}(k_{{\rm t}p}\rho)}{k_{{\rm t}p}\rho} \Bigg\}
\end{aligned}$$

and

$$\hat{\boldsymbol{z}} \cdot \boldsymbol{F}_n(\boldsymbol{r}) = \frac{\pi}{2k_0 d} \sum_{p=0}^{\infty} \varepsilon_p \frac{k_{\mathrm{t}p}}{k_0} \Bigg\{ g_{\overline{n}}^{+}(k_{\mathrm{t}p}, \phi) \mathrm{e}^{\mathrm{i}\pi p z_-/d} \cos(\pi p (z - z_-)/d) + g_{\overline{n}}^{-}(k_{\mathrm{t}p}, \phi) \mathrm{e}^{-\mathrm{i}\pi p z_+/d} \cos(\pi p (z - z_+)/d) \Bigg\} H_m^{(1)}(k_{\mathrm{t}p}\rho)$$

where the functions $g_n^{\pm}(k_{\mathrm{t}}, \phi)$ are, see (C.2)

$$g_n^{\pm}(k_{\mathrm{t}}, \phi) = \mathrm{i}^{-l+m} (\pm 1)^{l+m} C_{lm} \times \left(\mp \mathrm{i}\delta_{\tau 1} \Delta_l^m(k_z/k_0) \begin{Bmatrix} \cos m\phi \\ \sin m\phi \end{Bmatrix} - \delta_{\tau 2} \pi_l^m(k_z/k_0) \begin{Bmatrix} -\sin m\phi \\ \cos m\phi \end{Bmatrix} \right)$$

and the transverse wave number $k_{\mathrm{t}p}$ is defined in (8.1). Only a finite number of terms, identified as propagating modes [11, 27], contribute to the sum at large distances from the scatterer, *i.e.*, only those integers p satisfying $p \leq k_0 d/\pi$, since the Hankel functions are exponentially decreasing for purely imaginary arguments. The explicit evaluation of these integrals for frequencies below first cutoff frequency, *i.e.*, $k_0 d < \pi$, is made in Appendix E.1.

9 Scattered power and scattering cross section

The power transport of the scattered field is determined by the Poynting vector. The expression relevant for the power transport, using (C.15), is

$$\begin{aligned} P_{\mathrm{s}} &= \frac{1}{2} \operatorname{Re} \iint_{\rho=\text{constant}} (\boldsymbol{E}^{\mathrm{sec}} \times \boldsymbol{H}^{\mathrm{sec}*}) \cdot \hat{\boldsymbol{\rho}} \, \mathrm{d}S = \frac{1}{2k_0\eta_0} \operatorname{Re} \mathrm{i} \iint_{\rho=\text{constant}} (\boldsymbol{E}^{\mathrm{sec}} \times (\nabla \times \boldsymbol{E}^{\mathrm{sec}*})) \cdot \hat{\boldsymbol{\rho}} \, \mathrm{d}S \\ &= -\frac{1}{2k_0\eta_0} \operatorname{Im} \sum_{nn'n''n'''} T_{nn'} c_{n'} T^*_{n''n'''} c^*_{n'''} \iint_{\rho=\text{constant}} (\boldsymbol{F}_n \times (\nabla \times \boldsymbol{F}^*_{n''})) \cdot \hat{\boldsymbol{\rho}} \, \mathrm{d}S \\ &= \frac{1}{2\eta_0} \frac{d^2\pi}{(k_0 d)^3} \sum_{nn'n''n'''} T_{nn'} c_{n'} \left\{ 2I^{++}_{\overline{n}n'''}(k_0) + \sum_{p=1}^{[k_0 d/\pi]} I_{nn''}(k_{\mathrm{t}p}) \right\} T^*_{n''n'''} c^*_{n'''} \end{aligned}$$

For an incident plane wave, see Section 11.2, the scattering cross section becomes

$$\begin{aligned} \sigma_{\mathrm{s}} &= \frac{2\eta_0 P_{\mathrm{s}}}{|E_0|^2} \\ &= \frac{d^2\pi}{2(k_0 d)^3 |E_0|^2} \sum_{nn'n''n'''} T_{nn'} c_{n'} \left\{ 4I^{++}_{\overline{n}n'''}(k_0) + 2 \sum_{p=1}^{[k_0 d/\pi]} I_{nn''}(k_{\mathrm{t}p}) \right\} T^*_{n''n'''} c^*_{n'''} \end{aligned}$$

Note that the dimension of the scattering cross section is area, which, once again, shows that the problem is a three-dimensional problem, but shows many two-dimensional features.

10 Far field amplitude and the optical theorem

Let S be an arbitrary (cylindrical) surface between the plates that encloses the obstacle V_s. Provided the sources of the incident field, V_i, see Figure 2, lie outside the surface S, *e.g.*, plane wave incidence, we have from the Maxwell equations

$$\frac{1}{2}\,\mathrm{Re}\iint_S (\boldsymbol{E}\times\boldsymbol{H}^*)\cdot\hat{\boldsymbol{\nu}}\,\mathrm{d}S = \frac{1}{2}\,\mathrm{Re}\iint_{S_\mathrm{s}} (\boldsymbol{E}\times\boldsymbol{H}^*)\cdot\hat{\boldsymbol{\nu}}\,\mathrm{d}S = -P_\mathrm{a}$$

The right hand side is minus the power absorbed by the scatterer, P_a. For a PEC body this quantity is zero. The expression simply expresses power conservation in the scattering process. Separate in primary and secondary fields, and we get

$$2P_\mathrm{a} = -\,\mathrm{Re}\iint_S \left(\boldsymbol{E}^\mathrm{sec}\times\boldsymbol{H}^{\mathrm{sec}*} + \boldsymbol{E}^\mathrm{prim}\times\boldsymbol{H}^{\mathrm{sec}*} + \boldsymbol{E}^{\mathrm{sec}*}\times\boldsymbol{H}^\mathrm{prim}\right)\cdot\hat{\boldsymbol{\nu}}\,\mathrm{d}S$$

since with V_i outside S

$$\mathrm{Re}\iint_S \left(\boldsymbol{E}^\mathrm{prim}\times\boldsymbol{H}^{\mathrm{prim}*}\right)\cdot\hat{\boldsymbol{\nu}}\,\mathrm{d}S = 0$$

where the incident field is, see (11.4)

$$\boldsymbol{E}^\mathrm{prim}(\boldsymbol{r}) = \hat{\boldsymbol{z}}E_0\mathrm{e}^{\mathrm{i}k_0\hat{\boldsymbol{k}}_\mathrm{i}\cdot\boldsymbol{r}}$$

The value of integral on the right hand side is independent on the surface S as long as it encloses V_s, but not the sources of the incident field. Eventually, we evaluate the integral for a surface far away from the scatterer. Rewrite as

$$\begin{aligned}
2P_\mathrm{a} + 2P_\mathrm{s} &= -\,\mathrm{Re}\,E_0\iint_S \left(\hat{\boldsymbol{z}}\times\boldsymbol{H}^{\mathrm{sec}*} + \frac{1}{\eta_0}\boldsymbol{E}^{\mathrm{sec}*}\times(\hat{\boldsymbol{k}}_\mathrm{i}\times\hat{\boldsymbol{z}})\right)\cdot\hat{\boldsymbol{\nu}}\,\mathrm{e}^{\mathrm{i}k_0\hat{\boldsymbol{k}}_\mathrm{i}\cdot\boldsymbol{r}}\,\mathrm{d}S \\
&= -\,\mathrm{Re}\,E_0^*\iint_S \left(\hat{\boldsymbol{z}}\times\boldsymbol{H}^{\mathrm{sec}} + \frac{1}{\eta_0}\boldsymbol{E}^{\mathrm{sec}}\times(\hat{\boldsymbol{k}}_\mathrm{i}\times\hat{\boldsymbol{z}})\right)\cdot\hat{\boldsymbol{\nu}}\,\mathrm{e}^{-\mathrm{i}k_0\hat{\boldsymbol{k}}_\mathrm{i}\cdot\boldsymbol{r}}\,\mathrm{d}S
\end{aligned}$$

where we specified to a special incident field (plane wave incidence), where $\hat{\boldsymbol{k}}_\mathrm{i}\cdot\hat{\boldsymbol{z}} = 0$, see (11.4), and introduced the scattered power

$$P_\mathrm{s} = \frac{1}{2}\,\mathrm{Re}\iint_S (\boldsymbol{E}^\mathrm{sec}\times\boldsymbol{H}^{\mathrm{sec}*})\cdot\hat{\boldsymbol{\nu}}\,\mathrm{d}S$$

Insert (7.2), and we get

$$\begin{aligned}
2P_\mathrm{a} + 2P_\mathrm{s} = -\frac{1}{\eta_0}\,\mathrm{Re}\,E_0^*\sum_{nn'} T_{nn'}c_{n'} \\
\times\iint_S \left(\frac{1}{\mathrm{i}k_0}\hat{\boldsymbol{z}}\times(\nabla\times\boldsymbol{F}_n(\boldsymbol{r})) + \boldsymbol{F}_n(\boldsymbol{r})\times(\hat{\boldsymbol{k}}_\mathrm{i}\times\hat{\boldsymbol{z}})\right)\cdot\hat{\boldsymbol{\nu}}\,\mathrm{e}^{-\mathrm{i}k_0\hat{\boldsymbol{k}}_\mathrm{i}\cdot\boldsymbol{r}}\,\mathrm{d}S
\end{aligned}$$

Specialize to a cylindrical surface, $\rho = \text{constant}$, $\hat{\boldsymbol{\nu}} = \hat{\boldsymbol{\rho}}$.

$$
\begin{aligned}
&2P_{\mathrm{a}} + 2P_{\mathrm{s}} = -\frac{1}{\eta_0} \operatorname{Re} E_0^* \sum_{nn'} T_{nn'} c_{n'} \\
&\times \iint\limits_{\rho=\text{constant}} \left(\frac{1}{\mathrm{i}k_0} \left(\frac{\partial}{\partial \rho} \left(\hat{\boldsymbol{z}} \cdot \boldsymbol{F}_n(\boldsymbol{r}) \right) - \frac{\partial}{\partial z} \left(\hat{\boldsymbol{\rho}} \cdot \boldsymbol{F}_n(\boldsymbol{r}) \right) \right) + (\boldsymbol{F}_n(\boldsymbol{r}) \cdot \hat{\boldsymbol{z}})(\hat{\boldsymbol{k}}_{\mathrm{i}} \cdot \hat{\boldsymbol{\rho}}) \right) \mathrm{e}^{-\mathrm{i}k_0 \hat{\boldsymbol{k}}_{\mathrm{i}} \cdot \boldsymbol{r}} \, \mathrm{d}S \\
&= -\frac{1}{\eta_0} \operatorname{Re} E_0^* \sum_{nn'} T_{nn'} c_{n'} \iint\limits_{\rho=\text{constant}} \left(\frac{1}{\mathrm{i}k_0} \frac{\partial}{\partial \rho} \left(\hat{\boldsymbol{z}} \cdot \boldsymbol{F}_n(\boldsymbol{r}) \right) + (\boldsymbol{F}_n(\boldsymbol{r}) \cdot \hat{\boldsymbol{z}})(\hat{\boldsymbol{k}}_{\mathrm{i}} \cdot \hat{\boldsymbol{\rho}}) \right) \mathrm{e}^{-\mathrm{i}k_0 \hat{\boldsymbol{k}}_{\mathrm{i}} \cdot \boldsymbol{r}} \, \mathrm{d}S
\end{aligned}
$$

since the term containing the z derivative vanishes when integrating in the z variable. The component $\hat{\boldsymbol{z}} \cdot \boldsymbol{F}_n(\boldsymbol{r})$ is explicitly given in Section 8.4 and in Appendix C.

$$
\begin{aligned}
\hat{\boldsymbol{z}} \cdot \boldsymbol{F}_n(\boldsymbol{r}) = \frac{\pi}{2k_0 d} \sum_{p=0}^{\infty} \varepsilon_p \frac{k_{\mathrm{t}p}}{k_0} \Bigg\{ & g_{\overline{n}}^{+}(k_{\mathrm{t}p}, \phi) \mathrm{e}^{\mathrm{i}\pi p z_-/d} \cos(\pi p (z - z_-)/d) \\
& + g_{\overline{n}}^{-}(k_{\mathrm{t}p}, \phi) \mathrm{e}^{-\mathrm{i}\pi p z_+/d} \cos(\pi p (z - z_+)/d) \Bigg\} H_m^{(1)}(k_{\mathrm{t}p} \rho)
\end{aligned}
$$

Again, we conclude that the integration in the z variable gives zero contribution except for the fundamental mode $p = 0$, *i.e.*,

$$
\begin{aligned}
P_{\mathrm{a}} + P_{\mathrm{s}} = -\frac{\pi \rho}{2k_0 \eta_0} \operatorname{Re} E_0^* \sum_{nn'} T_{nn'} c_{n'} \\
\times \int_0^{2\pi} \left(-\mathrm{i} H_m^{(1)\prime}(k_0 \rho) + H_m^{(1)}(k_0 \rho)(\hat{\boldsymbol{k}}_{\mathrm{i}} \cdot \hat{\boldsymbol{\rho}}) \right) g_{\overline{n}}^{+}(k_0, \phi) \, \mathrm{e}^{-\mathrm{i}k_0 \hat{\boldsymbol{k}}_{\mathrm{i}} \cdot \boldsymbol{r}} \, \mathrm{d}\phi
\end{aligned}
$$

since $g_n^+(k_0, \phi) = g_n^-(k_0, \phi)$, see (E.1). Explicitly, we have

$$
\begin{aligned}
g_n^{\pm}(k_0, \phi) = -\mathrm{i}^{-l+m} C_{lm} \\
\times \left(\mathrm{i}\delta_{\tau 1} \Delta_l^m(0) \begin{Bmatrix} \cos m\phi \\ \sin m\phi \end{Bmatrix} + \delta_{\tau 2} \pi_l^m(0) \begin{Bmatrix} -\sin m\phi \\ \cos m\phi \end{Bmatrix} \right)
\end{aligned}
$$

The Hankel function has an asymptotic behavior for large arguments [1], *viz.*,

$$
H_m^{(1)}(z) = \left(\frac{2}{\pi z} \right)^{1/2} \mathrm{e}^{\mathrm{i}\left(z - \frac{m\pi}{2} - \frac{\pi}{4} \right)} \left(1 + O(1/z) \right)
$$

This leads to the asymptotic evaluation of the following integral ($\cos\phi = \hat{\boldsymbol{k}}_{\mathrm{i}} \cdot \hat{\boldsymbol{\rho}}$): In the limit as $\rho \to \infty$, we have

$$
\begin{aligned}
\lim_{\rho \to \infty} k_0 \rho \left(\frac{2}{\pi k_0 \rho} \right)^{1/2} \mathrm{e}^{-\mathrm{i}\left(\frac{m\pi}{2} + \frac{\pi}{4} \right)} \int_0^{2\pi} g(\phi) \left(1 + \cos\phi \right) \mathrm{e}^{\mathrm{i}k_0 \rho (1 - \cos\phi)} \, \mathrm{d}\phi \\
= k_0 \left(\frac{2}{\pi k_0} \right)^{1/2} \mathrm{e}^{-\mathrm{i}\left(\frac{m\pi}{2} + \frac{\pi}{4} \right)} 2g(0) \left(\frac{2\pi \mathrm{i}}{k_0} \right)^{1/2} = 4g(0) \mathrm{i}^{-m}
\end{aligned}
$$

The extinction power becomes

$$P_{\mathrm{a}} + P_{\mathrm{s}} = -\frac{1}{2\eta_0}\frac{4\pi}{k_0^2}\operatorname{Re} E_0^* \sum_{nn'} \mathrm{i}^{-m} T_{nn'} c_{n'} g_{\bar{n}}^{\pm}(k_0, 0)$$

We can identify the optical theorem, by noting that, to leading order in $1/(k_0\rho)$, the secondary field, integrated in the z direction between the plates, is, see (7.2) and (C.9)

$$\begin{aligned}\int_{z_-}^{z_+} \hat{\boldsymbol{z}} \cdot \boldsymbol{E}^{\mathrm{sec}}(\rho\hat{\boldsymbol{k}}_{\mathrm{i}} + z\hat{\boldsymbol{z}})\, \mathrm{d}z &= \sum_{nn'} T_{nn'} c_{n'} \int_{z_-}^{z_+} \hat{\boldsymbol{z}} \cdot \boldsymbol{F}_n(\rho\hat{\boldsymbol{k}}_{\mathrm{i}} + z\hat{\boldsymbol{z}})\, \mathrm{d}z \\ &= \sqrt{\frac{2}{\mathrm{i}\pi k_0\rho}}\frac{\pi}{k_0}\mathrm{e}^{\mathrm{i}k_0\rho} \sum_{nn'} \mathrm{i}^{-m} T_{nn'} c_{n'} g_{\bar{n}}^{\pm}(k_0, 0) \left(1 + O\left((k_0\rho)^{-1}\right)\right)\end{aligned}$$

Introduce the far field amplitude, $P(\hat{\boldsymbol{k}}_{\mathrm{i}})$, similar to the one defined in two dimension, see *e.g.*, [9].

$$P(\hat{\boldsymbol{k}}_{\mathrm{i}}) = \lim_{\rho\to\infty} \sqrt{\frac{\mathrm{i}\pi k_0\rho}{2}}\mathrm{e}^{-\mathrm{i}k_0\rho} \int_{z_-}^{z_+} \hat{\boldsymbol{z}} \cdot \boldsymbol{E}^{\mathrm{sec}}(\rho\hat{\boldsymbol{k}}_{\mathrm{i}} + z\hat{\boldsymbol{z}})\, \mathrm{d}z = \frac{\pi}{k_0} \sum_{nn'} \mathrm{i}^{-m} T_{nn'} c_{n'} g_{\bar{n}}^{\pm}(k_0, 0)$$

we get

$$P_{\mathrm{a}} + P_{\mathrm{s}} = -\frac{1}{2\eta_0}\frac{4}{k_0}\operatorname{Re}\left\{E_0^* P(\hat{\boldsymbol{k}}_{\mathrm{i}})\right\}$$

If we define scattering, absorption, and extinction cross section by division of the incident excitation power per area, $|E_0|^2/(2\eta_0)$, we obtain the optical theorem

$$\sigma_{\mathrm{ext}} = \sigma_{\mathrm{a}} + \sigma_{\mathrm{s}} = -\frac{4}{k_0}\operatorname{Re}\left\{\frac{E_0^* P(\hat{\boldsymbol{k}}_{\mathrm{i}})}{|E_0|^2}\right\} \tag{10.1}$$

This is formally the same as the optical theorem in two dimensions [9].

11 Examples of excitations

Several examples of explicit sources are of interest. In this section we examine the vertical electric dipole and the plane wave.

11.1 Vertical electric dipole

A first explicit example of an incident field is a vertical electric dipole located at $\boldsymbol{r}_0 = \boldsymbol{\rho}_0 + z_0\hat{\boldsymbol{z}} = \rho_0\left(\cos\phi_0\hat{\boldsymbol{x}} + \sin\phi_0\hat{\boldsymbol{y}}\right) + z_0\hat{\boldsymbol{z}}$, where $z_- < z_0 < z_+$. The expansion coefficients, $a_j^{\pm}(\boldsymbol{k}_{\mathrm{t}})$, of the incident field of this field in terms of planar spherical waves can be found from the transformation expression in (3.9) specialized to $\tau = 2$, $l = 1$, $m = 0$, and $\sigma = \mathrm{e}$.

$$\boldsymbol{E}_{\mathrm{i}}(\boldsymbol{r}) = \boldsymbol{u}_{2\mathrm{e}01}(k_0(\boldsymbol{r} - \boldsymbol{r}_0)) = \sum_{j=1,2} \iint_{\mathbb{R}^2} a_j^{\pm}(\boldsymbol{k}_{\mathrm{t}})\boldsymbol{\varphi}_j^{\pm}(\boldsymbol{k}_{\mathrm{t}}; \boldsymbol{r})\, \frac{\mathrm{d}k_x\, \mathrm{d}k_y}{k_0^2}, \quad z \gtrless z_0 \tag{11.1}$$

where

$$a_j^{\pm}(\boldsymbol{k}_{\mathrm{t}}) = 2\frac{k_0}{k_z}B_{2\mathrm{e}01j}^{\pm}(\boldsymbol{k}_{\mathrm{t}})\delta_{j2}\mathrm{e}^{-\mathrm{i}(\boldsymbol{k}_{\mathrm{t}}\pm k_z\hat{\boldsymbol{z}})\cdot\boldsymbol{r}_0} = 2\sqrt{\frac{3}{8\pi}}\frac{k_{\mathrm{t}}}{k_z}\delta_{j2}\mathrm{e}^{-\mathrm{i}(\boldsymbol{k}_{\mathrm{t}}\pm k_z\hat{\boldsymbol{z}})\cdot\boldsymbol{r}_0}$$

The expansion coefficients, a_n, in terms of regular spherical vector waves are

$$a_n = P_{2\mathrm{e}01n}(-\boldsymbol{d})$$

where the translation matrix $P_{nn'}$ is explicitly given in [6].

The primary field becomes, see (7.1)

$$\begin{aligned}\boldsymbol{E}^{\mathrm{prim}}(\boldsymbol{r}) = {} & 2\sqrt{\frac{3}{8\pi}}\iint_{\mathbb{R}^2}\frac{-\mathrm{sign}(z-z_0)\boldsymbol{k}_{\mathrm{t}}k_z + k_{\mathrm{t}}^2\hat{\boldsymbol{z}}}{4\pi k_0 k_{\mathrm{t}}}\mathrm{e}^{\mathrm{i}\boldsymbol{k}_{\mathrm{t}}\cdot(\boldsymbol{\rho}-\boldsymbol{\rho}_0)+\mathrm{i}k_z|z-z_0|}\frac{k_{\mathrm{t}}}{k_z}\frac{\mathrm{d}k_x\,\mathrm{d}k_y}{k_0^2} \\ & - 2\sqrt{\frac{3}{8\pi}}\iint_{\mathbb{R}^2}\frac{\mathrm{e}^{-\mathrm{i}k_z z_0}+\mathrm{e}^{\mathrm{i}k_z z_0}\mathrm{e}^{-2\mathrm{i}k_z z_+}}{1-\mathrm{e}^{-2\mathrm{i}k_z d}}\frac{-\boldsymbol{k}_{\mathrm{t}}k_z + k_{\mathrm{t}}^2\hat{\boldsymbol{z}}}{4\pi k_0 k_{\mathrm{t}}}\mathrm{e}^{\mathrm{i}\boldsymbol{k}_{\mathrm{t}}\cdot(\boldsymbol{\rho}-\boldsymbol{\rho}_0)+\mathrm{i}k_z z}\frac{k_{\mathrm{t}}}{k_z}\frac{\mathrm{d}k_x\,\mathrm{d}k_y}{k_0^2} \\ & - 2\sqrt{\frac{3}{8\pi}}\iint_{\mathbb{R}^2}\frac{\mathrm{e}^{-\mathrm{i}k_z z_0}\mathrm{e}^{2\mathrm{i}k_z z_-}+\mathrm{e}^{\mathrm{i}k_z z_0}}{1-\mathrm{e}^{-2\mathrm{i}k_z d}}\frac{\boldsymbol{k}_{\mathrm{t}}k_z + k_{\mathrm{t}}^2\hat{\boldsymbol{z}}}{4\pi k_0 k_{\mathrm{t}}}\mathrm{e}^{\mathrm{i}\boldsymbol{k}_{\mathrm{t}}\cdot(\boldsymbol{\rho}-\boldsymbol{\rho}_0)-\mathrm{i}k_z z}\frac{k_{\mathrm{t}}}{k_z}\frac{\mathrm{d}k_x\,\mathrm{d}k_y}{k_0^2}\end{aligned}$$

In particular, the vertical component is, see (C.1)

$$\begin{aligned}\boldsymbol{E}^{\mathrm{dir}}(\boldsymbol{r})\cdot\hat{\boldsymbol{z}} = {} & \sqrt{\frac{3}{8\pi}}\iint_{\mathbb{R}^2}\frac{k_{\mathrm{t}}}{k_0}J_0(k_{\mathrm{t}}|\boldsymbol{\rho}-\boldsymbol{\rho}_0|)\mathrm{e}^{\mathrm{i}k_z|z-z_0|}\frac{k_{\mathrm{t}}}{k_z}\frac{\mathrm{d}k_x\,\mathrm{d}k_y}{k_0^2} \\ & - \sqrt{\frac{3}{8\pi}}\int_0^{\infty}\frac{\mathrm{e}^{-\mathrm{i}k_z z_0}+\mathrm{e}^{\mathrm{i}k_z z_0}\mathrm{e}^{-2\mathrm{i}k_z z_+}}{1-\mathrm{e}^{-2\mathrm{i}k_z d}}\frac{k_{\mathrm{t}}}{k_0}J_0(k_{\mathrm{t}}|\boldsymbol{\rho}-\boldsymbol{\rho}_0|)\mathrm{e}^{\mathrm{i}k_z z}\frac{k_{\mathrm{t}}}{k_z}\frac{k_{\mathrm{t}}\,\mathrm{d}k_{\mathrm{t}}}{k_0^2} \\ & - \sqrt{\frac{3}{8\pi}}\int_0^{\infty}\frac{\mathrm{e}^{-\mathrm{i}k_z z_0}\mathrm{e}^{2\mathrm{i}k_z z_-}+\mathrm{e}^{\mathrm{i}k_z z_0}}{1-\mathrm{e}^{-2\mathrm{i}k_z d}}\frac{k_{\mathrm{t}}}{k_0}J_0(k_{\mathrm{t}}|\boldsymbol{\rho}-\boldsymbol{\rho}_0|)\mathrm{e}^{-\mathrm{i}k_z z}\frac{k_{\mathrm{t}}}{k_z}\frac{k_{\mathrm{t}}\,\mathrm{d}k_{\mathrm{t}}}{k_0^2}\end{aligned}$$

After using $2J_0(z) = H_0^{(1)}(z) + H_0^{(2)}(z)$ and $H_n^{(2)}(z\mathrm{e}^{-\mathrm{i}\pi}) = -\mathrm{e}^{\mathrm{i}n\pi}H_n^{(1)}(z)$, this expression leads to the following expression of the vertical component of the primary electric field, see also [10, p. 147]:

$$\boldsymbol{E}^{\mathrm{prim}}(\boldsymbol{r})\cdot\hat{\boldsymbol{z}} = C_0\int_C\frac{k_{\mathrm{t}}^3}{k_z}H_0^{(1)}(k_{\mathrm{t}}|\boldsymbol{\rho}-\boldsymbol{\rho}_0|)\left\{\mathrm{e}^{\mathrm{i}k_z|z-z_0|}+A(k_{\mathrm{t}})\mathrm{e}^{\mathrm{i}k_z z}+B(k_{\mathrm{t}})\mathrm{e}^{-\mathrm{i}k_z z}\right\}\mathrm{d}k_{\mathrm{t}}$$

where the contour C is depicted in Figure 4, and

$$\begin{cases}A(k_{\mathrm{t}}) = -\dfrac{\mathrm{e}^{-\mathrm{i}k_z z_0}+\mathrm{e}^{\mathrm{i}k_z z_0}\mathrm{e}^{-2\mathrm{i}k_z z_+}}{1-\mathrm{e}^{-2\mathrm{i}k_z d}} \\ B(k_{\mathrm{t}}) = -\dfrac{\mathrm{e}^{-\mathrm{i}k_z z_0}\mathrm{e}^{2\mathrm{i}k_z z_-}+\mathrm{e}^{\mathrm{i}k_z z_0}}{1-\mathrm{e}^{-2\mathrm{i}k_z d}}\end{cases}$$

and

$$C_0 = \sqrt{\frac{3}{8\pi}}\frac{1}{2k_0^3}$$

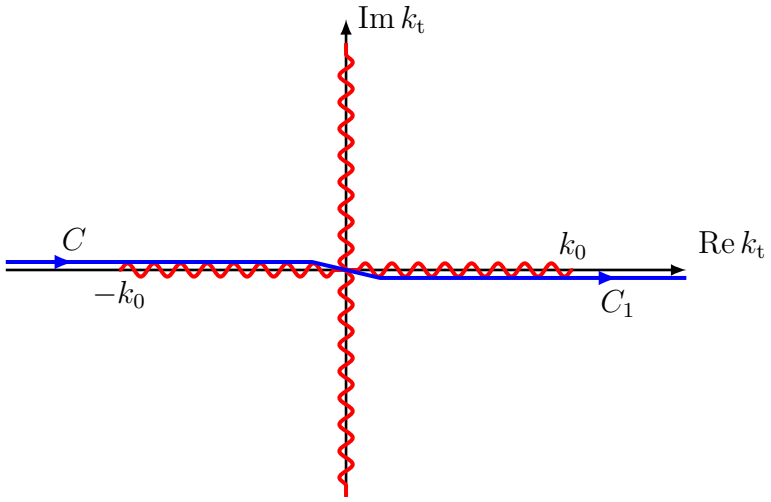

Figure 4: The two complex contours C_1 and C. The contour C_1 starts at the origin, and the contour C starts at infinity along the negative real axis. Both contours end at infinity along the positive real axis. The branch cuts are depicted in red.

Note that the function

$$\left(\mathrm{e}^{\mathrm{i}k_z|z-z_0|} + A(k_\mathrm{t})\mathrm{e}^{\mathrm{i}k_z z} + B(k_\mathrm{t})\mathrm{e}^{-\mathrm{i}k_z z}\right)/k_z$$

is an even function in k_z, and therefore has no branch point at $k_\mathrm{t} = \pm k_0$ ($k_z = 0$).

Calculus of residues gives

$$\begin{aligned}
\boldsymbol{E}^{\mathrm{prim}}(\boldsymbol{r})\cdot\hat{\boldsymbol{z}} &= \pi C_0 \sum_{p=0}^{\infty} \varepsilon_p \frac{k_{\mathrm{t}p}^2}{2d} H_0^{(1)}(k_{\mathrm{t}p}|\boldsymbol{\rho}-\boldsymbol{\rho}_0|)\Big\{\left(\mathrm{e}^{-\mathrm{i}p\pi z_0/d} + \mathrm{e}^{\mathrm{i}p\pi z_0/d}\mathrm{e}^{-2\mathrm{i}p\pi z_+/d}\right)\mathrm{e}^{\mathrm{i}p\pi z/d} \\
&\quad + \left(\mathrm{e}^{-\mathrm{i}p\pi z_0/d}\mathrm{e}^{2\mathrm{i}p\pi z_-/d} + \mathrm{e}^{\mathrm{i}p\pi z_0/d}\right)\mathrm{e}^{-\mathrm{i}p\pi z/d}\Big\} \\
&= \sqrt{\frac{3}{8\pi}}\frac{\pi}{2k_0 d}\sum_{p=0}^{\infty}\varepsilon_p \frac{k_{\mathrm{t}p}^2}{k_0^2} H_0^{(1)}(k_{\mathrm{t}p}|\boldsymbol{\rho}-\boldsymbol{\rho}_0|)\Big\{\mathrm{e}^{-\mathrm{i}p\pi(z_0-z_-)/d}\cos(\pi p(z-z_-)/d) \\
&\quad + \mathrm{e}^{-\mathrm{i}p\pi(z_+-z_0)/d}\cos(\pi p(z-z_+)/d)\Big\}
\end{aligned} \tag{11.2}$$

The explicit values of the remaining k_t integral evaluated below the first cutoff frequency is found in Appendix E.2.

Similarly, the horizontal components are, see (C.1)

$$\begin{aligned}\boldsymbol{E}_{\mathrm{t}}^{\mathrm{prim}}(\boldsymbol{r}) &= \mathrm{i}\sqrt{\frac{3}{8\pi}}\nabla_{\mathrm{t}}\int_0^\infty \frac{\mathrm{sign}(z-z_0)}{k_0}J_0(k_{\mathrm{t}}|\boldsymbol{\rho}-\boldsymbol{\rho}_0|)\mathrm{e}^{\mathrm{i}k_z|z-z_0|}\frac{k_{\mathrm{t}}\,\mathrm{d}k_{\mathrm{t}}}{k_0^2}\\ &\quad -\mathrm{i}\sqrt{\frac{3}{8\pi}}\nabla_{\mathrm{t}}\int_0^\infty \frac{\mathrm{e}^{-\mathrm{i}k_z z_0}+\mathrm{e}^{\mathrm{i}k_z z_0}\mathrm{e}^{-2\mathrm{i}k_z z_+}}{1-\mathrm{e}^{-2\mathrm{i}k_z d}}\frac{1}{k_0}J_0(k_{\mathrm{t}}|\boldsymbol{\rho}-\boldsymbol{\rho}_0|)\mathrm{e}^{\mathrm{i}k_z z}\frac{k_{\mathrm{t}}\,\mathrm{d}k_{\mathrm{t}}}{k_0^2}\\ &\quad +\mathrm{i}\sqrt{\frac{3}{8\pi}}\nabla_{\mathrm{t}}\int_0^\infty \frac{\mathrm{e}^{-\mathrm{i}k_z z_0}\mathrm{e}^{2\mathrm{i}k_z z_-}+\mathrm{e}^{\mathrm{i}k_z z_0}}{1-\mathrm{e}^{-2\mathrm{i}k_z d}}\frac{1}{k_0}J_0(k_{\mathrm{t}}|\boldsymbol{\rho}-\boldsymbol{\rho}_0|)\mathrm{e}^{-\mathrm{i}k_z z}\frac{k_{\mathrm{t}}\,\mathrm{d}k_{\mathrm{t}}}{k_0^2}\end{aligned}$$

or

$$\begin{aligned}\boldsymbol{E}_{\mathrm{t}}^{\mathrm{prim}}(\boldsymbol{r}) &= \mathrm{i}C_0\mathrm{sign}(z-z_0)\nabla_{\mathrm{t}}\int_C k_{\mathrm{t}}H_0^{(1)}(k_{\mathrm{t}}|\boldsymbol{\rho}-\boldsymbol{\rho}_0|)\mathrm{e}^{\mathrm{i}k_z|z-z_0|}\,\mathrm{d}k_{\mathrm{t}}\\ &\quad +\mathrm{i}C_0\nabla_{\mathrm{t}}\int_C A(k_{\mathrm{t}})k_{\mathrm{t}}H_0^{(1)}(k_{\mathrm{t}}|\boldsymbol{\rho}-\boldsymbol{\rho}_0|)\mathrm{e}^{\mathrm{i}k_z z}\,\mathrm{d}k_{\mathrm{t}}\\ &\quad -\mathrm{i}C_0\nabla_{\mathrm{t}}\int_C B(k_{\mathrm{t}})k_{\mathrm{t}}H_0^{(1)}(k_{\mathrm{t}}|\boldsymbol{\rho}-\boldsymbol{\rho}_0|)\mathrm{e}^{-\mathrm{i}k_z z}\,\mathrm{d}k_{\mathrm{t}}\end{aligned}$$

To evaluate the scattered field by this source, we also need to find the d_n vector, see (6.6)

$$\begin{aligned}d_n = -2\sqrt{\frac{3}{8\pi}}\iint_{\mathbb{R}^2}\Bigg\{&\mathrm{e}^{-\mathrm{i}k_z z_0}\frac{B_{n2}^{+\dagger}(\boldsymbol{k}_{\mathrm{t}})+\mathrm{e}^{2\mathrm{i}k_z z_-}B_{n2}^{-\dagger}(\boldsymbol{k}_{\mathrm{t}})}{1-\mathrm{e}^{-2\mathrm{i}k_z d}}\\ &+\mathrm{e}^{\mathrm{i}k_z z_0}\frac{B_{n2}^{-\dagger}(\boldsymbol{k}_{\mathrm{t}})+\mathrm{e}^{-2\mathrm{i}k_z z_+}B_{n2}^{+\dagger}(\boldsymbol{k}_{\mathrm{t}})}{1-\mathrm{e}^{-2\mathrm{i}k_z d}}-\mathrm{e}^{\mp\mathrm{i}k_z z_0}B_{n2}^{\pm\dagger}(\boldsymbol{k}_{\mathrm{t}})\Bigg\}\mathrm{e}^{-\mathrm{i}\boldsymbol{k}_{\mathrm{t}}\cdot\boldsymbol{r}_0}\frac{k_{\mathrm{t}}}{k_z}\,\frac{\mathrm{d}k_x\,\mathrm{d}k_y}{k_0^2}\end{aligned}$$

The choice of the plus or minus sign in this expression depends on whether $\hat{\boldsymbol{z}}\cdot\boldsymbol{r}_0 \gtrless 0$. From (C.1) we get

$$\frac{1}{2\pi}\int_0^{2\pi}\begin{Bmatrix}\cos m\beta\\ \sin m\beta\end{Bmatrix}\mathrm{e}^{\mathrm{i}\boldsymbol{k}_{\mathrm{t}}\cdot\boldsymbol{\rho}}\,\mathrm{d}\beta = \mathrm{i}^m\begin{Bmatrix}\cos m\phi\\ \sin m\phi\end{Bmatrix}J_m(k_{\mathrm{t}}\rho)$$

which gives

$$\begin{aligned}d_n = -4\pi\sqrt{\frac{3}{8\pi}}\int_0^\infty\Bigg\{&\mathrm{e}^{-\mathrm{i}k_z z_0}\frac{\mathrm{e}^{2\mathrm{i}k_z z_-}g_{\overline{n}}^{+}(k_{\mathrm{t}},\phi_0)+g_{\overline{n}}^{-}(k_{\mathrm{t}},\phi_0)}{1-\mathrm{e}^{-2\mathrm{i}k_z d}}\\ &+\mathrm{e}^{\mathrm{i}k_z z_0}\frac{\mathrm{e}^{-2\mathrm{i}k_z z_+}g_{\overline{n}}^{-}(k_{\mathrm{t}},\phi_0)+g_{\overline{n}}^{+}(k_{\mathrm{t}},\phi_0)}{1-\mathrm{e}^{-2\mathrm{i}k_z d}}-\mathrm{e}^{\mp\mathrm{i}k_z z_0}g_{\overline{n}}^{\mp}(k_{\mathrm{t}},\phi_0)\Bigg\}J_m(k_{\mathrm{t}}\rho_0)\frac{k_{\mathrm{t}}^2}{k_z}\,\frac{\mathrm{d}k_{\mathrm{t}}}{k_0^2}\end{aligned}$$

where $g_n^{\pm}(k_{\mathrm{t}},\phi)$ are defined in (C.2).

The remaining integration in the k_{t} variable can be transformed into a contour integration. Proceed as above, and we get

$$\begin{aligned}d_n = -2\pi\sqrt{\frac{3}{8\pi}}\int_C\Bigg\{&\mathrm{e}^{-\mathrm{i}k_z z_0}\frac{\mathrm{e}^{2\mathrm{i}k_z z_-}g_{\overline{n}}^{+}(k_{\mathrm{t}},\phi_0)+g_{\overline{n}}^{-}(k_{\mathrm{t}},\phi_0)}{1-\mathrm{e}^{-2\mathrm{i}k_z d}}\\ &+\mathrm{e}^{\mathrm{i}k_z z_0}\frac{\mathrm{e}^{-2\mathrm{i}k_z z_+}g_{\overline{n}}^{-}(k_{\mathrm{t}},\phi_0)+g_{\overline{n}}^{+}(k_{\mathrm{t}},\phi_0)}{1-\mathrm{e}^{-2\mathrm{i}k_z d}}-\mathrm{e}^{\mp\mathrm{i}k_z z_0}g_{\overline{n}}^{\mp}(k_{\mathrm{t}},\phi_0)\Bigg\}H_m^{(1)}(k_{\mathrm{t}}\rho_0)\frac{k_{\mathrm{t}}^2}{k_z}\,\frac{\mathrm{d}k_{\mathrm{t}}}{k_0^2}\end{aligned}$$

Calculus of residues gives

$$d_n = \frac{\pi^2}{k_0 d}\sqrt{\frac{3}{8\pi}}\sum_{p=0}^{\infty}\varepsilon_p\frac{k_{\mathrm{t}p}}{k_0}\Bigg\{\mathrm{e}^{-\mathrm{i}p\pi z_0/d}\left(\mathrm{e}^{2\mathrm{i}p\pi z_-/d}g_{\overline{n}}^{+}(k_{\mathrm{t}p},\phi_0)+g_{\overline{n}}^{-}(k_{\mathrm{t}p},\phi_0)\right)$$
$$+\mathrm{e}^{\mathrm{i}p\pi z_0/d}\left(\mathrm{e}^{-2\mathrm{i}p\pi z_+/d}g_{\overline{n}}^{-}(k_{\mathrm{t}p},\phi_0)+g_{\overline{n}}^{+}(k_{\mathrm{t}p},\phi_0)\right)\Bigg\}H_m^{(1)}(k_{\mathrm{t}p}\rho_0)$$
$$=\sqrt{\frac{3}{8\pi}}\frac{2\pi^2}{k_0 d}\sum_{p=0}^{\infty}\varepsilon_p\frac{k_{\mathrm{t}p}}{k_0}\Bigg\{\mathrm{e}^{\mathrm{i}p\pi z_-/d}g_{\overline{n}}^{+}(k_{\mathrm{t}p},\phi_0)\cos(\pi p(z_0-z_-)/d)$$
$$+\mathrm{e}^{-\mathrm{i}p\pi z_+/d}g_{\overline{n}}^{-}(k_{\mathrm{t}p},\phi_0)\cos(\pi p(z_+-z_0)/d)\Bigg\}H_m^{(1)}(k_{\mathrm{t}p}\rho_0)$$

The explicit values of the remaining k_{t} integral evaluated below the first cutoff frequency is found in Appendix E.3.

11.2 Plane wave incidence

As a second illustration of the results, we specialize to an incident field of a TEM wave excitation. We orient the x-axis such that the wave propagates in this direction, *i.e.*, $\boldsymbol{k}_{\mathrm{t}} = k_0\hat{\boldsymbol{x}}$. The appropriate expansion coefficients are:[2]

$$a_j^{\pm}(\boldsymbol{k}_{\mathrm{t}}) = -\delta_{j2}E_0k_0^2\pi\delta(\boldsymbol{k}_{\mathrm{t}}-k_0\hat{\boldsymbol{x}})\left(1-\mathrm{e}^{-2\mathrm{i}k_zd}\right)$$

and, see the consistency relation in (4.3)

$$a_n = 0$$

The incident field then is, see (4.1)

$$\boldsymbol{E}_{\mathrm{i}}(\boldsymbol{r}) = \sum_{j=1,2}\iint_{\mathbb{R}^2}a_j^{\pm}(\boldsymbol{k}_{\mathrm{t}})\boldsymbol{\varphi}_j^{\pm}(\boldsymbol{k}_{\mathrm{t}};\boldsymbol{r})\frac{\mathrm{d}k_x\,\mathrm{d}k_y}{k_0^2} = \boldsymbol{0},\quad \boldsymbol{r}\in V_{\pm}$$

with analytic continuation into the region between the plates, and, see (7.1)

$$\boldsymbol{E}_{\mathrm{s}}^{\mathrm{dir}}(\boldsymbol{r}) = -\sum_{j=1,2}\iint_{\mathbb{R}^2}\frac{a_j^{+}(\boldsymbol{k}_{\mathrm{t}})+a_j^{-}(\boldsymbol{k}_{\mathrm{t}})(-1)^j\mathrm{e}^{-2\mathrm{i}k_zz_+}}{1-\mathrm{e}^{-2\mathrm{i}k_zd}}\boldsymbol{\varphi}_j^{+}(\boldsymbol{k}_{\mathrm{t}};\boldsymbol{r})\,\frac{\mathrm{d}k_x\,\mathrm{d}k_y}{k_0^2}$$
$$-\sum_{j=1,2}\iint_{\mathbb{R}^2}\frac{a_j^{-}(\boldsymbol{k}_{\mathrm{t}})+a_j^{+}(\boldsymbol{k}_{\mathrm{t}})(-1)^j\mathrm{e}^{2\mathrm{i}k_zz_-}}{1-\mathrm{e}^{-2\mathrm{i}k_zd}}\boldsymbol{\varphi}_j^{-}(\boldsymbol{k}_{\mathrm{t}};\boldsymbol{r})\,\frac{\mathrm{d}k_x\,\mathrm{d}k_y}{k_0^2} = \hat{\boldsymbol{z}}E_0\mathrm{e}^{\mathrm{i}k_0x}\quad(11.3)$$

Then the primary electric field becomes

$$\boldsymbol{E}^{\mathrm{prim}}(\boldsymbol{r}) = \boldsymbol{E}_{\mathrm{i}}(\boldsymbol{r})+\boldsymbol{E}_{\mathrm{s}}^{\mathrm{dir}}(\boldsymbol{r}) = \hat{\boldsymbol{z}}E_0\mathrm{e}^{\mathrm{i}k_0x}\quad(11.4)$$

[2]To be more precise, replace $a_j^{\pm}(\boldsymbol{k}_{\mathrm{t}}) = \left(1-\mathrm{e}^{-2\mathrm{i}k_zd}\right)\hat{a}_j^{\pm}(\boldsymbol{k}_{\mathrm{t}})$ everywhere in the analysis, and then let $\hat{a}_j^{\pm}(\boldsymbol{k}_{\mathrm{t}}) = -\delta_{j2}E_0k_0^2\pi\delta(\boldsymbol{k}_{\mathrm{t}}-k_0\hat{\boldsymbol{x}})$.

The d_n vector, see (6.6), is

$$d_n = 2\pi E_0 \left(B_{n2}^{+\dagger}(k_0\hat{\boldsymbol{x}}) + B_{n2}^{-\dagger}(k_0\hat{\boldsymbol{x}}) \right) = 2\pi E_0 \left(B_{n2}^{+}(-k_0\hat{\boldsymbol{x}}) + B_{n2}^{-}(-k_0\hat{\boldsymbol{x}}) \right)$$

Insert the $B_{n2}(\boldsymbol{k}_{\mathrm{t}})$ from (3.11), and we obtain

$$d_n = -2\pi E_0 \mathrm{i}^{-l}(-1)^m C_{lm} \Big\{ \left(1 + (-1)^{l+m}\right) \delta_{\tau 1} \pi_l^m(0) \delta_{\sigma \mathrm{o}} + \mathrm{i} \left(1 - (-1)^{l+m}\right) \delta_{\tau 2} \Delta_l^m(0) \delta_{\sigma \mathrm{e}} \Big\}$$

or, see Appendix E

$$d_n = -4\pi E_0 \mathrm{i}^{-l}(-1)^m C_{lm} \left\{ \delta_{\tau 1} \pi_l^m(0) \delta_{\sigma \mathrm{o}} + \mathrm{i} \delta_{\tau 2} \Delta_l^m(0) \delta_{\sigma \mathrm{e}} \right\}$$

12 Numerical examples

In a few numerical examples, the analysis presented in this paper is illustrated. The verification of the numerical code has been verified with the optical theorem and the sum rule, see (10.1) and (12.2), both with good agreement.

12.1 Vertical electric dipole excitation

Let the source be a vertical electric dipole located at $\boldsymbol{r}_0 = -x_0\hat{\boldsymbol{x}} + z_0\hat{\boldsymbol{z}}$. This source was analyzed in Section 11.1. In all examples $x_0/d = 10$.

The absolute value of the vertical component of the electric field of the primary field, $|\hat{\boldsymbol{z}} \cdot \boldsymbol{E}^{\mathrm{prim}}(\boldsymbol{r})|$, see (11.2), as a function of frequency $k_0 d$ (up to five times the first cutoff frequency) is shown in Figure 5. The frequency interval below the second cutoff, $k_0 d \in [0, 2\pi]$, the red and the blue curves show no oscillations due to symmetry in the excitation, $z_0/d = 0$.

The absolute value of the vertical component of the secondary electric field, $|\hat{\boldsymbol{z}} \cdot \boldsymbol{E}^{\mathrm{sec}}(\boldsymbol{r})|$, at the point $\boldsymbol{r} = x\hat{\boldsymbol{x}} + z\hat{\boldsymbol{z}}$, as a function of frequency, $k_0 d$, (up to three times the first cutoff frequency) for a perfectly conducting sphere is depicted in Figure 6. The fields at two different vertical positions are shown, and only the contribution due to the propagating modes is included — no evanescent modes. The incident field is given by (11.1), and the curves are normalized with the absolute value of the vertical component of the primary field evaluated at the origin. In the normalization field, only the contribution of the fundamental mode is included, *i.e.*, all higher modes are ignored in the normalization field, since these higher modes show strong oscillatory behavior, see Figure 5, and for this reason they are unsuitable as normalization fields. In the frequency interval below the second cutoff, $k_0 d \in [0, 2\pi]$, the two curves are identical due to symmetry of the excitation, and there is no variation in the vertical component of scattered field.

If the sphere contains a dielectric material, which has a resonance below the first cutoff, $k_0 d = \pi$, the situation is different. This situation is depicted in Figure 7. In

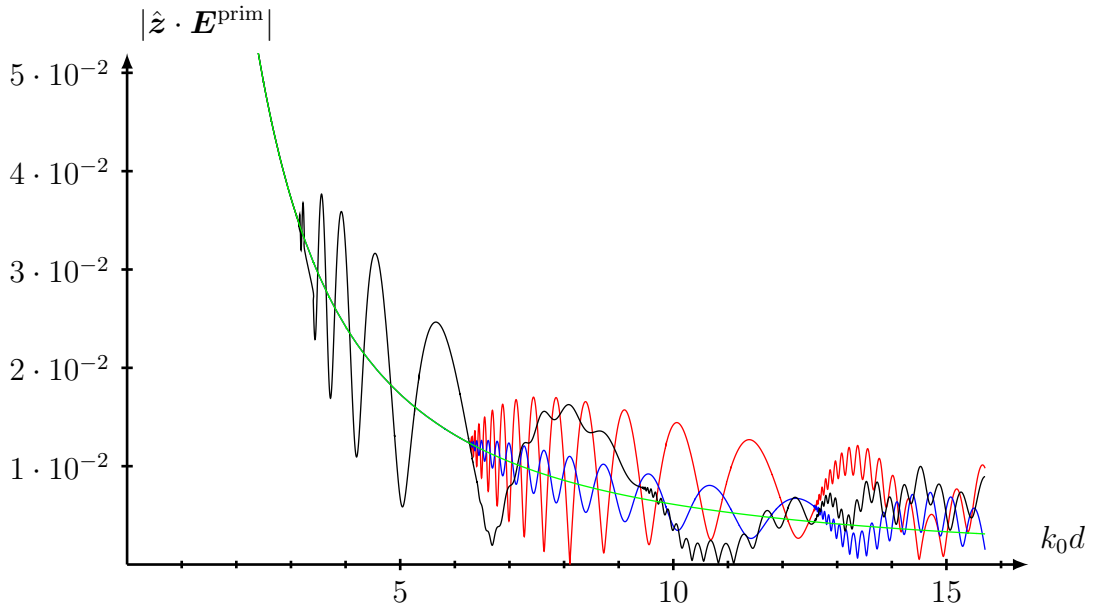

Figure 5: The absolute value of the vertical primary field, $|\hat{\boldsymbol{z}} \cdot \boldsymbol{E}^{\mathrm{prim}}(\boldsymbol{r})|$, at a fixed point $\boldsymbol{r}$ as a function of frequency, $k_0 d$, for a vertical electrical dipole located at $\boldsymbol{r}_0 = -x_0\hat{\boldsymbol{x}} + z_0\hat{\boldsymbol{z}}$, where $x_0/d = 10$ and $z_0/d = 0$ (red and blue curves), and $x_0/d = 10$ and $z_0/d = 0.2$ (black curve). The curve shows the contribution to the primary field due to the propagating modes. The locations of the planes are $z_+/d = 0.5$ and $z_-/d = -0.5$, and the field point is $\boldsymbol{r} = x\hat{\boldsymbol{x}} + z\hat{\boldsymbol{z}}$, where $x/d = 10$ and $z/d = 0$ (red curve) and $z/d = 0.3$ (blue and black curves). The green curve shows the contribution of the fundamental mode alone.

this example, we adopt a Lorentz model for the permittivity, *i.e.*,

$$\epsilon(\omega) = 1 - \frac{\omega_{\mathrm{p}}^2}{\omega^2 - \omega_0^2 + \mathrm{i}\nu\omega} \tag{12.1}$$

The explicit data of the example are given in the caption. Figure 7 shows a sharp resonance peak at about $k_0 d \approx 0.33$, which corresponds to $k_0 a \approx 0.15$. The curve is normalized in the same way as the curves in Figure 6.

In the next example, we illustrate the scattered power scattered by a perfectly conducting sphere excited by a vertical dipole, see (11.1). The result is shown in Figure 8. The result is normalized by the power flow of the fundamental mode of the primary field at the origin, see (11.2). The contributions of the higher modes are excluded in the normalization field, since these contributions oscillate to a great extent, see Figure 5.

12.2 Plane wave excitation

In the last numerical example, the first propagating mode is taken as the exciting field, which is a vertically polarized plane wave, see (11.4). In Figure 9, the scattering

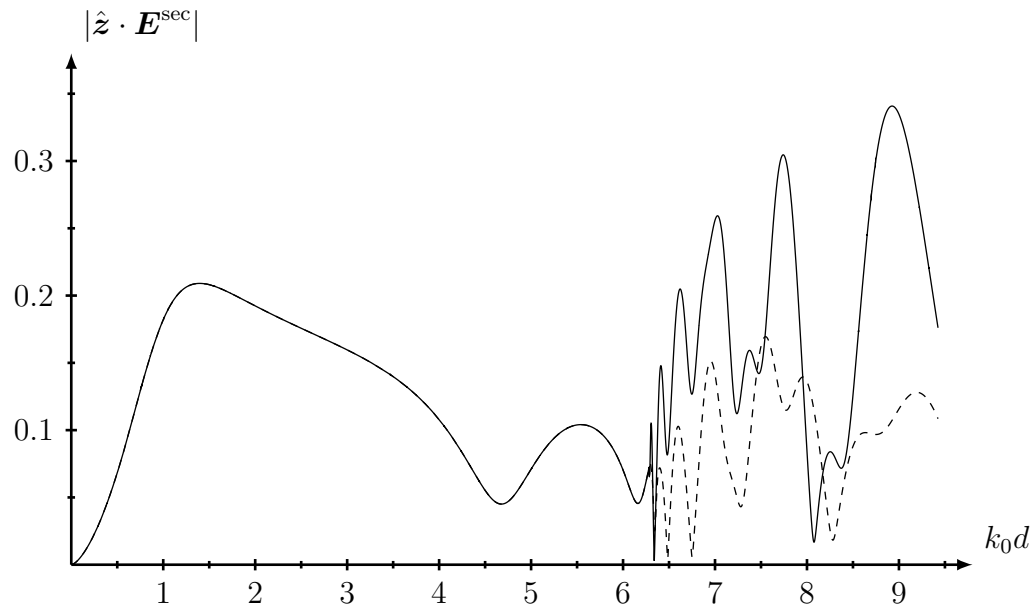

Figure 6: The absolute value of the vertical component of the secondary field, $|\hat{\boldsymbol{z}} \cdot \boldsymbol{E}^{\mathrm{sec}}(\boldsymbol{r})|$, at the point $\boldsymbol{r} = x\hat{\boldsymbol{x}} + z\hat{\boldsymbol{z}}$, where $x/d = 10$, as a function of frequency, $k_0 d$, for a vertical electrical dipole, see (11.1), located at $\boldsymbol{r}_0 = -x_0\hat{\boldsymbol{x}} + z_0\hat{\boldsymbol{z}}$, where $x_0/d = 10$ and $z_0/d = 0$. The locations of the planes are $z_+/d = 0.5$ and $z_-/d = -0.5$, and two different positions are shown, $z/d = 0$ (solid line) and $z/d = 0.3$ (dashed line). The scatterer is a perfectly conducting sphere of radius $a/d = 0.45$ located at the origin.

cross section is depicted as a function of $k_0 d$ for a perfectly conducting sphere of radius a. The scattering cross section is here equal to the extinction cross section. The results of two different radii are depicted. In this example, the frequency interval is such that the first three modes propagate at the highest frequency, *i.e.*, $0 \leq k_0 d \leq 3\pi$. The explicit data of the example are given in the caption.

Scattering by a perfectly conducting sphere in free space shows a resonance at about $k_0 a \approx 1$ [9]. As seen in Figure 9, the resonance is located at a slightly lower frequency, $k_0 a \approx 0.68$, when the sphere is confined between two parallel plates. Moreover, in free space, the scattering cross section remains almost constant after the first resonance. Located between the parallel plates, the scattering by the sphere shows interesting additional resonance behavior.

12.2.1 Sum rule

The appropriate sum rule for an incident plane wave, see (11.3), is [28]

$$\int_0^\infty \frac{\sigma_{\mathrm{ext}}(k)}{k^2}\, \mathrm{d}k = \frac{\pi}{2}\left(\hat{\boldsymbol{e}}^* \cdot \boldsymbol{\gamma}_{\mathrm{e}} \cdot \hat{\boldsymbol{e}} + (\hat{\boldsymbol{k}}_{\mathrm{i}} \times \hat{\boldsymbol{e}})^* \cdot \boldsymbol{\gamma}_{\mathrm{m}} \cdot (\hat{\boldsymbol{k}}_{\mathrm{i}} \times \hat{\boldsymbol{e}})\right) \tag{12.2}$$

This identity holds also for the parallel plate waveguide, provided the fundamental mode is considered. This identity is verified by numerical simulations for a dielectric

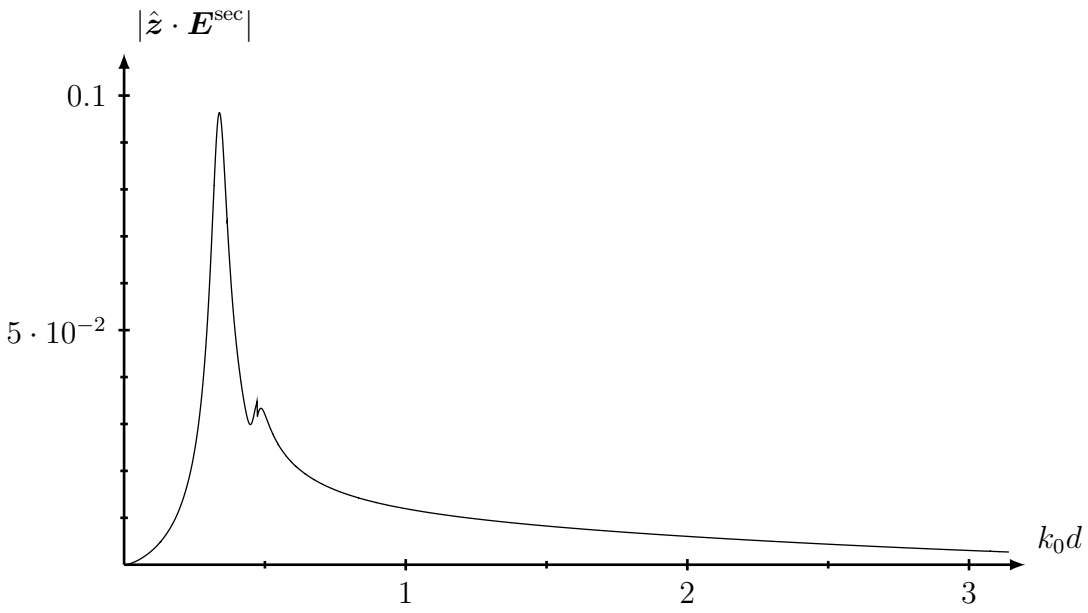

Figure 7: The absolute value of the vertical component of the secondary field, $|\hat{\boldsymbol{z}} \cdot \boldsymbol{E}^{\mathrm{sec}}(\boldsymbol{r})|$, at the point $\boldsymbol{r} = x\hat{\boldsymbol{x}} + z\hat{\boldsymbol{z}}$, where $x/d = 10$ and $z/d = 0.3$, as a function of frequency, $k_0 d$, for a vertical electrical dipole, see (11.1), located at $\boldsymbol{r}_0 = -x_0\hat{\boldsymbol{x}} + z_0\hat{\boldsymbol{z}}$, where $x_0/d = 10$ and $z_0/d = 0$. The curve shows the contribution due to the propagating modes. The locations of the planes are $z_+/d = 0.5$ and $z_-/d = -0.5$, and the scatterer is a non-magnetic, $\mu = 1$, dielectric sphere of radius $a/d = 0.45$ located at the origin. The data of the permittivity in the Lorentz model (12.1) are $\omega_{\mathrm{p}} = 0.7c_0/a$, $\omega_0 = 0.2c_0/a$, and $\nu = 0.05c_0/a$.

(Lorentz model) sphere to three decimal places.

13 Conclusions

By the use of the integral representation of the scattered field, the solution to a complex electromagnetic scattering problem of an obstacle inside a parallel plate waveguide has been solved. The solution is an extension of the null field method, originally proposed by Peter Waterman, to geometries with two planar interfaces. Similar geometries have been addressed in the past, see *e.g.*, [17–19, 21], but this problem shows more complexity. The approach is well suited to numerical implementation, and a series of numerical examples shows the usefulness of the method. Several ways of testing the numerical are suggested, *e.g.*, the optical theorem (appropriately formulated) and the sum rule. All these verifications show good agreement.

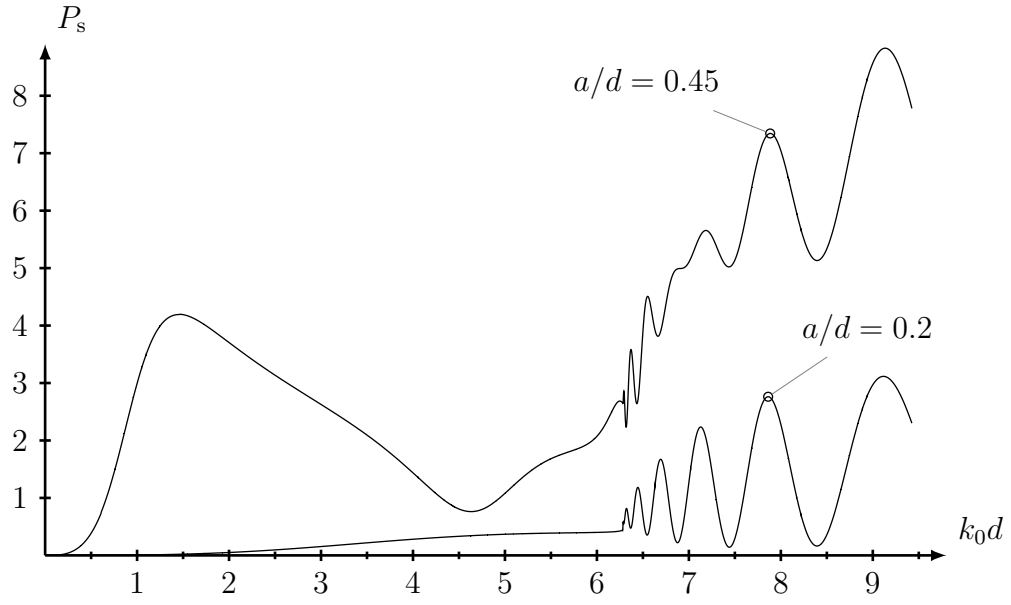

Figure 8: The scattered power P_s by a perfectly conducting sphere, centered at the origin, as a function of frequency, $k_0 d$, for a vertical electrical dipole, see (11.1), located at $\boldsymbol{r}_0 = -x_0\hat{\boldsymbol{x}} + z_0\hat{\boldsymbol{z}}$, where $x_0/d = 10$ and $z_0/d = 0$. The locations of the planes are $z_+/d = 0.5$ and $z_-/d = -0.5$.

Acknowledgement

The work reported in this paper has been performed by a grant from the Swedish Defence Materiel Administration, FMV. This support is gratefully acknowledged.

Appendix A Orthogonality relations

From the definitions of the planar vector waves in (3.4)

$$\begin{cases} \boldsymbol{\varphi}_1^{\pm}(\boldsymbol{k}_t;\boldsymbol{r}) = \dfrac{\hat{\boldsymbol{z}}\times\boldsymbol{k}_t}{4\pi \mathrm{i} k_t} \mathrm{e}^{\mathrm{i}\boldsymbol{k}_t\cdot\boldsymbol{\rho}\pm\mathrm{i}k_z z} \\ \boldsymbol{\varphi}_2^{\pm}(\boldsymbol{k}_t;\boldsymbol{r}) = \dfrac{\mp\boldsymbol{k}_t k_z + k_t^2\hat{\boldsymbol{z}}}{4\pi k_0 k_t} \mathrm{e}^{\mathrm{i}\boldsymbol{k}_t\cdot\boldsymbol{\rho}\pm\mathrm{i}k_z z} \end{cases} \qquad \begin{cases} \boldsymbol{\varphi}_1^{\pm\dagger}(\boldsymbol{k}_t;\boldsymbol{r}) = -\dfrac{\hat{\boldsymbol{z}}\times\boldsymbol{k}_t}{4\pi \mathrm{i} k_t} \mathrm{e}^{-\mathrm{i}\boldsymbol{k}_t\cdot\boldsymbol{\rho}\pm\mathrm{i}k_z z} \\ \boldsymbol{\varphi}_2^{\pm\dagger}(\boldsymbol{k}_t;\boldsymbol{r}) = \dfrac{\pm\boldsymbol{k}_t k_z + k_t^2\hat{\boldsymbol{z}}}{4\pi k_0 k_t} \mathrm{e}^{-\mathrm{i}\boldsymbol{k}_t\cdot\boldsymbol{\rho}\pm\mathrm{i}k_z z} \end{cases}$$

we get

$$\iint_S \boldsymbol{\varphi}_j^{\mp}(\boldsymbol{k}_t;\boldsymbol{r})\cdot\boldsymbol{\varphi}_{j'}^{\pm\dagger}(\boldsymbol{k}_t';\boldsymbol{r})\,\mathrm{d}x\,\mathrm{d}y = \frac{\delta_{jj'}}{16\pi^2}\iint_{\mathbb{R}^2} \mathrm{e}^{\mathrm{i}(\boldsymbol{k}_t-\boldsymbol{k}_t')\cdot\boldsymbol{\rho}}\,\mathrm{d}x\,\mathrm{d}y = \frac{\delta_{jj'}}{4}\delta(\boldsymbol{k}_t-\boldsymbol{k}_t')$$

Moreover, we have

$$\begin{cases} \hat{\boldsymbol{z}}\times\boldsymbol{\varphi}_1^{\pm}(\boldsymbol{k}_t;\boldsymbol{r}) = -\dfrac{\boldsymbol{k}_t}{4\pi \mathrm{i} k_t} \mathrm{e}^{\mathrm{i}\boldsymbol{k}_t\cdot\boldsymbol{\rho}\pm\mathrm{i}k_z z} \\ \hat{\boldsymbol{z}}\times\boldsymbol{\varphi}_2^{\pm}(\boldsymbol{k}_t;\boldsymbol{r}) = \mp\dfrac{\hat{\boldsymbol{z}}\times\boldsymbol{k}_t k_z}{4\pi k_0 k_t} \mathrm{e}^{\mathrm{i}\boldsymbol{k}_t\cdot\boldsymbol{\rho}\pm\mathrm{i}k_z z} \end{cases}$$

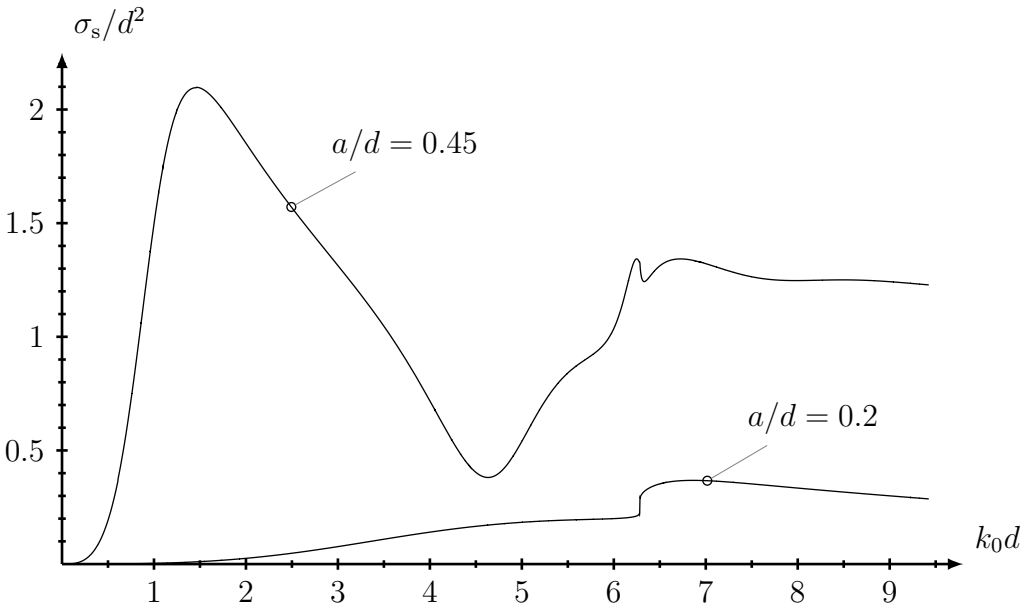

Figure 9: The scattering cross section, σ_s, for a PEC sphere of radius a, centered at the origin, as a function of $k_0 d$ and vertically polarized incident plane wave. The cross section is scaled with d^2. The locations of the planes are $z_+/d = 0.5$ and $z_-/d = -0.5$.

From these expression, we derive

$$\iint\limits_S \boldsymbol{\varphi}_{j'}^{\pm\dagger}(\boldsymbol{k}_t'; \boldsymbol{r}) \cdot \left(\hat{\boldsymbol{z}} \times \boldsymbol{\varphi}_j^{\mp}(\boldsymbol{k}_t; \boldsymbol{r})\right) \, \mathrm{d}x \, \mathrm{d}y = \mp \frac{k_z}{4\mathrm{i}k_0} \delta_{\bar{j}j'} \delta(\boldsymbol{k}_t - \boldsymbol{k}_t')$$

and

$$\iint\limits_S \boldsymbol{\varphi}_{j'}^{\pm\dagger}(\boldsymbol{k}_t'; \boldsymbol{r}) \cdot \left(\hat{\boldsymbol{z}} \times \boldsymbol{\varphi}_j^{\pm}(\boldsymbol{k}_t; \boldsymbol{r})\right) \, \mathrm{d}x \, \mathrm{d}y = \pm(-1)^j \frac{k_z}{4\mathrm{i}k_0} \mathrm{e}^{\pm 2\mathrm{i}k_z z_0} \delta_{\bar{j}j'} \delta(\boldsymbol{k}_t - \boldsymbol{k}_t')$$

where the dual index $\bar{j}$ is defined $\bar{1} = 2$ and $\bar{2} = 1$.

Furthermore, we get

$$\iint\limits_S \boldsymbol{\varphi}_{j'}^{\pm}(\boldsymbol{k}_t; \boldsymbol{r}) \cdot \left(\hat{\boldsymbol{z}} \times \boldsymbol{\varphi}_{\bar{j}}^{\mp}(\boldsymbol{k}_t'; \boldsymbol{r})\right) \, \mathrm{d}x \, \mathrm{d}y = \mp \frac{k_z}{4\mathrm{i}k_0} \delta_{jj'} \delta(\boldsymbol{k}_t + \boldsymbol{k}_t')$$

The orthogonality relations in (3.6) and (6.1) are then proved.

Appendix B The $A_{nn'}$ matrix

The evaluation of the integrals in the A matrix in (6.7)

$$A_{nn'} = -2\sum_{j=1,2}\iint_{\mathbb{R}^2} B_{nj}^{-\dagger}(\boldsymbol{k}_\mathrm{t})\frac{B_{n'j}^{-}(\boldsymbol{k}_\mathrm{t}) + (-1)^j \mathrm{e}^{2\mathrm{i}k_z z_-} B_{n'j}^{+}(\boldsymbol{k}_\mathrm{t})}{1-\mathrm{e}^{-2\mathrm{i}k_z d}}\frac{k_0}{k_z}\frac{\mathrm{d}k_x\,\mathrm{d}k_y}{k_0^2}$$
$$-2\sum_{j=1,2}\iint_{\mathbb{R}^2} B_{nj}^{+\dagger}(\boldsymbol{k}_\mathrm{t})\frac{B_{n'j}^{+}(\boldsymbol{k}_\mathrm{t}) + (-1)^j \mathrm{e}^{-2\mathrm{i}k_z z_+} B_{n'j}^{-}(\boldsymbol{k}_\mathrm{t})}{1-\mathrm{e}^{-2\mathrm{i}k_z d}}\frac{k_0}{k_z}\frac{\mathrm{d}k_x\,\mathrm{d}k_y}{k_0^2}$$

is somewhat technical, and we prefer to collect the results in this appendix.

We proceed in two steps in cylinder coordinates (k_t,β) of $\boldsymbol{k}_\mathrm{t}$, *i.e.*,

$$\boldsymbol{k}_\mathrm{t} = k_\mathrm{t}(\hat{\boldsymbol{x}}\cos\beta + \hat{\boldsymbol{y}}\sin\beta)$$

The first step involves the β integration. Define (upper and lower signs on the left- and right-hand sides are read together)

$$G_{nn'}^{\pm}(t) = \sum_{j=1,2}\int_0^{2\pi} B_{nj}^{\pm\dagger}(\boldsymbol{k}_\mathrm{t})B_{n'j}^{\pm}(\boldsymbol{k}_\mathrm{t})\,\mathrm{d}\beta$$

and

$$H_{nn'}^{\pm}(t) = \sum_{j=1,2}\int_0^{2\pi} (-1)^j B_{nj}^{\pm\dagger}(\boldsymbol{k}_\mathrm{t})B_{n'j}^{\mp}(\boldsymbol{k}_\mathrm{t})\,\mathrm{d}\beta$$

where $k_z = k_0 t$. We get

$$A_{nn'} = -2\int_{\mathrm{i}\infty}^{1}\frac{\mathrm{e}^{2\mathrm{i}k_0 z_- t}H_{nn'}^{-}(t) + G_{nn'}^{-}(t) + G_{nn'}^{+}(t) + \mathrm{e}^{-2\mathrm{i}k_0 z_+ t}H_{nn'}^{+}(t)}{1-\mathrm{e}^{-2\mathrm{i}k_0 dt}}\,\mathrm{d}t$$

where we have used $k_\mathrm{t}\,\mathrm{d}k_\mathrm{t} = -k_z\,\mathrm{d}k_z = -k_z k_0\,\mathrm{d}t$.

The functions $G_{nn'}^{\pm}(t)$ and $H_{nn'}^{\pm}(t)$ are readily computed by orthogonality over the interval $[0,2\pi)$. The integrands in $G_{nn'}^{\pm}(t)$ are

$$\begin{cases} B_{n1}^{\pm\dagger}(\boldsymbol{k}_\mathrm{t})B_{n'1}^{\pm}(\boldsymbol{k}_\mathrm{t}) = \mathrm{i}^{l-l'}C_{lm}C_{l'm'}(\pm1)^{l+m+l'+m'} \\ \qquad\times\left\{\pm\mathrm{i}\delta_{\tau 1}\Delta_l^m(t)\begin{Bmatrix}\cos m\beta\\ \sin m\beta\end{Bmatrix} - \delta_{\tau 2}\pi_l^m(t)\begin{Bmatrix}-\sin m\beta\\ \cos m\beta\end{Bmatrix}\right\} \\ \qquad\times\left\{\mp\mathrm{i}\delta_{\tau' 1}\Delta_{l'}^{m'}(t)\begin{Bmatrix}\cos m'\beta\\ \sin m'\beta\end{Bmatrix} - \delta_{\tau' 2}\pi_{l'}^{m'}(t)\begin{Bmatrix}-\sin m'\beta\\ \cos m'\beta\end{Bmatrix}\right\} \\ B_{n2}^{\pm\dagger}(\boldsymbol{k}_\mathrm{t})B_{n'2}^{\pm}(\boldsymbol{k}_\mathrm{t}) = \mathrm{i}^{l-l'}C_{lm}C_{l'm'}(\pm1)^{l+m+l'+m'} \\ \qquad\times\left\{-\delta_{\tau 1}\pi_l^m(t)\begin{Bmatrix}-\sin m\beta\\ \cos m\beta\end{Bmatrix} \pm \mathrm{i}\delta_{\tau 2}\Delta_l^m(t)\begin{Bmatrix}\cos m\beta\\ \sin m\beta\end{Bmatrix}\right\} \\ \qquad\times\left\{-\delta_{\tau' 1}\pi_{l'}^{m'}(t)\begin{Bmatrix}-\sin m'\beta\\ \cos m'\beta\end{Bmatrix} \mp \mathrm{i}\delta_{\tau' 2}\Delta_{l'}^{m'}(t)\begin{Bmatrix}\cos m'\beta\\ \sin m'\beta\end{Bmatrix}\right\} \end{cases}$$

This results in

$$G^{\pm}_{nn'}(t) = C'_{ll'm}\delta_{mm'}\mathrm{i}^{l-l'}(\pm 1)^{l+l'}\Big\{\delta_{\sigma\sigma'}\delta_{\tau\tau'}\left(\Delta^m_l(t)\Delta^m_{l'}(t)+\pi^m_l(t)\pi^m_{l'}(t)\right) \pm \mathrm{i}\delta_{\overline{\sigma}\sigma'}\delta_{\overline{\tau}\tau'}(-1)^{\sigma}\left(\Delta^m_l(t)\pi^m_{l'}(t)+\pi^m_l(t)\Delta^m_{l'}(t)\right)\Big\}$$

where the dual indices $\overline{\sigma}$ and $\overline{\tau}$, $\overline{\mathrm{e}}=\mathrm{o}$, $\overline{\mathrm{o}}=\mathrm{e}$ and $\overline{1}=2$, $\overline{2}=1$, have been employed, and where

$$C'_{ll'm} = \sqrt{\frac{2l+1}{2}\frac{(l-m)!}{(l+m)!}}\sqrt{\frac{2l'+1}{2}\frac{(l'-m)!}{(l'+m)!}}, \quad (-1)^{\sigma} = \begin{cases} -1, & \sigma=\mathrm{e} \\ 1, & \sigma=\mathrm{o} \end{cases}$$

The integrands in $H^{\pm}_{nn'}(t)$ are

$$\begin{cases} B^{\pm\dagger}_{n1}(\boldsymbol{k}_{\mathrm{t}})B^{\mp}_{n'1}(\boldsymbol{k}_{\mathrm{t}}) = \mathrm{i}^{l-l'}C_{lm}C_{l'm'}(\pm 1)^{l+m}(\mp 1)^{l'+m'} \\ \qquad \times\left\{\pm\mathrm{i}\delta_{\tau 1}\Delta^m_l(t)\begin{Bmatrix}\cos m\beta\\ \sin m\beta\end{Bmatrix} - \delta_{\tau 2}\pi^m_l(t)\begin{Bmatrix}-\sin m\beta\\ \cos m\beta\end{Bmatrix}\right\} \\ \qquad \times\left\{\pm\mathrm{i}\delta_{\tau' 1}\Delta^{m'}_{l'}(t)\begin{Bmatrix}\cos m'\beta\\ \sin m'\beta\end{Bmatrix} - \delta_{\tau' 2}\pi^{m'}_{l'}(t)\begin{Bmatrix}-\sin m'\beta\\ \cos m'\beta\end{Bmatrix}\right\} \\ B^{\pm\dagger}_{n2}(\boldsymbol{k}_{\mathrm{t}})B^{\mp}_{n'2}(\boldsymbol{k}_{\mathrm{t}}) = \mathrm{i}^{l-l'}C_{lm}C_{l'm'}(\pm 1)^{l+m}(\mp 1)^{l'+m'} \\ \qquad \times\left\{-\delta_{\tau 1}\pi^m_l(t)\begin{Bmatrix}-\sin m\beta\\ \cos m\beta\end{Bmatrix} \pm \mathrm{i}\delta_{\tau 2}\Delta^m_l(t)\begin{Bmatrix}\cos m\beta\\ \sin m\beta\end{Bmatrix}\right\} \\ \qquad \times\left\{-\delta_{\tau' 1}\pi^{m'}_{l'}(t)\begin{Bmatrix}-\sin m'\beta\\ \cos m'\beta\end{Bmatrix} \pm \mathrm{i}\delta_{\tau' 2}\Delta^{m'}_{l'}(t)\begin{Bmatrix}\cos m'\beta\\ \sin m'\beta\end{Bmatrix}\right\} \end{cases}$$

This results in

$$H^{\pm}_{nn'}(t) = C'_{ll'm}\delta_{mm'}\mathrm{i}^{l-l'}(\pm 1)^{l+m}(\mp 1)^{l'+m} \times\Big\{\delta_{\sigma\sigma'}\delta_{\tau\tau'}(-1)^{\tau+1}\left(\Delta^m_l(t)\Delta^m_{l'}(t)+\pi^m_l(t)\pi^m_{l'}(t)\right) \pm \mathrm{i}\delta_{\overline{\sigma}\sigma'}\delta_{\overline{\tau}\tau'}(-1)^{\sigma+\tau}\left(\Delta^m_l(t)\pi^m_{l'}(t)+\pi^m_l(t)\Delta^m_{l'}(t)\right)\Big\}$$

Notice that $G^{+}_{nn'}(t) = G^{-}_{n'n}(t)$ and $H^{\pm}_{n'n}(t)$ is symmetric, *i.e.*, $H^{\pm}_{nn'}(t) = H^{\pm}_{n'n}(t)$.

The structure of the $A_{nn'}$ matrix in the τ and σ indices is

$$A_{nn'} = \delta_{mm'}\begin{array}{c} \\ 1\mathrm{e} \\ 2\mathrm{o} \\ 1\mathrm{o} \\ 2\mathrm{e}\end{array}\begin{array}{c}\begin{array}{cccc}1\mathrm{e} & 2\mathrm{o} & 1\mathrm{o} & 2\mathrm{e}\end{array}\\ \begin{pmatrix} A^1_{ll'm} & A^2_{ll'm} & 0 & 0 \\ A^3_{ll'm} & A^4_{ll'm} & 0 & 0 \\ 0 & 0 & A^1_{ll'm} & A^5_{ll'm} \\ 0 & 0 & A^6_{ll'm} & A^4_{ll'm}\end{pmatrix}\end{array}$$

and we observe that the index pairs $\{1\mathrm{e},2\mathrm{o}\}$ and $\{1\mathrm{o},2\mathrm{e}\}$ do not couple.

All entries in the $A_{nn'}$ matrix can be written in terms of a combination of the integrals

$$I^1_{ll'm}(k_0z,k_0d)=\int_{\mathrm{i}\infty}^{1}\frac{\Delta^m_l(t)\Delta^m_{l'}(t)+\pi^m_l(t)\pi^m_{l'}(t)}{1-\mathrm{e}^{-2\mathrm{i}k_0dt}}\mathrm{e}^{-2\mathrm{i}k_0zt}\,\mathrm{d}t$$
$$=\sum_{k=0}^{l+l'}a_k(l,l',m)\int_{\mathrm{i}\infty}^{1}\frac{t^k\mathrm{e}^{-2\mathrm{i}k_0zt}}{1-\mathrm{e}^{-2\mathrm{i}k_0dt}}\,\mathrm{d}t$$

and

$$I^2_{ll'm}(k_0z,k_0d)=\int_{\mathrm{i}\infty}^{1}\frac{\Delta^m_l(t)\pi^m_{l'}(t)+\pi^m_l(t)\Delta^m_{l'}(t)}{1-\mathrm{e}^{-2\mathrm{i}k_0dt}}\mathrm{e}^{-2\mathrm{i}k_0zt}\,\mathrm{d}t$$
$$=\sum_{k=0}^{l+l'-1}b_k(l,l',m)\int_{\mathrm{i}\infty}^{1}\frac{t^k\mathrm{e}^{-2\mathrm{i}k_0zt}}{1-\mathrm{e}^{-2\mathrm{i}k_0dt}}\,\mathrm{d}t$$

for some real-valued coefficients $a_k(l,l',m)$ and $b_k(l,l',m)$. This is clear since, see (3.12)

$$\Delta^m_l(t)=-\frac{(1-t^2)^{1/2}}{\sqrt{l(l+1)}}P^{m\prime}_l(t),\quad \pi^m_l(t)=\frac{m}{\sqrt{l(l+1)}\,(1-t^2)^{1/2}}P^m_l(t)$$

with special case

$$\Delta^0_l(t)=-\frac{1}{\sqrt{l(l+1)}}P^1_l(t),\quad \pi^0_l(t)=0$$

and

$$\Delta^m_l(t)\Delta^m_{l'}(t)+\pi^m_l(t)\pi^m_{l'}(t)=\sum_{k=0}^{l+l'}a_k(l,l',m)t^k$$
$$\Delta^m_l(t)\pi^m_{l'}(t)+\pi^m_l(t)\Delta^m_{l'}(t)=\sum_{k=0}^{l+l'-1}b_k(l,l',m)t^k$$

Both integrals $I^1_{ll'm}(k_0z,k_0d)$ and $I^2_{ll'm}(k_0z,k_0d)$ are symmetric in the l and l' indices.

The matrix entries of $A_{nn'}$ therefore are

$$A_{\tau\sigma ml\tau\sigma'l'm'}=-2\delta_{\sigma\sigma'}\delta_{mm'}C'_{ll'm}\mathrm{i}^{l-l'}\Big\{(-1)^{l+m+\tau+1}I^1_{ll'm}(-k_0z_-,k_0d)+I^1_{ll'm}(0,k_0d)$$
$$+(-1)^{l+l'}I^1_{ll'm}(0,k_0d)+(-1)^{l'+m+\tau+1}I^1_{ll'm}(k_0z_+,k_0d)\Big\}$$

and

$$A_{\tau\sigma ml\bar\tau\sigma'l'm'}=-2\mathrm{i}\delta_{\bar\sigma\sigma'}\delta_{mm'}C'_{ll'm}\mathrm{i}^{l-l'}(-1)^{\sigma}\Big\{-(-1)^{l+m+\tau}I^2_{ll'm}(-k_0z_-,k_0d)$$
$$+I^2_{ll'm}(0,k_0d)-(-1)^{l+l'}I^2_{ll'm}(0,k_0d)+(-1)^{l'+m+\tau}I^2_{ll'm}(k_0z_+,k_0d)\Big\}$$

The integrals $I^1_{ll'm}(k_0z, k_0d)$ and $I^2_{ll'm}(k_0z, k_0d)$ can both be evaluated in terms of the Lerch function [13], see Section B.1.

B.1 Lerch function

The main result in this section is that for $b > a > 0$, $n = 0, 1, 2, \ldots$

$$I_n(a,b) = \int_{\mathrm{i}\infty}^{1} \frac{t^n \mathrm{e}^{-\mathrm{i}at}}{1 - \mathrm{e}^{-\mathrm{i}bt}}\,\mathrm{d}t = \mathrm{e}^{\mathrm{i}(b-a)} \sum_{k=1}^{n+1} \frac{\mathrm{i}^k n!}{(n+1-k)!b^k} \Phi(\mathrm{e}^{\mathrm{i}b}, k, 1 - a/b)$$

where the Lerch function is [13]

$$\Phi(\beta, \nu, \mu) = \sum_{n=0}^{\infty} \frac{\beta^n}{(\mu+n)^\nu}$$

From [13, p. 353] we have

$$\int_0^\infty \frac{x^{\nu-1}\mathrm{e}^{-\mu x}}{1 - \beta \mathrm{e}^{-x}}\,\mathrm{d}x = \Gamma(\nu) \sum_{n=0}^{\infty} \frac{\beta^n}{(\mu+n)^\nu}, \quad \mathrm{Re}\,\mu > 0, |\beta| \le 1, \beta \neq 1, \mathrm{Re}\,\nu > 0$$

The sum on the right-hand side is Lerch function

$$\Phi(\beta, \nu, \mu) = \sum_{n=0}^{\infty} \frac{\beta^n}{(\mu+n)^\nu}$$

Introduce the parametrization of the integration path $t = 1 + \mathrm{i}x$, $x \in [0, \infty)$.

$$I_n(a,b) = \mathrm{i} \int_0^\infty \frac{(1+\mathrm{i}x)^n \mathrm{e}^{\mathrm{i}(b-a)(1+\mathrm{i}x)}}{1 - \mathrm{e}^{\mathrm{i}b(1+\mathrm{i}x)}}\,\mathrm{d}x = \mathrm{i}\mathrm{e}^{\mathrm{i}(b-a)} \int_0^\infty \frac{(1+\mathrm{i}x)^n \mathrm{e}^{-(b-a)x}}{1 - \mathrm{e}^{\mathrm{i}b}\mathrm{e}^{-bx}}\,\mathrm{d}x$$

The binomial expansion of the numerator implies

$$\begin{aligned} I_n(a,b) &= \mathrm{i}\mathrm{e}^{\mathrm{i}(b-a)} \sum_{k=0}^{n} \binom{n}{k} \mathrm{i}^k \int_0^\infty \frac{x^k \mathrm{e}^{-(b-a)x}}{1 - \mathrm{e}^{\mathrm{i}b}\mathrm{e}^{-bx}}\,\mathrm{d}x \\ &= \mathrm{i}\mathrm{e}^{\mathrm{i}(b-a)} \sum_{k=0}^{n} \binom{n}{k} \mathrm{i}^k \int_0^\infty \frac{b^{-k-1} y^k \mathrm{e}^{-(1-a/b)y}}{1 - \mathrm{e}^{\mathrm{i}b}\mathrm{e}^{-y}}\,\mathrm{d}y \end{aligned}$$

and in terms of Lerch function, we get

$$I_n(a,b) = \mathrm{e}^{\mathrm{i}(b-a)} \sum_{k=0}^{n} \frac{\mathrm{i}^{k+1} n!}{(n-k)!b^{k+1}} \Phi(\mathrm{e}^{\mathrm{i}b}, k+1, 1 - a/b)$$

The integrals $I^1_{ll'm}(k_0z, k_0d)$ and $I^2_{ll'm}(k_0z, k_0d)$ are

$$I^1_{ll'm}(k_0z, k_0d) = \sum_{k=0}^{l+l'} a_k(l, l', m) I_k(2k_0z, 2k_0d)$$

and

$$I^2_{ll'm}(k_0z, k_0d) = \sum_{k=0}^{l+l'-1} b_k(l, l', m) I_k(2k_0z, 2k_0d)$$

Appendix C The $\boldsymbol{F}_n(\boldsymbol{r})$ vector

The $\boldsymbol{F}_n(\boldsymbol{r})$ vector has the formal form, see (7.3) and (3.5)

$$\boldsymbol{F}_n(\boldsymbol{r}) = \frac{1}{k_0}\hat{\boldsymbol{z}} \times \nabla G_n(\boldsymbol{r}) + \frac{1}{k_0^2}\nabla \times (\hat{\boldsymbol{z}} \times \nabla H_{\overline{n}}(\boldsymbol{r}))$$

where

$$G_n(\boldsymbol{r}) = -\frac{1}{2\pi}\iint\limits_{\mathbb{R}^2}\left\{ B_{n1}^{\pm}(\boldsymbol{k}_\mathrm{t})\mathrm{e}^{\mathrm{i}\boldsymbol{k}_\mathrm{t}\cdot\boldsymbol{\rho}+\mathrm{i}k_z|z|} - \frac{B_{n1}^{+}(\boldsymbol{k}_\mathrm{t}) - B_{n1}^{-}(\boldsymbol{k}_\mathrm{t})\mathrm{e}^{-2\mathrm{i}k_z z_+}}{1-\mathrm{e}^{-2\mathrm{i}k_z d}}\mathrm{e}^{\mathrm{i}\boldsymbol{k}_\mathrm{t}\cdot\boldsymbol{\rho}+\mathrm{i}k_z z} \right.$$
$$\left. - \frac{B_{n1}^{-}(\boldsymbol{k}_\mathrm{t}) - B_{n1}^{+}(\boldsymbol{k}_\mathrm{t})\mathrm{e}^{2\mathrm{i}k_z z_-}}{1-\mathrm{e}^{-2\mathrm{i}k_z d}}\mathrm{e}^{\mathrm{i}\boldsymbol{k}_\mathrm{t}\cdot\boldsymbol{\rho}-\mathrm{i}k_z z} \right\}\frac{\mathrm{d}k_x\,\mathrm{d}k_y}{k_z k_\mathrm{t}}$$

and using (3.13)

$$H_n(\boldsymbol{r}) = -\frac{1}{2\pi}\iint\limits_{\mathbb{R}^2}\left\{ B_{n1}^{\pm}(\boldsymbol{k}_\mathrm{t})\mathrm{e}^{\mathrm{i}\boldsymbol{k}_\mathrm{t}\cdot\boldsymbol{\rho}+\mathrm{i}k_z|z|} - \frac{B_{n1}^{+}(\boldsymbol{k}_\mathrm{t}) + B_{n1}^{-}(\boldsymbol{k}_\mathrm{t})\mathrm{e}^{-2\mathrm{i}k_z z_+}}{1-\mathrm{e}^{-2\mathrm{i}k_z d}}\mathrm{e}^{\mathrm{i}\boldsymbol{k}_\mathrm{t}\cdot\boldsymbol{\rho}+\mathrm{i}k_z z} \right.$$
$$\left. - \frac{B_{n1}^{-}(\boldsymbol{k}_\mathrm{t}) + B_{n1}^{+}(\boldsymbol{k}_\mathrm{t})\mathrm{e}^{2\mathrm{i}k_z z_-}}{1-\mathrm{e}^{-2\mathrm{i}k_z d}}\mathrm{e}^{\mathrm{i}\boldsymbol{k}_\mathrm{t}\cdot\boldsymbol{\rho}-\mathrm{i}k_z z} \right\}\frac{\mathrm{d}k_x\,\mathrm{d}k_y}{k_z k_\mathrm{t}}$$

and the dual index of n is defined as $\overline{n} = \overline{\tau}\sigma ml$.

Both these functions satisfy

$$\nabla^2 G_n(\boldsymbol{r}) = -k_0^2 G_n(\boldsymbol{r}), \quad \nabla^2 H_n(\boldsymbol{r}) = -k_0^2 H_n(\boldsymbol{r})$$

and

$$\nabla_\mathrm{t}^2 G_n(\boldsymbol{r}) = -k_\mathrm{t}^2 G_n(\boldsymbol{r}), \quad \nabla_\mathrm{t}^2 H_n(\boldsymbol{r}) = -k_\mathrm{t}^2 H_n(\boldsymbol{r})$$

Perform the integration in polar coordinates, $\boldsymbol{k}_\mathrm{t} = k_\mathrm{t}(\cos\beta\hat{\boldsymbol{x}} + \sin\beta\hat{\boldsymbol{y}})$, and the integration in β gives

$$G_n(\boldsymbol{r}) = -\int_0^\infty \left\{ g_n^{\pm}(k_\mathrm{t},\phi)\mathrm{e}^{\mathrm{i}k_z|z|} \right.$$
$$\left. - \frac{g_n^{+}(k_\mathrm{t},\phi)\left(\mathrm{e}^{\mathrm{i}k_z z} - \mathrm{e}^{\mathrm{i}k_z(2z_- - z)}\right) + g_n^{-}(k_\mathrm{t},\phi)\left(\mathrm{e}^{-\mathrm{i}k_z z} - \mathrm{e}^{\mathrm{i}k_z(z-2z_+)}\right)}{1-\mathrm{e}^{-2\mathrm{i}k_z d}} \right\} J_m(k_\mathrm{t}\rho)\,\frac{\mathrm{d}k_\mathrm{t}}{k_z}$$

and

$$H_n(\boldsymbol{r}) = -\int_0^\infty \left\{ g_n^{\pm}(k_\mathrm{t},\phi)\mathrm{e}^{\mathrm{i}k_z|z|} \right.$$
$$\left. - \frac{g_n^{+}(k_\mathrm{t},\phi)\left(\mathrm{e}^{\mathrm{i}k_z z} + \mathrm{e}^{\mathrm{i}k_z(2z_- - z)}\right) + g_n^{-}(k_\mathrm{t},\phi)\left(\mathrm{e}^{-\mathrm{i}k_z z} + \mathrm{e}^{\mathrm{i}k_z(z-2z_+)}\right)}{1-\mathrm{e}^{-2\mathrm{i}k_z d}} \right\} J_m(k_\mathrm{t}\rho)\,\frac{\mathrm{d}k_\mathrm{t}}{k_z}$$

where we used [1]

$$\frac{1}{2\pi}\int_0^{2\pi}\begin{Bmatrix}\cos m\beta\\ \sin m\beta\end{Bmatrix}\mathrm{e}^{\mathrm{i}\boldsymbol{k}_\mathrm{t}\cdot\boldsymbol{\rho}}\,\mathrm{d}\beta=\mathrm{i}^m\begin{Bmatrix}\cos m\phi\\ \sin m\phi\end{Bmatrix}J_m(k_\mathrm{t}\rho) \tag{C.1}$$

and

$$\begin{aligned}g_n^{\pm}(k_\mathrm{t},\phi)&=\mathrm{i}^{-l+m+\tau}(\pm1)^{l+m}C_{lm}\\ &\times\left(\mp\delta_{\tau1}\Delta_l^m(k_z/k_0)\begin{Bmatrix}\cos m\phi\\ \sin m\phi\end{Bmatrix}+\delta_{\tau2}\pi_l^m(k_z/k_0)\begin{Bmatrix}-\sin m\phi\\ \cos m\phi\end{Bmatrix}\right)\end{aligned} \tag{C.2}$$

Notice that as functions of the complex k_t variable these functions have symmetry relations, *e.g.*, $g_n^{\pm}(k_\mathrm{t}\mathrm{e}^{-\mathrm{i}\pi},\phi)=\mathrm{e}^{-\mathrm{i}(m+1)\pi}g_n^{\pm}(k_\mathrm{t},\phi)$, since $\sin\left(z\mathrm{e}^{-\mathrm{i}\pi}\right)=\mathrm{e}^{-\mathrm{i}\pi}\sin z$, and $\cos\left(z\mathrm{e}^{-\mathrm{i}\pi}\right)=\cos z$. Moreover, $g_n^{\pm}(k_\mathrm{t},\phi)\to g_n^{\mp}(k_\mathrm{t},\phi)$ as $k_z\to-k_z$. For real argument (both k_t and k_z real), we also have $(g_n^{\pm}(k_\mathrm{t},\phi))^*=g_n^{\mp}(k_\mathrm{t},\phi)$.

The remaining integral in the k_t variable is performed by calculus of residues. A typical integral is

$$\begin{aligned}\int_0^\infty J_m(k_\mathrm{t}\rho)h(k_\mathrm{t})\,\mathrm{d}k_\mathrm{t}&=\frac{1}{2}\int_0^\infty\left(H_m^{(1)}(k_\mathrm{t}\rho)+H_m^{(2)}(k_\mathrm{t}\rho)\right)h(k_\mathrm{t})\,\mathrm{d}k_\mathrm{t}\\ &=\frac{1}{2}\int_0^\infty\left(H_m^{(1)}(k_\mathrm{t}\rho)-\mathrm{e}^{\mathrm{i}m\pi}H_m^{(1)}(k_\mathrm{t}\rho\mathrm{e}^{\mathrm{i}\pi})\right)h(k_\mathrm{t})\,\mathrm{d}k_\mathrm{t}\\ &=\frac{1}{2}\int_0^\infty H_m^{(1)}(k_\mathrm{t}\rho)h(k_\mathrm{t})\,\mathrm{d}k_\mathrm{t}+\frac{1}{2}\mathrm{e}^{\mathrm{i}(m+1)\pi}\int_{-\infty}^0 H_m^{(1)}(k_\mathrm{t}\rho)h(k_\mathrm{t}\mathrm{e}^{-\mathrm{i}\pi})\,\mathrm{d}k_\mathrm{t}\end{aligned}$$

where we used $H_m^{(2)}(k_\mathrm{t}\rho\mathrm{e}^{-\mathrm{i}\pi})=-\mathrm{e}^{\mathrm{i}m\pi}H_m^{(1)}(k_\mathrm{t}\rho)$. If $h(k_\mathrm{t}\mathrm{e}^{-\mathrm{i}\pi})=\mathrm{e}^{-\mathrm{i}(m+1)\pi}h(k_\mathrm{t})$, then

$$\begin{aligned}\int_{C_1}J_m(k_\mathrm{t}\rho)h(k_\mathrm{t})\,\mathrm{d}k_\mathrm{t}&=\int_0^\infty J_m(k_\mathrm{t}\rho)h(k_\mathrm{t})\,\mathrm{d}k_\mathrm{t}\\ &=\frac{1}{2}\int_{-\infty}^\infty H_m^{(1)}(k_\mathrm{t}\rho)h(k_\mathrm{t})\,\mathrm{d}k_\mathrm{t}=\frac{1}{2}\int_C H_m^{(1)}(k_\mathrm{t}\rho)h(k_\mathrm{t})\,\mathrm{d}k_\mathrm{t}\end{aligned}$$

where the contours C_1 and C are depicted in Figure 4. Rewrite in terms of the contour integral C as

$$\begin{aligned}G_n(\boldsymbol{r})=-\frac{1}{2}\int_C\Bigg\{&g_n^{\pm}(k_\mathrm{t},\phi)\mathrm{e}^{\mathrm{i}k_z|z|}\\ &-\frac{g_n^{+}(k_\mathrm{t},\phi)\left(\mathrm{e}^{\mathrm{i}k_zz}-\mathrm{e}^{\mathrm{i}k_z(2z_--z)}\right)+g_n^{-}(k_\mathrm{t},\phi)\left(\mathrm{e}^{-\mathrm{i}k_zz}-\mathrm{e}^{\mathrm{i}k_z(z-2z_+)}\right)}{1-\mathrm{e}^{-2\mathrm{i}k_zd}}\Bigg\}H_m^{(1)}(k_\mathrm{t}\rho)\,\frac{\mathrm{d}k_\mathrm{t}}{k_z}\end{aligned}$$

and

$$\begin{aligned}H_n(\boldsymbol{r})=-\frac{1}{2}\int_C\Bigg\{&g_n^{\pm}(k_\mathrm{t},\phi)\mathrm{e}^{\mathrm{i}k_z|z|}\\ &-\frac{g_n^{+}(k_\mathrm{t},\phi)\left(\mathrm{e}^{\mathrm{i}k_zz}+\mathrm{e}^{\mathrm{i}k_z(2z_--z)}\right)+g_n^{-}(k_\mathrm{t},\phi)\left(\mathrm{e}^{-\mathrm{i}k_zz}+\mathrm{e}^{\mathrm{i}k_z(z-2z_+)}\right)}{1-\mathrm{e}^{-2\mathrm{i}k_zd}}\Bigg\}H_m^{(1)}(k_\mathrm{t}\rho)\,\frac{\mathrm{d}k_\mathrm{t}}{k_z}\end{aligned}$$

Closing the contour in the upper k_t plane gives residue contributions at the poles $k_\mathrm{t} = k_{\mathrm{t}p}$, but the branch cut for $H_0(k_\mathrm{t}\rho)$ is not crossed. The contributions of the residues at the poles, $k_\mathrm{t} = k_{\mathrm{t}p} = (k_0^2 - p^2\pi^2/d^2)^{1/2}$ are, *cf.*, the residues in Section D

$$\begin{aligned} G_n(\boldsymbol{r}) &= -\frac{\pi}{4k_0 d}\sum_{p=1}^{\infty}\varepsilon_p\frac{k_0}{k_{\mathrm{t}p}}\Big\{g_n^+(k_{\mathrm{t}p},\phi)\left(\mathrm{e}^{\mathrm{i}\pi pz/d} - \mathrm{e}^{-\mathrm{i}\pi p(z-2z_-)/d}\right) \\ &\qquad + g_n^-(k_{\mathrm{t}p},\phi)\left(\mathrm{e}^{-\mathrm{i}\pi pz/d} - \mathrm{e}^{-\mathrm{i}\pi p(2z_+-z)/d}\right)\Big\}H_m^{(1)}(k_{\mathrm{t}p}\rho) \\ &= -\frac{\mathrm{i}\pi}{2k_0 d}\sum_{p=1}^{\infty}\varepsilon_p\frac{k_0}{k_{\mathrm{t}p}}\Big\{g_n^+(k_{\mathrm{t}p},\phi)\mathrm{e}^{\mathrm{i}\pi pz_-/d}\sin(\pi p(z-z_-)/d) \\ &\qquad - g_n^-(k_{\mathrm{t}p},\phi)\mathrm{e}^{-\mathrm{i}\pi pz_+/d}\sin(\pi p(z-z_+)/d)\Big\}H_m^{(1)}(k_{\mathrm{t}p}\rho) \end{aligned} \tag{C.3}$$

and

$$\begin{aligned} H_n(\boldsymbol{r}) &= -\frac{\pi}{4k_0 d}\sum_{p=0}^{\infty}\varepsilon_p\frac{k_0}{k_{\mathrm{t}p}}\Big\{g_n^+(k_{\mathrm{t}p},\phi)\left(\mathrm{e}^{\mathrm{i}\pi pz/d} + \mathrm{e}^{-\mathrm{i}\pi p(z-2z_-)/d}\right) \\ &\qquad + g_n^-(k_{\mathrm{t}p},\phi)\left(\mathrm{e}^{-\mathrm{i}\pi pz/d} + \mathrm{e}^{-\mathrm{i}\pi p(2z_+-z)/d}\right)\Big\}H_m^{(1)}(k_{\mathrm{t}p}\rho) \\ &= -\frac{\pi}{2k_0 d}\sum_{p=0}^{\infty}\varepsilon_p\frac{k_0}{k_{\mathrm{t}p}}\Big\{g_n^+(k_{\mathrm{t}p},\phi)\mathrm{e}^{\mathrm{i}\pi pz_-/d}\cos(\pi p(z-z_-)/d) \\ &\qquad + g_n^-(k_{\mathrm{t}p},\phi)\mathrm{e}^{-\mathrm{i}\pi pz_+/d}\cos(\pi p(z-z_+)/d)\Big\}H_m^{(1)}(k_{\mathrm{t}p}\rho) \end{aligned} \tag{C.4}$$

Only a finite number of terms contribute in the sum is not exponentially decreasing, *i.e.*, only those p values satisfying $p \le k_0 d/\pi$, contribute to the radiated field. The functions $G_n(\boldsymbol{r})$ and $H_n(\boldsymbol{r})$ satisfy

$$\nabla\times(\hat{\boldsymbol{z}}\times\nabla G_n) = \hat{\boldsymbol{z}}\nabla^2 G_n - \frac{\partial}{\partial z}\nabla G_n = -\hat{\boldsymbol{z}}k_0^2 G_n - \nabla\frac{\partial}{\partial z}G_n$$

and

$$\nabla\times(\hat{\boldsymbol{z}}\times\nabla H_n) = -\hat{\boldsymbol{z}}k_0^2 H_n - \nabla\frac{\partial}{\partial z}H_n$$

This implies

$$\begin{cases} \hat{\boldsymbol{z}}\cdot(\nabla\times(\hat{\boldsymbol{z}}\times\nabla G_n)) = \nabla_\mathrm{t}^2 G_n = -k_\mathrm{t}^2 G_n(\boldsymbol{r}) \\ \hat{\boldsymbol{z}}\cdot(\nabla\times(\hat{\boldsymbol{z}}\times\nabla H_n)) = \nabla_\mathrm{t}^2 H_n = -k_\mathrm{t}^2 H_n(\boldsymbol{r}) \end{cases} \tag{C.5}$$

Notice that on $\boldsymbol{r}_\pm = \boldsymbol{\rho} + z_\pm\hat{\boldsymbol{z}}$

$$G_n(\boldsymbol{r}_\pm) = 0, \quad \nabla_\mathrm{t} G_n(\boldsymbol{r}_\pm) = 0, \quad \frac{\partial}{\partial z}H_n(\boldsymbol{r}_\pm) = 0 \tag{C.6}$$

In terms of the circular cylindrical coordinate system, the components are

$$\boldsymbol{F}_n(\boldsymbol{r}) = \hat{\boldsymbol{\rho}} F_{n\rho}(\boldsymbol{r}) + \hat{\boldsymbol{\phi}} F_{n\phi}(\boldsymbol{r}) + \hat{\boldsymbol{z}} F_{nz}(\boldsymbol{r})$$

where

$$\begin{aligned}
\hat{\boldsymbol{\rho}} \cdot \boldsymbol{F}_n(\boldsymbol{r}) &= -\frac{1}{k_0} \hat{\boldsymbol{\phi}} \cdot \nabla G_n(\boldsymbol{r}) - \frac{1}{k_0^2} \hat{\boldsymbol{\rho}} \cdot \nabla \frac{\partial}{\partial z} H_{\overline{n}} \\
&= \frac{\mathrm{i}\pi}{2k_0 d} \sum_{p=1}^{\infty} \varepsilon_p \Bigg\{ \frac{\partial g_n^+(k_{\mathrm{t}p}, \phi)}{\partial \phi} \mathrm{e}^{\mathrm{i}\pi p z_-/d} \sin(\pi p (z - z_-)/d) \frac{H_m^{(1)}(k_{\mathrm{t}p}\rho)}{k_{\mathrm{t}p}\rho} \\
&\quad - \frac{\partial g_n^-(k_{\mathrm{t}p}, \phi)}{\partial \phi} \mathrm{e}^{-\mathrm{i}\pi p z_+/d} \sin(\pi p (z - z_+)/d) \frac{H_m^{(1)}(k_{\mathrm{t}p}\rho)}{k_{\mathrm{t}p}\rho} \\
&\quad + \mathrm{i} \frac{p\pi}{k_0 d} g_{\overline{n}}^+(k_{\mathrm{t}p}, \phi) \mathrm{e}^{\mathrm{i}\pi p z_-/d} \sin(\pi p (z - z_-)/d) H_m^{(1)\prime}(k_{\mathrm{t}p}\rho) \\
&\quad + \mathrm{i} \frac{p\pi}{k_0 d} g_{\overline{n}}^-(k_{\mathrm{t}p}, \phi) \mathrm{e}^{-\mathrm{i}\pi p z_+/d} \sin(\pi p (z - z_+)/d) H_m^{(1)\prime}(k_{\mathrm{t}p}\rho) \Bigg\}
\end{aligned} \tag{C.7}$$

and

$$\begin{aligned}
\hat{\boldsymbol{\phi}} \cdot \boldsymbol{F}_n(\boldsymbol{r}) &= \frac{1}{k_0} \hat{\boldsymbol{\rho}} \cdot \nabla G_n(\boldsymbol{r}) - \frac{1}{k_0^2} \hat{\boldsymbol{\phi}} \cdot \nabla \frac{\partial}{\partial z} H_{\overline{n}} \\
&= \frac{\mathrm{i}\pi}{2k_0 d} \sum_{p=1}^{\infty} \varepsilon_p \Bigg\{ - g_n^+(k_{\mathrm{t}p}, \phi) \mathrm{e}^{\mathrm{i}\pi p z_-/d} \sin(\pi p (z - z_-)/d) H_m^{(1)\prime}(k_{\mathrm{t}p}\rho) \\
&\quad + g_n^-(k_{\mathrm{t}p}, \phi) \mathrm{e}^{-\mathrm{i}\pi p z_+/d} \sin(\pi p (z - z_+)/d) H_m^{(1)\prime}(k_{\mathrm{t}p}\rho) \\
&\quad + \mathrm{i} \frac{p\pi}{k_0 d} \frac{\partial g_{\overline{n}}^+(k_{\mathrm{t}p}, \phi)}{\partial \phi} \mathrm{e}^{\mathrm{i}\pi p z_-/d} \sin(\pi p (z - z_-)/d) \frac{H_m^{(1)}(k_{\mathrm{t}p}\rho)}{k_{\mathrm{t}p}\rho} \\
&\quad + \mathrm{i} \frac{p\pi}{k_0 d} \frac{\partial g_{\overline{n}}^-(k_{\mathrm{t}p}, \phi)}{\partial \phi} \mathrm{e}^{-\mathrm{i}\pi p z_+/d} \sin(\pi p (z - z_+)/d) \frac{H_m^{(1)}(k_{\mathrm{t}p}\rho)}{k_{\mathrm{t}p}\rho} \Bigg\}
\end{aligned} \tag{C.8}$$

and

$$\begin{aligned}
\hat{\boldsymbol{z}} \cdot \boldsymbol{F}_n(\boldsymbol{r}) &= \frac{\pi}{2k_0 d} \sum_{p=0}^{\infty} \varepsilon_p \frac{k_{\mathrm{t}p}}{k_0} \Bigg\{ g_{\overline{n}}^+(k_{\mathrm{t}p}, \phi) \mathrm{e}^{\mathrm{i}\pi p z_-/d} \cos(\pi p (z - z_-)/d) \\
&\quad + g_{\overline{n}}^-(k_{\mathrm{t}p}, \phi) \mathrm{e}^{-\mathrm{i}\pi p z_+/d} \cos(\pi p (z - z_+)/d) \Bigg\} H_m^{(1)}(k_{\mathrm{t}p}\rho)
\end{aligned} \tag{C.9}$$

C.1 Power flux

To compute the power flux in the $\hat{\boldsymbol{\nu}}$ direction, we need to evaluate the following integral: $(\hat{\boldsymbol{\nu}} \cdot \hat{\boldsymbol{z}} = 0)$

$$\begin{aligned}\frac{1}{k_0}\hat{\boldsymbol{\nu}} \cdot (\boldsymbol{F}_n \times (\nabla \times \boldsymbol{F}^*_{n'})) = \hat{\boldsymbol{\nu}} \cdot \Bigg\{ &\left(\frac{1}{k_0}\hat{\boldsymbol{z}} \times \nabla G_n + \frac{1}{k_0^2}\nabla \times (\hat{\boldsymbol{z}} \times \nabla H_{\overline{n}})\right) \\ &\times \left(\frac{1}{k_0^2}\nabla \times (\hat{\boldsymbol{z}} \times \nabla G^*_{n'}) + \frac{1}{k_0}\hat{\boldsymbol{z}} \times \nabla H^*_{\overline{n'}}\right)\Bigg\} \\ = \frac{1}{k_0^3}\hat{\boldsymbol{\nu}} \cdot \{&(\hat{\boldsymbol{z}} \times \nabla G_n) \times (\nabla \times (\hat{\boldsymbol{z}} \times \nabla G^*_{n'}))\} \\ + \frac{1}{k_0^4}\hat{\boldsymbol{\nu}} \cdot \{&(\nabla \times (\hat{\boldsymbol{z}} \times \nabla H_{\overline{n}})) \times (\nabla \times (\hat{\boldsymbol{z}} \times \nabla G^*_{n'}))\} \\ + \frac{1}{k_0^3}\hat{\boldsymbol{\nu}} \cdot \big\{&(\nabla \times (\hat{\boldsymbol{z}} \times \nabla H_{\overline{n}})) \times \big(\hat{\boldsymbol{z}} \times \nabla H^*_{\overline{n'}}\big)\big\}\end{aligned}$$

Rewrite as, see (C.5)

$$\begin{aligned}\frac{1}{k_0}\hat{\boldsymbol{\nu}} \cdot (\boldsymbol{F}_n \times (\nabla \times \boldsymbol{F}^*_{n'})) = &\frac{1}{k_0^3}\left(\hat{\boldsymbol{\nu}} \cdot \nabla_{\mathrm{t}} G_n\right)\nabla_{\mathrm{t}}^2 G^*_{n'} - \frac{1}{k_0^3}\left(\hat{\boldsymbol{\nu}} \cdot \nabla_{\mathrm{t}} H^*_{\overline{n'}}\right)\nabla_{\mathrm{t}}^2 H_{\overline{n}} \\ &+ \frac{1}{k_0^4}\hat{\boldsymbol{\nu}} \cdot \left\{\left(\hat{\boldsymbol{z}}k_0^2 H_{\overline{n}} + \nabla\frac{\partial}{\partial z}H_{\overline{n}}\right) \times \left(\hat{\boldsymbol{z}}k_0^2 G^*_{n'} + \nabla\frac{\partial}{\partial z}G^*_{n'}\right)\right\} \\ = &\frac{1}{k_0^3}\left(\hat{\boldsymbol{\nu}} \cdot \nabla_{\mathrm{t}} G_n\right)\nabla_{\mathrm{t}}^2 G^*_{n'} - \frac{1}{k_0^3}\left(\hat{\boldsymbol{\nu}} \cdot \nabla_{\mathrm{t}} H^*_{\overline{n'}}\right)\nabla_{\mathrm{t}}^2 H_{\overline{n}} \\ &- \frac{1}{k_0^2}\hat{\boldsymbol{\nu}} \cdot \left\{H_{\overline{n}}\nabla_{\mathrm{t}} \times \left(\hat{\boldsymbol{z}}\frac{\partial}{\partial z}G^*_{n'}\right) - G^*_{n'}\nabla_{\mathrm{t}} \times \left(\hat{\boldsymbol{z}}\frac{\partial}{\partial z}H_{\overline{n}}\right)\right\} \\ &+ \frac{1}{k_0^4}\hat{\boldsymbol{\nu}} \cdot \left\{\nabla \times \left(\frac{\partial}{\partial z}H_{\overline{n}}\nabla\frac{\partial}{\partial z}G^*_{n'}\right)\right\}\end{aligned} \tag{C.10}$$

If we integrate over a cylindrical surface between the two parallel plates, $z = z_\pm$, the last term vanishes due to Stokes' theorem, and the fact that $\partial_z H_n$ vanishes on $z = z_\pm$, see (C.6). The second last term also vanishes, since the term can rewrite as

$$\begin{aligned}&\hat{\boldsymbol{\nu}} \cdot \left\{H_{\overline{n}}\nabla_{\mathrm{t}} \times \left(\hat{\boldsymbol{z}}\frac{\partial}{\partial z}G^*_{n'}\right) - G^*_{n'}\nabla_{\mathrm{t}} \times \left(\hat{\boldsymbol{z}}\frac{\partial}{\partial z}H_{\overline{n}}\right)\right\} \\ =&\hat{\boldsymbol{\nu}} \cdot \left\{H_{\overline{n}}\nabla_{\mathrm{t}} \times \left(\hat{\boldsymbol{z}}\frac{\partial}{\partial z}G^*_{n'}\right) + \frac{\partial}{\partial z}H_{\overline{n}}\nabla_{\mathrm{t}} \times (\hat{\boldsymbol{z}}G^*_{n'}) - \nabla_{\mathrm{t}} \times \left(\hat{\boldsymbol{z}}\left(\frac{\partial}{\partial z}H_{\overline{n}}\right)G^*_{n'}\right)\right\} \\ =&\frac{\partial}{\partial z}\hat{\boldsymbol{\nu}} \cdot \{H_{\overline{n}}\nabla_{\mathrm{t}} \times (\hat{\boldsymbol{z}}G^*_{n'})\} - \hat{\boldsymbol{\nu}} \cdot \left\{\nabla_{\mathrm{t}} \times \left(\hat{\boldsymbol{z}}\left(\frac{\partial}{\partial z}H_{\overline{n}}\right)G^*_{n'}\right)\right\}\end{aligned}$$

and both these terms vanish when integrating over a cylindrical surface between the two parallel plates, $z = z_\pm$ — the first term due to an exact z derivative and the fact that $\nabla_{\mathrm{t}} G^*_{n'}$ vanishes on $z = z_\pm$, and the second term vanishes due to Stokes' theorem and the fact that $G^*_{n'}$ vanishes on $z = z_\pm$, see (C.6). The conclusion of this

analysis is that only the first two terms in (C.10) contribute to the final result of an integral over a cylindrical surface between the two parallel plates, $z = z_{\pm}$.

To evaluate the power flux through a cylindrical surface, we need to evaluate four canonical integrals w.r.t. z, *viz.*, ($d = z_+ - z_-$, $p, p' = 0, 1, 2, \ldots$)

$$\begin{aligned}
&\int_{z_-}^{z_+} \sin\left(\pi p(z - z_-)/d\right) \sin\left(\pi p'(z - z_-)/d\right)\, \mathrm{d}z \\
&\quad = \int_{z_-}^{z_+} \sin\left(\pi p(z - z_+)/d\right) \sin\left(\pi p'(z - z_+)/d\right)\, \mathrm{d}z \\
&\quad = \frac{d}{\pi} \int_0^{\pi} \sin pt \sin p't\, \mathrm{d}t = \frac{d}{2}\delta_{pp'}(1 - \delta_{p0}) \\
&\int_{z_-}^{z_+} \sin\left(\pi p(z - z_-)/d\right) \sin\left(\pi p'(z - z_+)/d\right)\, \mathrm{d}z \\
&\quad = \int_{z_-}^{z_+} \sin\left(\pi p(z - z_+)/d\right) \sin\left(\pi p'(z - z_-)/d\right)\, \mathrm{d}z \\
&\quad = \frac{d}{\pi} \int_0^{\pi} \sin pt \sin p'(t - \pi)\, \mathrm{d}t = (-1)^p \frac{d}{2}\delta_{pp'}(1 - \delta_{p0})
\end{aligned}$$

and

$$\begin{aligned}
&\int_{z_-}^{z_+} \cos\left(\pi p(z - z_-)/d\right) \cos\left(\pi p'(z - z_-)/d\right)\, \mathrm{d}z \\
&\quad = \int_{z_-}^{z_+} \cos\left(\pi p(z - z_+)/d\right) \cos\left(\pi p'(z - z_+)/d\right)\, \mathrm{d}z \\
&\quad = \frac{d}{\pi} \int_0^{\pi} \cos pt \cos p't\, \mathrm{d}t = \frac{d}{\varepsilon_p}\delta_{pp'}
\end{aligned}$$

where ε_p is the Neumann factor, and similarly

$$\begin{aligned}
&\int_{z_-}^{z_+} \cos\left(\pi p(z - z_-)/d\right) \cos\left(\pi p'(z - z_+)/d\right)\, \mathrm{d}z \\
&\quad = \int_{z_-}^{z_+} \cos\left(\pi p(z - z_+)/d\right) \cos\left(\pi p'(z - z_-)/d\right)\, \mathrm{d}z \\
&\quad = \frac{d}{\pi} \int_0^{\pi} \cos pt \cos p'(t - \pi)\, \mathrm{d}t = (-1)^p \frac{d}{\varepsilon_p}\delta_{pp'}
\end{aligned}$$

The two canonical integrals w.r.t. z, then become ($d = z_+ - z_-$, $p, p' = 0, 1, 2, \ldots$)

$$\begin{aligned}
&\int_{z_-}^{z_+} \left\{ a^- \sin\left(\pi p(z - z_-)/d\right) + a^+ \sin\left(\pi p(z - z_+)/d\right) \right\} \\
&\qquad \left\{ b^- \sin\left(\pi p'(z - z_-)/d\right) + b^+ \sin\left(\pi p'(z - z_+)/d\right) \right\} \mathrm{d}z \\
&\quad = \frac{d}{2}\delta_{pp'}(1 - \delta_{p0}) \left(a^+ b^+ + a^- b^- + (-1)^p (a^+ b^- + a^+ b^-) \right) \\
&\quad = \frac{d}{2}\delta_{pp'}(1 - \delta_{p0}) \left(a^+ + (-1)^p a^- \right) \left(b^+ + (-1)^p b^- \right)
\end{aligned} \tag{C.11}$$

and

$$\begin{aligned}
&\int_{z_-}^{z_+} \left\{ a^- \cos\left(\pi p(z-z_-)/d\right) + a^+ \cos\left(\pi p(z-z_+)/d\right) \right\} \\
&\qquad \left\{ b^- \cos\left(\pi p'(z-z_-)/d\right) + b^+ \cos\left(\pi p'(z-z_+)/d\right) \right\} \mathrm{d}z \\
=&\frac{d}{\varepsilon_p}\delta_{pp'}\left(a^+b^+ + a^-b^- + (-1)^p(a^+b^- + a^+b^-)\right) \\
=&\frac{d}{\varepsilon_p}\delta_{pp'}\left(a^+ + (-1)^p a^-\right)\left(b^+ + (-1)^p b^-\right)
\end{aligned} \tag{C.12}$$

Only considering the propagating modes, *i.e.*, only terms in the sums with integers $p < k_0 d/\pi$, the power flux P through a cylindrical surface S, $\rho =$ constant, $\hat{\boldsymbol{\nu}} = \hat{\boldsymbol{\rho}}$, then becomes, see (C.10), (C.3), (C.4), (C.11), and (C.12)

$$\begin{aligned}
&\frac{1}{k_0}\iint_S \hat{\boldsymbol{\rho}} \cdot \left(\boldsymbol{F}_n \times (\nabla \times \boldsymbol{F}^*_{n'})\right) \mathrm{d}S = \frac{1}{k_0^3}\iint_S \hat{\boldsymbol{\rho}} \cdot \left\{ \nabla_{\mathrm{t}} G_n \nabla_{\mathrm{t}}^2 G^*_{n'} - \nabla_{\mathrm{t}}^2 H_{\overline{n}} \nabla_{\mathrm{t}} H^*_{\overline{n'}} \right\} \mathrm{d}S \\
=&\rho d \left(\frac{\pi}{2k_0 d}\right)^2 \sum_{p=0}^{[k_0 d/\pi]} \varepsilon_p \frac{k_{\mathrm{t}p}}{k_0} H_m^{(1)}(k_{\mathrm{t}p}\rho) H_{m'}^{(1)\prime *}(k_{\mathrm{t}p}\rho) \\
&\times \int_0^{2\pi} \left(g^+_{\overline{n}}(k_{\mathrm{t}p},\phi)\mathrm{e}^{\mathrm{i}\pi p z_-/d} + (-1)^p g^-_{\overline{n}}(k_{\mathrm{t}p},\phi)\mathrm{e}^{-\mathrm{i}\pi p z_+/d}\right) \\
&\qquad \left(g^{+\,*}_{\overline{n'}}(k_{\mathrm{t}p},\phi)\mathrm{e}^{-\mathrm{i}\pi p z_-/d} + (-1)^p g^{-\,*}_{\overline{n'}}(k_{\mathrm{t}p},\phi)\mathrm{e}^{\mathrm{i}\pi p z_+/d}\right) \mathrm{d}\phi \\
&- 2\rho d \left(\frac{\pi}{2k_0 d}\right)^2 \sum_{p=1}^{[k_0 d/\pi]} \frac{k_{\mathrm{t}p}}{k_0} H_m^{(1)\prime}(k_{\mathrm{t}p}\rho) H_{m'}^{(1)*}(k_{\mathrm{t}p}\rho) \\
&\times \int_0^{2\pi} \left(g^+_{n}(k_{\mathrm{t}p},\phi)\mathrm{e}^{\mathrm{i}\pi p z_-/d} - (-1)^p g^-_{n}(k_{\mathrm{t}p},\phi)\mathrm{e}^{-\mathrm{i}\pi p z_+/d}\right) \\
&\qquad \left(g^{+\,*}_{n'}(k_{\mathrm{t}p},\phi)\mathrm{e}^{-\mathrm{i}\pi p z_-/d} - (-1)^p g^{-\,*}_{n'}(k_{\mathrm{t}p},\phi)\mathrm{e}^{\mathrm{i}\pi p z_+/d}\right) \mathrm{d}\phi
\end{aligned}$$

Note that the value of the flux is independent of the surface S as long as the surface encloses the scatterer S_{s}. We will use this fact, and evaluate the flux in the limit as the cylindrical surface approaches infinity, *i.e.*, $\rho \to \infty$.

It is convenient to introduce the following notion (read the first (second) $\pm$ on the left-hand side together with the first (second) $\pm$ sign on the right-hand side):

$$I^{\pm\pm}_{nn'}(k_{\mathrm{t}p}) = \int_0^{2\pi} g^{\pm}_n(k_{\mathrm{t}p},\phi) g^{\pm\,*}_{n'}(k_{\mathrm{t}p},\phi)\, \mathrm{d}\phi$$

Since for *propagating* modes $(g^{\pm}_n(k_{\mathrm{t}},\phi))^* = g^{\mp}_n(k_{\mathrm{t}},\phi)$, we have

$$\left(I^{+\pm}_{nn'}(k_{\mathrm{t}p})\right)^* = I^{-\mp}_{nn'}(k_{\mathrm{t}p}), \quad \left(I^{-\pm}_{nn'}(k_{\mathrm{t}p})\right)^* = I^{+\mp}_{nn'}(k_{\mathrm{t}p}) \tag{C.13}$$

We also have the symmetries

$$\left(I^{+\pm}_{nn'}(k_{\mathrm{t}p})\right)^* = I^{\pm+}_{n'n}(k_{\mathrm{t}p}), \quad \left(I^{-\pm}_{nn'}(k_{\mathrm{t}p})\right)^* = I^{\pm-}_{n'n}(k_{\mathrm{t}p}) \tag{C.14}$$

Explicit values of $I^{\pm\pm}_{nn'}(k_{\mathrm{t}p})$ for $m > 0$

$$I^{+\pm}_{nn'}(k_{\mathrm{t}p}) = \pi\delta_{mm'}\mathrm{i}^{l'-l}C_{lm}C_{l'm}(\pm 1)^{l'+m}$$
$$\Big\{\delta_{\sigma\sigma'}\left\{\pm\delta_{\tau 1}\delta_{\tau' 1}\Delta^m_l(p\pi/k_0d)\Delta^m_{l'}(p\pi/k_0d) + \delta_{\tau 2}\delta_{\tau' 2}\pi^m_l(p\pi/k_0d)\pi^m_{l'}(p\pi/k_0d)\right\}$$
$$-\mathrm{i}\delta_{\sigma\overline{\sigma'}}(-1)^{\sigma}\left\{\delta_{\tau 1}\delta_{\tau' 2}\Delta^m_l(p\pi/k_0d)\pi^m_{l'}(p\pi/k_0d) \pm \delta_{\tau 2}\delta_{\tau' 1}\pi^m_l(p\pi/k_0d)\Delta^m_{l'}(p\pi/k_0d)\right\}\Big\}$$

and

$$I^{-\pm}_{nn'}(k_{\mathrm{t}p}) = \pi\delta_{mm'}\mathrm{i}^{l'-l}C_{lm}C_{l'm}(-1)^{l+m}(\pm 1)^{l'+m}$$
$$\Big\{\delta_{\sigma\sigma'}\left\{\mp\delta_{\tau 1}\delta_{\tau' 1}\Delta^m_l(p\pi/k_0d)\Delta^m_{l'}(p\pi/k_0d) + \delta_{\tau 2}\delta_{\tau' 2}\pi^m_l(p\pi/k_0d)\pi^m_{l'}(p\pi/k_0d)\right\}$$
$$+\mathrm{i}\delta_{\sigma\overline{\sigma'}}(-1)^{\sigma}\left\{\delta_{\tau 1}\delta_{\tau' 2}\Delta^m_l(p\pi/k_0d)\pi^m_{l'}(p\pi/k_0d) \mp \delta_{\tau 2}\delta_{\tau' 1}\pi^m_l(p\pi/k_0d)\Delta^m_{l'}(p\pi/k_0d)\right\}\Big\}$$

where the function $g^{\pm}_n(k_{\mathrm{t}}, \phi)$ in (C.2) has been used, and where

$$(-1)^{\sigma} = \begin{cases} -1, & \sigma = \mathrm{e} \\ 1, & \sigma = \mathrm{o} \end{cases}$$

The explicit values for $m = 0$ are

$$I^{+\pm}_{nn'}(k_{\mathrm{t}p}) = \pm 2\pi\delta_{mm'}\mathrm{i}^{l'-l}C_{lm}C_{l'm}(\pm 1)^{l'}\delta_{\sigma\mathrm{e}}\delta_{\sigma'\mathrm{e}}\delta_{\tau 1}\delta_{\tau' 1}\Delta^m_l(p\pi/k_0d)\Delta^m_{l'}(p\pi/k_0d)$$

and

$$I^{-\pm}_{nn'}(k_{\mathrm{t}p}) = \mp 2\pi\delta_{mm'}\mathrm{i}^{l'-l}C_{lm}C_{l'm}(-1)^{l}(\pm 1)^{l'}\delta_{\sigma\mathrm{e}}\delta_{\sigma'\mathrm{e}}\delta_{\tau 1}\delta_{\tau' 1}\Delta^m_l(p\pi/k_0d)\Delta^m_{l'}(p\pi/k_0d)$$

This integral is diagonal in the m index, and we get

$$\frac{1}{k_0}\iint_S \hat{\boldsymbol{\rho}}\cdot(\boldsymbol{F}_n \times (\nabla \times \boldsymbol{F}^*_{n'}))\,\mathrm{d}S$$
$$= \rho d\left(\frac{\pi}{2k_0d}\right)^2 \sum_{p=0}^{[k_0d/\pi]} \varepsilon_p \frac{k_{\mathrm{t}p}}{k_0} H^{(1)}_m(k_{\mathrm{t}p}\rho)H^{(1)'*}_m(k_{\mathrm{t}p}\rho)$$
$$\times\left(I^{++}_{\overline{n}\overline{n'}}(k_{\mathrm{t}p}) + I^{--}_{\overline{n}\overline{n'}}(k_{\mathrm{t}p}) + I^{+-}_{\overline{n}\overline{n'}}(k_{\mathrm{t}p})\mathrm{e}^{2\pi\mathrm{i}pz_-/d} + I^{-+}_{\overline{n}\overline{n'}}(k_{\mathrm{t}p})\mathrm{e}^{-2\pi\mathrm{i}pz_+/d}\right)$$
$$- 2\rho d\left(\frac{\pi}{2k_0d}\right)^2 \sum_{p=1}^{[k_0d/\pi]} \frac{k_{\mathrm{t}p}}{k_0} H^{(1)'}_m(k_{\mathrm{t}p}\rho)H^{(1)*}_m(k_{\mathrm{t}p}\rho)$$
$$\times\left(I^{++}_{nn'}(k_{\mathrm{t}p}) + I^{--}_{nn'}(k_{\mathrm{t}p}) - I^{+-}_{nn'}(k_{\mathrm{t}p})\mathrm{e}^{2\pi\mathrm{i}pz_-/d} - I^{-+}_{nn'}(k_{\mathrm{t}p})\mathrm{e}^{-2\pi\mathrm{i}pz_+/d}\right)$$

We extract the first mode, $p = 0$, $k_{\mathrm{t}p} = k_0$, since this is special is special and always propagate. The result is (use $I^{++}_{nn'}(k_0) = I^{+-}_{nn'}(k_0) = I^{-+}_{nn'}(k_0) = I^{--}_{nn'}(k_0)$)

$$
\begin{aligned}
&\frac{1}{k_0}\iint_S \hat{\boldsymbol{\rho}}\cdot(\boldsymbol{F}_n\times(\nabla\times\boldsymbol{F}^*_{n'}))\,\mathrm{d}S \\
&\quad= 4\rho d\left(\frac{\pi}{2k_0 d}\right)^2 H^{(1)}_m(k_0\rho)H^{(1)\prime *}_m(k_0\rho)I^{++}_{\overline{n}\overline{n'}}(k_0) \\
&\qquad + 2\rho d\left(\frac{\pi}{2k_0 d}\right)^2 \sum_{p=1}^{[k_0 d/\pi]} \frac{k_{\mathrm{t}p}}{k_0} H^{(1)}_m(k_{\mathrm{t}p}\rho)H^{(1)\prime *}_m(k_{\mathrm{t}p}\rho) \\
&\qquad \times\left(I^{++}_{\overline{n}\overline{n'}}(k_{\mathrm{t}p}) + I^{--}_{\overline{n}\overline{n'}}(k_{\mathrm{t}p}) + I^{+-}_{\overline{n}\overline{n'}}(k_{\mathrm{t}p})\mathrm{e}^{2\pi\mathrm{i}pz_+/d} + I^{-+}_{\overline{n}\overline{n'}}(k_{\mathrm{t}p})\mathrm{e}^{-2\pi\mathrm{i}pz_+/d}\right) \\
&\qquad - 2\rho d\left(\frac{\pi}{2k_0 d}\right)^2 \sum_{p=1}^{[k_0 d/\pi]} \frac{k_{\mathrm{t}p}}{k_0} H^{(1)\prime}_m(k_{\mathrm{t}p}\rho)H^{(1)*}_m(k_{\mathrm{t}p}\rho) \\
&\qquad \times\left(I^{++}_{nn'}(k_{\mathrm{t}p}) + I^{--}_{nn'}(k_{\mathrm{t}p}) - I^{+-}_{nn'}(k_{\mathrm{t}p})\mathrm{e}^{2\pi\mathrm{i}pz_+/d} - I^{-+}_{nn'}(k_{\mathrm{t}p})\mathrm{e}^{-2\pi\mathrm{i}pz_+/d}\right)
\end{aligned}
$$

Notice that all entries of $I^{++}_{\overline{n}\overline{n'}}(k_0)$ are real-valued, since $\pi^m_l(0)$ has only non-zero values for $l+m$ even, and $\Delta^m_l(0)$ has only non-zero values for $l+m$ odd.

Keeping only the dominant contribution as $\rho\to\infty$ (use the asymptotic value of the Hankel function as $\rho\to\infty$ [3, 12]) gives

$$
\begin{aligned}
\frac{1}{k_0}\iint_S \hat{\boldsymbol{\rho}}\cdot(\boldsymbol{F}_n\times(\nabla\times\boldsymbol{F}^*_{n'}))\,\mathrm{d}S = -\frac{\mathrm{i}d^2\pi}{(k_0 d)^3}\Bigg\{ & 2I^{++}_{\overline{n}\overline{n'}}(k_0) \\
&+ \sum_{p=1}^{[k_0 d/\pi]}\Bigg(I^{++}_{\overline{n}\overline{n'}}(k_{\mathrm{t}p}) + I^{--}_{\overline{n}\overline{n'}}(k_{\mathrm{t}p}) + I^{+-}_{\overline{n}\overline{n'}}(k_{\mathrm{t}p})\mathrm{e}^{2\pi\mathrm{i}pz_+/d} + I^{-+}_{\overline{n}\overline{n'}}(k_{\mathrm{t}p})\mathrm{e}^{-2\pi\mathrm{i}pz_+/d} \\
&\quad + I^{++}_{nn'}(k_{\mathrm{t}p}) + I^{--}_{nn'}(k_{\mathrm{t}p}) - I^{+-}_{nn'}(k_{\mathrm{t}p})\mathrm{e}^{2\pi\mathrm{i}pz_+/d} - I^{-+}_{nn'}(k_{\mathrm{t}p})\mathrm{e}^{-2\pi\mathrm{i}pz_+/d}\Bigg)\Bigg\}
\end{aligned}
$$

The $I^{\pm\pm}_{nn'}(k_{\mathrm{t}p})$ in terms of the $\tau\sigma$ indices are ($m>0$, for $m=0$ only $\tau\sigma = 1\mathrm{e}$ survives)

$$
I^{++}_{nn'} = \pi\delta_{mm'}\mathrm{i}^{l'-l}C_{lm}C_{l'm}
\begin{array}{c} \\ 1\mathrm{e} \\ 2\mathrm{o} \\ 1\mathrm{o} \\ 2\mathrm{e} \end{array}
\begin{array}{c}
\begin{array}{cccc} 1\mathrm{e} & 2\mathrm{o} & 1\mathrm{o} & 2\mathrm{e} \end{array} \\
\begin{pmatrix}
\Delta^m_l\Delta^m_{l'} & \mathrm{i}\Delta^m_l\pi^m_{l'} & 0 & 0 \\
-\mathrm{i}\pi^m_l\Delta^m_{l'} & \pi^m_l\pi^m_{l'} & 0 & 0 \\
0 & 0 & \Delta^m_l\Delta^m_{l'} & -\mathrm{i}\Delta^m_l\pi^m_{l'} \\
0 & 0 & \mathrm{i}\pi^m_l\Delta^m_{l'} & \pi^m_l\pi^m_{l'}
\end{pmatrix}
\end{array}
$$

$$
I^{+-}_{nn'} = \pi\delta_{mm'}\mathrm{i}^{l'-l}C_{lm}C_{l'm}(-1)^{l'+m}
\begin{array}{c} \\ 1\mathrm{e} \\ 2\mathrm{o} \\ 1\mathrm{o} \\ 2\mathrm{e} \end{array}
\begin{array}{c}
\begin{array}{cccc} 1\mathrm{e} & 2\mathrm{o} & 1\mathrm{o} & 2\mathrm{e} \end{array} \\
\begin{pmatrix}
-\Delta^m_l\Delta^m_{l'} & \mathrm{i}\Delta^m_l\pi^m_{l'} & 0 & 0 \\
\mathrm{i}\pi^m_l\Delta^m_{l'} & \pi^m_l\pi^m_{l'} & 0 & 0 \\
0 & 0 & -\Delta^m_l\Delta^m_{l'} & -\mathrm{i}\Delta^m_l\pi^m_{l'} \\
0 & 0 & -\mathrm{i}\pi^m_l\Delta^m_{l'} & \pi^m_l\pi^m_{l'}
\end{pmatrix}
\end{array}
$$

$$I^{-+}_{nn'} = \pi\delta_{mm'}\mathrm{i}^{l'-l}C_{lm}C_{l'm}(-1)^{l+m}\begin{array}{c} \\ 1\mathrm{e} \\ 2\mathrm{o} \\ 1\mathrm{o} \\ 2\mathrm{e} \end{array}\begin{array}{c} \begin{array}{cccc} 1\mathrm{e} & 2\mathrm{o} & 1\mathrm{o} & 2\mathrm{e} \end{array} \\ \begin{pmatrix} -\Delta^m_l\Delta^m_{l'} & -\mathrm{i}\Delta^m_l\pi^m_{l'} & 0 & 0 \\ -\mathrm{i}\pi^m_l\Delta^m_{l'} & \pi^m_l\pi^m_{l'} & 0 & 0 \\ 0 & 0 & -\Delta^m_l\Delta^m_{l'} & \mathrm{i}\Delta^m_l\pi^m_{l'} \\ 0 & 0 & \mathrm{i}\pi^m_l\Delta^m_{l'} & \pi^m_l\pi^m_{l'} \end{pmatrix} \end{array}$$

$$I^{--}_{nn'} = \pi\delta_{mm'}\mathrm{i}^{l'-l}C_{lm}C_{l'm}(-1)^{l+l'}\begin{array}{c} \\ 1\mathrm{e} \\ 2\mathrm{o} \\ 1\mathrm{o} \\ 2\mathrm{e} \end{array}\begin{array}{c} \begin{array}{cccc} 1\mathrm{e} & 2\mathrm{o} & 1\mathrm{o} & 2\mathrm{e} \end{array} \\ \begin{pmatrix} \Delta^m_l\Delta^m_{l'} & -\mathrm{i}\Delta^m_l\pi^m_{l'} & 0 & 0 \\ \mathrm{i}\pi^m_l\Delta^m_{l'} & \pi^m_l\pi^m_{l'} & 0 & 0 \\ 0 & 0 & \Delta^m_l\Delta^m_{l'} & \mathrm{i}\Delta^m_l\pi^m_{l'} \\ 0 & 0 & -\mathrm{i}\pi^m_l\Delta^m_{l'} & \pi^m_l\pi^m_{l'} \end{pmatrix} \end{array}$$

and the matrices with dual indices:

$$I^{++}_{\overline{n}\overline{n'}} = \pi\delta_{mm'}\mathrm{i}^{l'-l}C_{lm}C_{l'm}\begin{array}{c} \\ 1\mathrm{e} \\ 2\mathrm{o} \\ 1\mathrm{o} \\ 2\mathrm{e} \end{array}\begin{array}{c} \begin{array}{cccc} 1\mathrm{e} & 2\mathrm{o} & 1\mathrm{o} & 2\mathrm{e} \end{array} \\ \begin{pmatrix} \pi^m_l\pi^m_{l'} & \mathrm{i}\pi^m_l\Delta^m_{l'} & 0 & 0 \\ -\mathrm{i}\Delta^m_l\pi^m_{l'} & \Delta^m_l\Delta^m_{l'} & 0 & 0 \\ 0 & 0 & \pi^m_l\pi^m_{l'} & -\mathrm{i}\pi^m_l\Delta^m_{l'} \\ 0 & 0 & \mathrm{i}\Delta^m_l\pi^m_{l'} & \Delta^m_l\Delta^m_{l'} \end{pmatrix} \end{array}$$

$$I^{+-}_{\overline{n}\overline{n'}} = \pi\delta_{mm'}\mathrm{i}^{l'-l}C_{lm}C_{l'm}(-1)^{l'+m}\begin{array}{c} \\ 1\mathrm{e} \\ 2\mathrm{o} \\ 1\mathrm{o} \\ 2\mathrm{e} \end{array}\begin{array}{c} \begin{array}{cccc} 1\mathrm{e} & 2\mathrm{o} & 1\mathrm{o} & 2\mathrm{e} \end{array} \\ \begin{pmatrix} \pi^m_l\pi^m_{l'} & -\mathrm{i}\pi^m_l\Delta^m_{l'} & 0 & 0 \\ -\mathrm{i}\Delta^m_l\pi^m_{l'} & -\Delta^m_l\Delta^m_{l'} & 0 & 0 \\ 0 & 0 & \pi^m_l\pi^m_{l'} & \mathrm{i}\pi^m_l\Delta^m_{l'} \\ 0 & 0 & \mathrm{i}\Delta^m_l\pi^m_{l'} & -\Delta^m_l\Delta^m_{l'} \end{pmatrix} \end{array}$$

$$I^{-+}_{\overline{n}\overline{n'}} = \pi\delta_{mm'}\mathrm{i}^{l'-l}C_{lm}C_{l'm}(-1)^{l+m}\begin{array}{c} \\ 1\mathrm{e} \\ 2\mathrm{o} \\ 1\mathrm{o} \\ 2\mathrm{e} \end{array}\begin{array}{c} \begin{array}{cccc} 1\mathrm{e} & 2\mathrm{o} & 1\mathrm{o} & 2\mathrm{e} \end{array} \\ \begin{pmatrix} \pi^m_l\pi^m_{l'} & \mathrm{i}\pi^m_l\Delta^m_{l'} & 0 & 0 \\ \mathrm{i}\Delta^m_l\pi^m_{l'} & -\Delta^m_l\Delta^m_{l'} & 0 & 0 \\ 0 & 0 & \pi^m_l\pi^m_{l'} & -\mathrm{i}\pi^m_l\Delta^m_{l'} \\ 0 & 0 & -\mathrm{i}\Delta^m_l\pi^m_{l'} & -\Delta^m_l\Delta^m_{l'} \end{pmatrix} \end{array}$$

$$I^{--}_{\overline{n}\overline{n'}} = \pi\delta_{mm'}\mathrm{i}^{l'-l}C_{lm}C_{l'm}(-1)^{l+l'}\begin{array}{c} \\ 1\mathrm{e} \\ 2\mathrm{o} \\ 1\mathrm{o} \\ 2\mathrm{e} \end{array}\begin{array}{c} \begin{array}{cccc} 1\mathrm{e} & 2\mathrm{o} & 1\mathrm{o} & 2\mathrm{e} \end{array} \\ \begin{pmatrix} \pi^m_l\pi^m_{l'} & -\mathrm{i}\pi^m_l\Delta^m_{l'} & 0 & 0 \\ \mathrm{i}\Delta^m_l\pi^m_{l'} & \Delta^m_l\Delta^m_{l'} & 0 & 0 \\ 0 & 0 & \pi^m_l\pi^m_{l'} & \mathrm{i}\pi^m_l\Delta^m_{l'} \\ 0 & 0 & -\mathrm{i}\Delta^m_l\pi^m_{l'} & \Delta^m_l\Delta^m_{l'} \end{pmatrix} \end{array}$$

The following sum has to be evaluated (the row and column indices are sup-

pressed, $m > 0$, for $m = 0$ only $\tau\sigma = 1\mathrm{e}$ and $\tau\sigma = 2\mathrm{e}$ survive):

$$
\begin{aligned}
I_{nn'}(k_{\mathrm{t}p}) &= I^{++}_{\overline{n}\overline{n'}}(k_{\mathrm{t}p}) + I^{--}_{\overline{n}\overline{n'}}(k_{\mathrm{t}p}) + I^{+-}_{\overline{n}\overline{n'}}(k_{\mathrm{t}p})\mathrm{e}^{2\pi\mathrm{i}pz_+/d} + I^{-+}_{\overline{n}\overline{n'}}(k_{\mathrm{t}p})\mathrm{e}^{-2\pi\mathrm{i}pz_+/d} \\
&\quad + I^{++}_{nn'}(k_{\mathrm{t}p}) + I^{--}_{nn'}(k_{\mathrm{t}p}) - I^{+-}_{nn'}(k_{\mathrm{t}p})\mathrm{e}^{2\pi\mathrm{i}pz_+/d} - I^{-+}_{nn'}(k_{\mathrm{t}p})\mathrm{e}^{-2\pi\mathrm{i}pz_+/d} \\
&= \pi\delta_{mm'}\mathrm{i}^{l'-l}C_{lm}C_{l'm}
\begin{pmatrix}
\chi_{ll'm} & \mathrm{i}\psi_{ll'm} & 0 & 0 \\
-\mathrm{i}\psi_{ll'm} & \chi_{ll'm} & 0 & 0 \\
0 & 0 & \chi_{ll'm} & -\mathrm{i}\psi_{ll'm} \\
0 & 0 & \mathrm{i}\psi_{ll'm} & \chi_{ll'm}
\end{pmatrix} \\
&\quad + \pi\delta_{mm'}\mathrm{i}^{l'-l}C_{lm}C_{l'm}(-1)^{l+l'}
\begin{pmatrix}
\chi_{ll'm} & -\mathrm{i}\psi_{ll'm} & 0 & 0 \\
\mathrm{i}\psi_{ll'm} & \chi_{ll'm} & 0 & 0 \\
0 & 0 & \chi_{ll'm} & \mathrm{i}\psi_{ll'm} \\
0 & 0 & -\mathrm{i}\psi_{ll'm} & \chi_{ll'm}
\end{pmatrix} \\
&\quad + \pi\delta_{mm'}\mathrm{i}^{l'-l}C_{lm}C_{l'm}(-1)^{l'+m}
\begin{pmatrix}
\chi_{ll'm} & -\mathrm{i}\psi_{ll'm} & 0 & 0 \\
-\mathrm{i}\psi_{ll'm} & -\chi_{ll'm} & 0 & 0 \\
0 & 0 & \chi_{ll'm} & \mathrm{i}\psi_{ll'm} \\
0 & 0 & \mathrm{i}\psi_{ll'm} & -\chi_{ll'm}
\end{pmatrix}\mathrm{e}^{2\pi\mathrm{i}pz_+/d} \\
&\quad + \pi\delta_{mm'}\mathrm{i}^{l'-l}C_{lm}C_{l'm}(-1)^{l+m}
\begin{pmatrix}
\chi_{ll'm} & \mathrm{i}\psi_{ll'm} & 0 & 0 \\
\mathrm{i}\psi_{ll'm} & -\chi_{ll'm} & 0 & 0 \\
0 & 0 & \chi_{ll'm} & -\mathrm{i}\psi_{ll'm} \\
0 & 0 & -\mathrm{i}\psi_{ll'm} & -\chi_{ll'm}
\end{pmatrix}\mathrm{e}^{-2\pi\mathrm{i}pz_+/d}
\end{aligned}
$$

where the new combinations $\chi_{ll'm} = \Delta^m_l\Delta^m_{l'} + \pi^m_l\pi^m_{l'}$ and $\psi_{ll'm} = \Delta^m_l\pi^m_{l'} + \pi^m_l\Delta^m_{l'}$ have been introduced. Notice that these functions are all symmetric in l and l', and that for propagating modes $I_{nn'} = I^*_{n'n}$.

The relevant sum in the computation of the flux density is

$$
\begin{aligned}
&\frac{1}{k_0}\iint\limits_S \hat{\boldsymbol{\rho}}\cdot(\boldsymbol{F}_n\times(\nabla\times\boldsymbol{F}^*_{n'}))\,\mathrm{d}S - \frac{1}{k_0}\iint\limits_S \hat{\boldsymbol{\rho}}\cdot(\boldsymbol{F}^*_{n'}\times(\nabla\times\boldsymbol{F}_n))\,\mathrm{d}S \\
&\quad = -\frac{\mathrm{i}d^2\pi}{(k_0d)^3}\left\{2I^{++}_{\overline{n}\overline{n'}}(k_0) + 2I^{++*}_{\overline{n'}\overline{n}}(k_0) + \sum_{p=1}^{[k_0d/\pi]}\left(I_{nn'}(k_{\mathrm{t}p}) + I^*_{n'n}(k_{\mathrm{t}p})\right)\right\} \qquad \text{(C.15)} \\
&\quad = \frac{2\mathrm{i}d^2\pi}{(k_0d)^3}\left\{2I^{++}_{\overline{n}\overline{n'}}(k_0) + \sum_{p=1}^{[k_0d/\pi]} I_{nn'}(k_{\mathrm{t}p})\right\}
\end{aligned}
$$

Appendix D Calculus of residues

The generic denominator of the integrals has the form

$$f(k_{\mathrm{t}}) = \left(1 - \mathrm{e}^{-2\mathrm{i}k_zd}\right)k_z$$

The derivative is

$$\frac{\mathrm{d}f(k_{\mathrm{t}})}{\mathrm{d}k_{\mathrm{t}}} = \left(2\mathrm{i}k_zd\mathrm{e}^{-2\mathrm{i}k_zd} + 1 - \mathrm{e}^{-2\mathrm{i}k_zd}\right)\frac{\mathrm{d}k_z}{\mathrm{d}k_{\mathrm{t}}} = -\left(2\mathrm{i}k_zd\mathrm{e}^{-2\mathrm{i}k_zd} + 1 - \mathrm{e}^{-2\mathrm{i}k_zd}\right)\frac{k_{\mathrm{t}}}{k_z}$$

which at the poles, $k_\mathrm{t} = k_{\mathrm{t}p}$ in (8.1), assumes the values

$$\frac{\mathrm{d}f(k_{\mathrm{t}p})}{\mathrm{d}k_\mathrm{t}} = \begin{cases} \mp 2\mathrm{i}\left(k_0^2 d^2 - p^2\pi^2\right)^{1/2}, & p = 1, 2, \ldots \\ \mp 4\mathrm{i}k_0 d, & p = 0 \end{cases}$$

where the upper (lower) sign holds for the poles on the red (green) contour in Figure 4. More compactly, with the Neumann factor, $\varepsilon_p = 2 - \delta_{p0}$

$$\frac{\mathrm{d}f(k_{\mathrm{t}p})}{\mathrm{d}k_\mathrm{t}} = \mp\frac{4\mathrm{i}}{\varepsilon_p}\left(k_0^2 d^2 - p^2\pi^2\right)^{1/2}, \quad p = 0, 1, 2, \ldots$$

The residues then become

$$\mathrm{Res}\,\frac{1}{\left(1 - \mathrm{e}^{-2\mathrm{i}k_z d}\right)k_z}\bigg|_{k_\mathrm{t}=k_{\mathrm{t}p}} = \frac{\mp\varepsilon_p}{4\mathrm{i}\left(k_0^2 d^2 - p^2\pi^2\right)^{1/2}}, \quad p = 0, 1, 2, \ldots \tag{D.1}$$

Similarly,

$$\mathrm{Res}\,\frac{1}{1 - \mathrm{e}^{-2\mathrm{i}k_z d}}\bigg|_{k_\mathrm{t}=k_{\mathrm{t}p}} = \frac{\mp p\pi}{2\mathrm{i}d\left(k_0^2 d^2 - p^2\pi^2\right)^{1/2}}, \quad p = 0, 1, 2, \ldots \tag{D.2}$$

and for $p = 0$

$$\mathrm{Res}\,\frac{1}{k_z}\bigg|_{k_\mathrm{t}=k_{\mathrm{t}0}} = -\,\frac{k_z}{k_\mathrm{t}}\bigg|_{k_\mathrm{t}=k_{\mathrm{t}0}} = 0 \tag{D.3}$$

Appendix E Evaluation of integrals at frequencies below first cutoff

As a first illustration of the results, we specialize to an incident field with a frequency below the first cutoff frequency $k_0 d = \pi$, *i.e.*, at frequencies in the interval $0 < f < c_0/2d$. Under this condition, only one pole, $p = 0$ in (8.1) ($k_\mathrm{t} = k_0$), contributes to the radiated field — all other poles give exponentially decreasing contributions in the lateral direction. This pole has residues, see (D.1) and (D.3)

$$\mathrm{Res}\,\frac{1}{\left(1 - \mathrm{e}^{-2\mathrm{i}k_z d}\right)k_z}\bigg|_{k_\mathrm{t}=k_0} = -\frac{1}{4\mathrm{i}k_0 d}, \quad \mathrm{Res}\,\frac{1}{k_z}\bigg|_{k_\mathrm{t}=k_0} = 0$$

Both the vertical component of $\boldsymbol{F}_n(\boldsymbol{r})$ and the d_n vector contain the functions $g_n^{\pm}(k_\mathrm{t}, \phi)$, which at $k_\mathrm{t} = k_0$ simplify to, see (C.2)

$$\begin{aligned} g_n^{\pm}(k_0, \phi) &= \mathrm{i}^{-l+m}(\pm 1)^{l+m} C_{lm} \\ &\quad \times \left(\mp\mathrm{i}\delta_{\tau 1}\Delta_l^m(0)\begin{Bmatrix}\cos m\phi \\ \sin m\phi\end{Bmatrix} - \delta_{\tau 2}\pi_l^m(0)\begin{Bmatrix}-\sin m\phi \\ \cos m\phi\end{Bmatrix}\right) \end{aligned}$$

and from Section 3.4 we get

$$\Delta_l^m(0) = -\frac{1}{\sqrt{l(l+1)}}P_l^{m\prime}(0), \quad \pi_l^m(0) = \frac{m}{\sqrt{l(l+1)}}P_l^m(0)$$

where

$$P_l^m(0) = \begin{cases} (-1)^{(l-m)/2} \dfrac{(l+m)!}{2^l \left(\frac{l-m}{2}\right)! \left(\frac{l+m}{2}\right)!}, & l+m \text{ even} \\ 0, & l+m \text{ odd} \end{cases}$$

and

$$P_l^{m\prime}(0) = \begin{cases} 0, & l+m \text{ even} \\ (l+m)P_{l-1}^m(0) = -(l-m+1)P_{l+1}^m(0), & l+m \text{ odd} \end{cases}$$

This implies

$$\begin{aligned} g_n^{\pm}(k_0,\phi) = &-\mathrm{i}^{-l+m} C_{lm} \\ &\times \left(\mathrm{i}\delta_{\tau 1} \Delta_l^m(0) \begin{Bmatrix} \cos m\phi \\ \sin m\phi \end{Bmatrix} + \delta_{\tau 2} \pi_l^m(0) \begin{Bmatrix} -\sin m\phi \\ \cos m\phi \end{Bmatrix} \right) \end{aligned} \tag{E.1}$$

E.1 The vertical component of $\boldsymbol{F}_n(\boldsymbol{r})$

The vertical component of the $\boldsymbol{F}_n(\boldsymbol{r})$ vector is, see (C.9)

$$\hat{\boldsymbol{z}} \cdot \boldsymbol{F}_n(\boldsymbol{r}) = \pi \frac{g_{\overline{n}}^{+}(k_0,\phi) + g_{\overline{n}}^{-}(k_0,\phi)}{2k_0 d} H_m^{(1)}(k_0\rho)$$

which simplifies to

$$\begin{aligned} \hat{\boldsymbol{z}} \cdot \boldsymbol{F}_n(\boldsymbol{r}) = &-\frac{\mathrm{i}^{-l+m}\pi C_{lm}}{k_0 d} \\ &\times \left(\delta_{\tau 1} \pi_l^m(0) \begin{Bmatrix} -\sin m\phi \\ \cos m\phi \end{Bmatrix} + \mathrm{i}\delta_{\tau 2} \Delta_l^m(0) \begin{Bmatrix} \cos m\phi \\ \sin m\phi \end{Bmatrix} \right) H_m^{(1)}(k_0\rho) \end{aligned}$$

At $\boldsymbol{r} = x\hat{\boldsymbol{x}}$ this expression simplifies further to

$$\hat{\boldsymbol{z}} \cdot \boldsymbol{F}_n(x\hat{\boldsymbol{x}}) = -\frac{\mathrm{i}^{-l+m}\pi C_{lm}}{k_0 d} \left(\delta_{\tau 1} \delta_{\sigma \mathrm{o}} \pi_l^m(0) + \mathrm{i}\delta_{\tau 2} \delta_{\sigma \mathrm{e}} \Delta_l^m(0) \right) H_m^{(1)}(k_0 x)$$

This quantity is non-zero only for the combinations $\{\tau, \sigma, l+m\} = \{1, \mathrm{o}, \text{even}\}$ and $\{\tau, \sigma, l+m\} = \{2, \mathrm{e}, \text{odd}\}$.

E.2 The primary field

The primary field at a frequency below the first cutoff frequency $k_0 d = \pi$, *i.e.*, at frequencies in the interval $0 < f < c_0/2d$ is now evaluated. Then only the pole at $k_{\mathrm{t}} = k_0$ contributes when the contour is closed in the upper half complex k_{t} plane. The result is

$$\boldsymbol{E}^{\mathrm{prim}}(\boldsymbol{r}) \cdot \hat{\boldsymbol{z}} = 2\pi\mathrm{i} \frac{C_0 k_0^3}{\mathrm{i}k_0 d} H_0^{(1)}(k_0|\boldsymbol{\rho} - \boldsymbol{\rho}_0|) = \sqrt{\frac{3}{8\pi}} \frac{\pi}{k_0 d} H_0^{(1)}(k_0|\boldsymbol{\rho} - \boldsymbol{\rho}_0|)$$

E.3 The d_n vector

The evaluation of the d_n vector below cutoff follows the same procedure. We have

$$d_n = 2\pi^2 \sqrt{\frac{3}{8\pi}} \frac{g_{\overline{n}}^{+}(k_0, \phi_0) + g_{\overline{n}}^{-}(k_0, \phi_0)}{k_0 d} H_m^{(1)}(k_0 \rho_0)$$

With the results and notation from above, we get

$$d_n = -4\pi^2 \sqrt{\frac{3}{8\pi}} \frac{\mathrm{i}^{-l+m} C_{lm}}{k_0 d} \times \left(\delta_{\tau 1} \pi_l^m(0) \begin{Bmatrix} -\sin m\phi_0 \\ \cos m\phi_0 \end{Bmatrix} + \mathrm{i}\delta_{\tau 2} \Delta_l^m(0) \begin{Bmatrix} \cos m\phi_0 \\ \sin m\phi_0 \end{Bmatrix} \right) H_m^{(1)}(k_0 \rho_0)$$

At $\boldsymbol{r} = -x_0 \hat{\boldsymbol{x}}$ this expression simplifies to

$$d_n = -4\pi^2 \sqrt{\frac{3}{8\pi}} \frac{\mathrm{i}^{-l-m} C_{lm}}{k_0 d} \left(\delta_{\tau 1} \delta_{\sigma \mathrm{o}} \pi_l^m(0) + \mathrm{i}\delta_{\tau 2} \delta_{\sigma \mathrm{e}} \Delta_l^m(0) \right) H_m^{(1)}(k_0 x_0)$$

Again, this quantity is non-zero only for the combinations $\{\tau, \sigma, l+m\} = \{1, \mathrm{o}, \mathrm{even}\}$ and $\{\tau, \sigma, l+m\} = \{2, \mathrm{e}, \mathrm{odd}\}$.

References

[1] M. Abramowitz and I. A. Stegun, editors. *Handbook of Mathematical Functions.* Applied Mathematics Series No. 55. National Bureau of Standards, Washington D.C., 1970.

[2] A. Bernland. *Integral Identities for Passive Systems and Spherical Waves in Scattering and Antenna Problems.* PhD thesis, Lund University, 2012.

[3] N. Bleistein and R. A. Handelsman. *Asymptotic Expansions of Integrals.* Dover Publications, New York, 1986.

[4] A. Boström and A. Karlsson. Broad-band synthetic seismograms for a spherical inhomogeneity in a many-layered elastic half-space. *Geophys. J. R. Astr. Soc.*, **89**(2), 527–547, May 1984.

[5] A. Boström and A. Karlsson. Exact synthetic seismograms for an inhomogeneity in a layered elastic half-space. *Geophys. J. R. Astr. Soc.*, **79**, 835–862, 1984.

[6] A. Boström, G. Kristensson, and S. Ström. Transformation properties of plane, spherical and cylindrical scalar and vector wave functions. In V. V. Varadan, A. Lakhtakia, and V. K. Varadan, editors, *Field Representations and Introduction to Scattering*, Acoustic, Electromagnetic and Elastic Wave Scattering, chapter 4, pages 165–210. Elsevier Science Publishers, Amsterdam, 1991.

[7] A. Boström and P. Olsson. Transmission and reflection of electromagnetic waves by an obstacle inside a waveguide. *J. Appl. Phys.*, **52**(3), 1187–1196, 1981.

[8] A. Boström and G. Kristensson. Scattering of a pulsed Rayleigh wave by a spherical cavity in an elastic half space. *Wave Motion*, **5**(2), 137–143, 1983.

[9] J. J. Bowman, T. B. A. Senior, and P. L. E. Uslenghi. *Electromagnetic and Acoustic Scattering by Simple Shapes*. North-Holland, Amsterdam, 1969.

[10] W. C. Chew. *Waves and fields in inhomogeneous media*. IEEE Press, Piscataway, NJ, 1995.

[11] R. E. Collin. *Field Theory of Guided Waves*. IEEE Press, New York, second edition, 1991.

[12] L. B. Felsen and N. Marcuvitz. *Radiation and scattering of waves*. IEEE Press, Piscataway, NJ, 1994. (Originally published by Prentice-Hall in 1973).

[13] I. S. Gradshteyn and I. M. Ryzhik. *Table of Integrals, Series, and Products*. Academic Press, San Diego, seventh edition, 2007.

[14] M. Gustafsson, C. Sohl, and G. Kristensson. Physical limitations on antennas of arbitrary shape. *Proc. R. Soc. A*, **463**, 2589–2607, 2007.

[15] M. Gustafsson, I. Vakili, S. E. B. Keskin, D. Sjöberg, and C. Larsson. Optical theorem and forward scattering sum rule for periodic structures. *IEEE Trans. Antennas Propagat.*, **60**(8), 3818–3826, 2012.

[16] A. Karlsson. Scattering of Rayleigh-Lamb waves from a 2D-cavity in an elastic plate. *Wave Motion*, **6**, 205–222, 1984.

[17] A. Karlsson and G. Kristensson. Electromagnetic scattering from subteranean obstacles in a stratified ground. *Radio Sci.*, **18**(3), 345–356, 1983.

[18] G. Kristensson. Electromagnetic scattering from buried inhomogeneities—a general three-dimensional formalism. *J. Appl. Phys.*, **51**(7), 3486–3500, 1980.

[19] G. Kristensson. The electromagnetic field in a layered earth induced by an arbitrary stationary current distribution. *Radio Sci.*, **18**(3), 357–368, 1983.

[20] G. Kristensson. The polarizability and the capacitance change of a bounded object in a parallel plate capacitor. *Physica Scripta*, **86**(3), 035405, 2012.

[21] G. Kristensson and S. Ström. Scattering from buried inhomogeneities — a general three-dimensional formalism. *J. Acoust. Soc. Am.*, **64**(3), 917–936, 1978.

[22] C. Larsson, S. E. Bayer, M. Gustafsson, G. Kristensson, D. Sjöberg, C. Sohl, and I. Vakili. Scattering measurements in a parallel plate waveguide – first results. In *Proceedings of the XXXth URSI General Assembly*, page B06.6, 2011.

[23] C. Larsson, C. Sohl, M. Gustafsson, and G. Kristensson. Wideband extinction measurements for thin and planar samples. Technical Report LUTEDX/(TEAT-7166)/1–10/(2008), Lund University, Department of Electrical and Information Technology, P.O. Box 118, S-221 00 Lund, Sweden, 2008. http://www.eit.lth.se.

[24] C. Larsson, M. Gustafsson, and G. Kristensson. Polarimetric measurements of the extinction cross section. In *International Conference on Electromagnetics in Advanced Applications (ICEAA)*, pages 311–314, Turin, Italy, September 14–18 2009.

[25] C. Larsson, M. Gustafsson, and G. Kristensson. Wideband microwave measurements of the extinction cross section — experimental techniques. Technical Report LUTEDX/(TEAT-7182)/1–22/(2009), Lund University, Department of Electrical and Information Technology, P.O. Box 118, S-221 00 Lund, Sweden, 2009. `http://www.eit.lth.se`.

[26] C. Larsson, C. Sohl, M. Gustafsson, and G. Kristensson. Measuring the extinction cross section. In *3rd European Conference on Antennas and Propagation*, pages 3633–3636, Berlin, Germany, March 23–27 2009.

[27] D. M. Pozar. *Microwave Engineering*. John Wiley & Sons, New York, third edition, 2005.

[28] C. Sohl, M. Gustafsson, and G. Kristensson. Physical limitations on broadband scattering by heterogeneous obstacles. *J. Phys. A: Math. Theor.*, **40**, 11165–11182, 2007.

[29] S. Ström. Introduction to integral representations and integral equations for time-harmonic acoustic, electromagnetic and elastodynamic wave fields. In V. V. Varadan, A. Lakhtakia, and V. K. Varadan, editors, *Field Representations and Introduction to Scattering*, volume 1 of *Handbook on Acoustic, Electromagnetic and Elastic Wave Scattering*, chapter 2, pages 37–141. Elsevier Science Publishers, Amsterdam, 1991.

[30] P. Waterman. Matrix formulation of electromagnetic scattering. *Proc. IEEE*, **53**(8), 805–812, August 1965.